

**Dynamic modeling of branches and knot formation in  
loblolly pine (*Pinus taeda* L.) trees**

by

Guillermo Trincado

Dissertation submitted to the Faculty of the  
Virginia Polytechnic Institute and State University  
in partial fulfillment of the requirements for the degree of

Doctor of Philosophy

in

Forestry

Dr. Harold E. Burkhart, Chair

Dr. Earl Kline

Dr. Richard G. Oderwald

Dr. Philip J. Radtke

Dr. Marion R. Reynolds, Jr.

June 15, 2006

Blacksburg, Virginia

**Keywords:** branch growth, knot shape, individual-tree growth models, loblolly pine.

Copyright 2006, Guillermo Trincado.

**Dynamic modeling of branches and knot formation in  
loblolly pine (*Pinus taeda* L.) trees**

by

Guillermo Trincado

(ABSTRACT)

A stochastic framework to simulate the process of initiation, diameter growth, death and self-pruning of branches in loblolly pine (*Pinus taeda* L.) trees was developed. A data set was obtained from a destructive sampling of whorl sections from 34 trees growing under different initial spacing. Data from dissected branches were used to develop a model for representing knot shape, which assumed that the live portion of a knot can be modeled by a one-parameter equation and the dead portion by assuming a cylindrical shape. For the developed knot model analytical expressions were derived for estimating the volume of knots (live/dead portions) for three types of branch conditions on simulated trees: (i) live branches, (ii) non-occluded dead branches, and (iii) occluded dead branches. This model was intended to recover information on knots shape and volume during the simulation process of branch dynamics.

Three different components were modeled and hierarchically connected: *whorl*, *branches* and *knots*. For each new growing season, whorls and branches are assigned stochastically along and around the stem. Thereafter, branch diameter growth is predicted as function of relative location within the live crown and stem growth. Using a taper equation, the spatial location (X,Y,Z) of both live and dead portion of simulated knots is maintained in order to create a 3D representation of the internal stem structure. At the end of the projection period information on (i) vertical trend of branch diameter and location along and around the stem, (ii) volume of knots, and (iii) spatial location, size and type (live and dead) of knots can be obtained.

The proposed branch model was linked to the individual-tree growth and yield model PTAEDA3.1 to evaluate the effect of initial spacing and thinning intensity on branch growth in sawtimber trees. The use of the dynamic branch model permitted generation of additional information on sawlog quality under different management regimes. The arithmetic mean diameter of the largest four branches, one from each radial quadrant of the log (i.e. Branch Index, BI) and the number of whorls per log were considered as indicators of sawlog quality.

The developed framework makes it possible to include additional wood properties in the simulation system, allowing linkage with industrial conversion processes (e.g. sawing simulation). This integrated modeling system should promote further research to obtain necessary data on crown and branch dynamics to validate the overall performance of the proposed branch model and to improve its components.

## ACKNOWLEDGEMENTS

This study was supported by the Loblolly Pine Growth and Yield Research Cooperative, the Sustainable Engineered Materials Institute and USDA/CSREES Fund Number 2005-06172 at Virginia Tech. I would like to thank Dr. Harold Burkhart for the opportunity to complete my graduate education in Blacksburg and for his limitless support of my research interests. Having the opportunity to interact with Dr. Burkhart has provided a great base for my successful advancement in academia and research. I would also like to extend my thanks to Dr. Phillip J. Radtke, Dr. Earl Kline, Dr. Richard G. Oderwald, and Dr. Marion R. Reynolds Jr. for serving on my advisory committee. During the development of this study helpful technical direction were kindly provided by Dr. Carolyn Copenhaver and Dr. Rien Visser. My thanks go to Tal Roberts and Noah Adams for invaluable help in the dissection and measurement of wood samples.

A special thanks to Ralph Amateis for consultation on technical topics and the opportunity to participate in a variety of activities within the Coop. Our conversations in the field were an invaluable experience that helped me to understand the real meaning and importance of long-term research in forestry.

Thanks also to my fellow graduate students, the faculty and staff for making my time in the Forestry Department the most enjoyable experience, with special thanks to Sue Snow who from the beginning to the end helped me in many different ways. A special recognition to the academic support and friendship received from Jason Henning during my whole period of study. Thank you to all the friends of our family in Blacksburg, in particular the Burkhart's , the Amateis's , Eddie and Sue Snow, Jason and Katie Henning, Nathan and Shana Smith, the Hareu's, the Scaglia's, Kevin and Star Packard, the Choi's, Paige Parrish, Curtis VanderSchaaf and Nathan Herring. For the sacrifices, patience, encouragement and love required to complete this journey I would like to thank my wife Marlene, and our daughters Valentina and Rebeca. Finally, I would like to extend my deepest appreciation to my parents and sister in Chile for their consistent unconditional support and love.

# TABLE OF CONTENTS

|  |            |
|--|------------|
| <b>Abstract</b>  | <b>ii</b>  |
| <b>Acknowledgements</b>  | <b>iv</b>  |
| <b>List of Tables</b>  | <b>vii</b> |
| <b>List of Figures</b>   | <b>ix</b>  |
| <b>Chapter 1. Introduction and Objectives</b>  | <b>1</b>   |
| 1.1 Introduction   | 1          |
| 1.2 Objectives   | 4          |
| 1.3 Literature Cited   | 5          |
| <b>Chapter 2. Literature Review</b>  | <b>10</b>  |
| 2.1. Introduction  | 10         |
| 2.2 Modeling external branch characteristics   | 10         |
| 2.3 Modeling branch development and dynamics   | 27         |
| 2.4 Measurement and modeling of knot shape   | 29         |
| 2.5 Conclusions  | 35         |
| 2.6 Literature cited   | 36         |
| <b>Chapter 3. A Simple Model to Represent Knots in Simulated<br/>    Loblolly pine Trees</b> | <b>43</b>  |
| 3.1 Introduction   | 44         |
| 3.2 Data   | 45         |
| 3.2.1 Loblolly pine spacing trial  | 45         |
| 3.2.2 Collection of branch data  | 46         |
| 3.3 Methods  | 47         |
| 3.3.1 Dissection and measurement of knots  | 47         |
| 3.3.2 Reconstruction of knot profiles  | 49         |
| 3.3.3 Model development  | 54         |
| 3.3.4 Volume estimate for branches internally attached to the stem                           | 55         |
| 3.3.5 Model fitting and validation   | 59         |
| 3.4 Results and Discussion   | 61         |
| 3.4.2 Testing for knot curvature   | 61         |
| 3.4.2 Knot profile model   | 62         |
| 3.4.3 Practical implementation   | 68         |
| 3.5 Conclusions  | 73         |
| 3.6 Acknowledgements   | 77         |
| 3.7 Literature Cited   | 78         |

|  |            |
|--|------------|
| <b>Chapter 4. A Stochastic Framework for Modeling Branch Development and Knot Formation in Loblolly pine</b>         | <b>81</b>  |
| 4.1 Introduction   | 82         |
| 4.2 Literature Review  | 84         |
| 4.2.1 Branch dynamics of loblolly pine   | 84         |
| 4.2.2 Previous work on modeling branch characteristics   | 86         |
| 4.3 Data   | 89         |
| 4.3.1 Loblolly pine spacing trial  | 89         |
| 4.3.2 Collection of branch data  | 90         |
| 4.4 Methods  | 92         |
| 4.4.1 Reconstruction of whorl location and frequency per growing season  | 92         |
| 4.4.2 Dissection of branches and reconstruction of branch attributes   | 94         |
| 4.4.3 Dynamic modeling of branches along and around the stem   | 95         |
| 4.4.4 Incorporation of branch model into PTAEDA 3.1  | 101        |
| 4.5 Results and Discussion   | 102        |
| 4.5.1 Modeling whorl components  | 102        |
| 4.5.2 Modeling branch components   | 108        |
| 4.5.3 Prediction of branch diameter growth and internal stem structure   | 127        |
| 4.5.4 Application, limitations and future work   | 137        |
| 4.6 Conclusions  | 140        |
| 4.7 Acknowledgements   | 141        |
| 4.8 Literature Cited   | 141        |
| <br>   |            |
| <b>Chapter 5. Simulating the Impact of Initial Spacing and Thinning Intensity on Sawlog Quality in Loblolly pine</b> | <b>149</b> |
| 5.1 Introduction   | 150        |
| 5.2 Material and Methods   | 152        |
| 5.2.1 Simulation of first-order branch dynamics  | 152        |
| 5.2.2 Effect of initial spacing and thinning intensity on sawlog production  | 152        |
| 5.2.3 Assessment of sawlog quality   | 154        |
| 5.3 Results and Discussion   | 154        |
| 5.3.1 Effect of initial spacing  | 154        |
| 5.3.2 Effect of thinning intensity   | 160        |
| 5.4 Conclusions  | 166        |
| 5.5 Acknowledgements   | 168        |
| 5.6 Literature Cited   | 168        |
| <br>   |            |
| <b>Chapter 6. Conclusions and Recommendations</b>  | <b>170</b> |
| 6.1 Modeling knot shape in simulated trees   | 170        |
| 6.2 Modeling branch dynamics and knot formation  | 171        |
| 6.3 Simulating the effects to initial spacing and thinning on sawlog quality   | 174        |
| <br>   |            |
| <b>Appendix. Simulator Input/Output and Fortran Code</b>   | <b>176</b> |

## List of Tables

|   |     |
|---|-----|
| Table 3.1. Location of sampled whorl sections along the stem for the selected trees, where DBH is diameter at breast height and H is total tree height.     | 48  |
| Table 3.2. Number of times the null hypothesis $H_0: \beta_2 = 0$ was accepted (n= 218 branch profiles).  | 63  |
| Table 3.3. Parameter estimates and goodness-of-fit for the fitting and validation data sets.  | 65  |
| Table 3.4. Parameter estimates and goodness-of-fit for the fitting and validation data sets.  | 67  |
| Table 3.5. Validation of the knot profile model where residuals are calculated by the model developed using the other data set.                             | 69  |
| Table 3.6. Parameter estimate and goodness-of-fit for the entire data set.  | 70  |
| Table 3.7. Branch characteristics for a simulated whorl composed of three branches.   | 72  |
| Table 3.8. Spatial location of simulated branches.  | 74  |
| Table 3.9. Variables required for computing knot volume. All values are given in cm.  | 75  |
| Table 3.10. Computed knot volumes for the live and dead portions for the simulated branches.  | 76  |
| Table 4.1. Number of sampled trees per initial spacing and sampled whorl sections per tree.   | 91  |
| Table 4.2. Number of whorls produced and mean relative location (%) within a growing season.  | 103 |
| Table 4.3. Number of branches per whorl disaggregated by the number of whorls produced per annual shoot.  | 110 |
| Table 4.4. Probability and cumulative probability for the number of branches (x) in each whorl, assuming that three whorls were formed in a growing season. | 113 |
| Table 4.5. Difference angle (in degrees) for consecutive whorls having the same number of branches (NB) obtained by Doruska and Burkhart (1994).            | 116 |

|  |     |
|--|-----|
| Table 4.6. Parameter estimates and goodness of fit test for the Weibull probability density function (p.d.f.).   | 118 |
| Table 4.7. Parameter estimates and mean square error for the candidate equations to predict branch diameter increment ( $\Delta BD$ ).                             | 123 |
| Table 4.8. Simulated growth for a dominant tree using PTAEDA3.1.   | 128 |
| Table 5.1. Production of sawtimber trees, sawlog volume and log volume at age 30 years under different initial spacing (Coastal Plain, SI=65 ft).                  | 155 |
| Table 5.2. Average branch index for the first and second 16-ft butt sawlog disaggregated by DBH-classes and initial spacing.                                       | 159 |
| Table 5.3. Production of sawtimber trees, sawlog volume and log volume at 30 years old under different thinning intensities for an initial spacing of 8 ft x 8 ft. | 162 |
| Table 5.4. Average branch index for the first and second 16-ft butt sawlog disaggregated by DBH-classes and thinning intensities.                                  | 165 |



## List of Figures

|   |    |
|---|----|
| Figure 2.1. Simulated vertical trend of branch characteristics for Douglas-fir trees (Adapted from Roeh and Maguire 1997).  | 17 |
| Figure 2.2. Simulated branch characteristics for trees of different social status (a) predicted number of branches in a new whorl, (b) probability of a branch to be alive and (c) proportion of the actual number of branches on a whorl to the predicted initial number below the crown, where $\Delta h$ is the height increment and whorl is the whorl number (Adapted from Mäkinen and Colin 1999).        | 20 |
| Figure 2.3. Internode length (Adapted from Grace and Carson (1993).   | 23 |
| Figure 2.4. Simulation of branch characteristics for Douglas-fir trees (a) prediction of number of branches as function of shoot length, (b) empirical relative frequency of branches across relative depth into annual shoot, (c) prediction of relative branch diameter and relative depth into annual shoot, and (d) predicted vertical trend of maximum branch diameter (Adapted from Maguire et al. 1994). | 25 |
| Figure 2.5. Dissection techniques proposed by (a) Maguire and Hann (1987) for Douglas-fir and (b) Fujimori (1993) for hinoki cypress (Adapted from Maguire and Hann 1987 and Fujimori 1993).  | 28 |
| Figure 2.6. Dissection techniques used to study knot geometry (a) flitch method, (b) disk method and (c) peeling method.  | 31 |
| Figure 2.7. Dissection technique utilized to study the morphology of knots (Adapted from Lemieux et al. 2001).  | 33 |
| Figure 2.8. Representation of knot shape (Adapted from Samson et al. 1996).   | 34 |
| Figure 3.1. Procedure used for dissecting branches: (a) identification of target branches, (b) tangential cut for consistent positioning of the sample on the band saw and (c) sawing branch into approximately 3 mm slices parallel to stem pith.  | 50 |
| Figure 3.2. Reconstruction of knot profiles (a) measured branch profile, (b) smoothed branch profile with interpolated branch diameters at a given branch age in the R/T plane and (c) smoothed branch profile with branch diameters perpendicular to branch pith.  | 52 |
| Figure 3.3. Smoothing of branch measurements (a) fitting a growth curve to the diameter measurements of a dissected branch, and (b) linear regression through the branch pith.  | 53 |

|  |     |
|--|-----|
| Figure 3.4. Type of branch conditions on simulated trees (a) live branch, (b) non-occluded dead branch, and (c) occluded dead branch, where $r$ and $r'$ represent the stem radius at the height a branch arises from the stem bole. | 56  |
| Figure 3.5. Randomly selected knot profiles for the live portion, where $\beta_2$ was found to be significant ( $\alpha=0.001$ ).  | 64  |
| Figure 3.6. Relationship between the random effect parameter $b_i$ and the maximum branch radius $R_i$ for the (a) fitting and (b) validation datasets.  | 66  |
| Figure 3.7. Observed and modeled relative knot profiles for different values of maximum branch radius ( $R$ ) in mm.   | 71  |
| Figure 4.1. Reconstruction of whorl location within each growing season until tree age 8 years old.  | 93  |
| Figure 4.2. Relationship between the different entities and components for the proposed branch growth model, where $A_b$ = branch age, $H_b$ = height of the branch above the ground and HLC = height to live crown.                 | 96  |
| Figure 4.3. Relationships between (a) observed number of whorls versus height increment and (b) mean number of whorls vs height increment classes.   | 104 |
| Figure 4.4. Predicted response probabilities for the number of whorls produced within a growing season.  | 106 |
| Figure 4.5. Empirical distribution of the number of branches per whorl for the destructive data set.   | 111 |
| Figure 4.6. Relationship between parameter $\theta$ and whorl number. The line represents the fit of equation (4.7).   | 112 |
| Figure 4.7. Empirical distribution and fit of the Weibull probability distribution function for (a) branch inclination ( $BI$ ) and (b) the initial branch diameter ( $IBD$ ).   | 117 |
| Figure 4.8. Relationships between branch diameter increment ( $\Delta BD$ ) with (a) branch age ( $BA$ ), (b) increment in branch length ( $\Delta BL$ ), and (c) relative position of the branch within the live crown ( $Z$ ).     | 121 |
| Figure 4.9. Studentized residuals for equation (4.23) plotted versus predicted values.   | 124 |
| Figure 4.10. Probability of a branch to self-prune after branch death, where $\theta_0 = 4$ years and $\theta_1 = 11$ years.   | 126 |

|  |     |
|--|-----|
| Figure 4.11. Simulated (a) number of whorls per growing season and (b) number of branches per whorl, where consecutive points with similar symbol belong to the same growing season.   | 129 |
| Figure 4.12. Vertical trend of simulated branch diameters.   | 131 |
| Figure 4.13. Internal stem structure in terms of ring-width (left-side) and branch defects (right-side) derived for the simulated tree (DBH = 10.7 inches, TH = 72.7 feet and HLC = 48.7 feet), where a: zone with live branches, b: zone with dead branches and c: clear-wood zone. | 132 |
| Figure 4.14. Volume of individual knots along the stem (a) total knot volume, (b) live knot volume and (c) dead knot volume.   | 134 |
| Figure 4.15. Cumulative knot volume along the stem for the total, live and dead portions.  | 136 |
| Figure 4.16. Three-dimensional representation of internal branches (knots) indicating live and dead portions.  | 138 |
| Figure 5.1. Mean response profiles for the (a) branch index (BI) and (b) number of whorls for the first (●) and second (○) 16-ft butt sawlog under different initial spacing.  | 156 |
| Figure 5.2. Relationships between branch index (BI) and the diameter at breast height for three different initial spacing for the first and second 16-ft butt sawlogs.   | 158 |
| Figure 5.3. Mean response profiles for the (a) branch index (BI) and (b) number of whorls for the first (●) and second (○) 16-ft butt sawlog under different thinning intensities.   | 163 |
| Figure 5.4. Relationships between branch index (BI) and the diameter at breast height for different thinning intensities for the first and second 16-ft butt sawlogs.  | 164 |

# Chapter 1

## Introduction and Objectives

### 1.1 Introduction

Loblolly pine (*Pinus taeda* L.) plantations are intensively managed, providing raw material for pulp and paper industries as well as for solid and composite wood products (Daniels et al. 2002). In plantations managed for production of solid wood products, quality and value of standing trees, logs and lumber depends on factors such as the number, position and size of branches. Branches included in the wood of the stem originate knots, which decrease the strength and stiffness of wood intended for structural uses and influences the appearance of timber (Whiteside et al. 1977, Briggs 1996, Gartner 2005). Their effect on mechanical properties is due to interruption of continuity and change in the direction of wood fibers (Grace et al. 1999). Furthermore, compression wood produced at the base of branches to support their angle has a detrimental effect on wood quality (Schultz 1997). Haygreen and Bowyer (1996) state that for sawlog and veneer production, size and frequency of knots are the single most important determinant of quality. From a management perspective the importance is that these two product categories account for most of the value of a stand (Amateis and Burkhart 2005).

For southern pines, the size and location of knots in relation to board width are the key factors used to grading dimension lumber (Clark and McAlister 1998). However, despite of the importance of knots in the manufacture of solid wood products, there is limited empirical data and few studies on the development of first-order branches and knot formation under different management practices. In contrast, a number of studies investigated specific gravity and its response to silvicultural practices because it is a determining factor of pulp yield and most mechanical wood properties (Tassisa and Burkhart 1998, Phillips 2002, Clark and Daniels 2002, Daniels et al. 2002, Mora 2003).

Branch development in loblolly pine trees is greatly influenced by genetic, site quality and environmental conditions (Bridgwater et al. 1985, Bridgwater 1990, Mudano et al. 1992). Initial planting density and spacing (e.g. Sharma et al. 2002, Clark et al. 1994, Amateis et al. 2004), thinning (e.g. Baldwin et al. 2000), pruning (e.g. Clark et al. 2004) and fertilization (e.g. Yu et al. 2003) also affect crown and branch development. Thus, quality of logs and wood produced can be controlled by defining adequately the timing and intensity of silvicultural treatments.

Growth and yield models have been developed to support management decisions, incorporating the effect of intensive management practices on volume production. However, until now they do not account for wood quality differentials in predicted volumes (Clark et al. 1994). Crown dimensions have been included in individual-tree growth and yield models as surrogates for photosynthetic potential and as predictors for other growth components (Daniels and Burkhart 1975, Maguire and Hann 1990). Research have focused on modeling crown recession process (Dyer and Burkhart 1987, Short and Burkhart 1992, Liu et al. 1995), crown profiles (Doruska and Mays 1998), crown shape (Baldwin et al. 1995, Baldwin and Peterson 1997), foliage weight and surface area (Baldwin and Peterson 1997), and branch biomass (Zhang et al. 2004). For loblolly pine the only model able to describe the tree crown at branch-level is that of Doruska and Burkhart (1994). They presented a system of equations for predicting the external location and distribution of first-order branches along and around the stem. However, some of the limitations of this model are that it permits the modeling of branches only at one point in time and prediction of external branch characteristics is limited to the crown. From a wood quality perspective this model does not provide information on knots characteristics along the stem.

Dynamic modeling of first-order branches would extend the utility of existing individual-tree growth models to more accurately quantify value of raw material. Simulated trees with detailed internal structure can meet data needs while reducing the time and cost involved in destructive data collection as lumber grade recovery studies (Clark and McAlister 1998, Hilpp and Pelkki 2003). Information on internal stem

structure can be accomplished by linking individual-tree growth model output with information on knot size and location to existing bucking and sawing simulators (Todoroki 1997, Lemieux et al. 2001, Lemieux et al. 2002). Data for simulating wood processing are obtained by scanning sample logs to obtain information on log shape. Afterwards, the log is peeled to get information on internal defects (Pinto et al. 2003, Pinto et al. 2005). Hence, forest management and industrial processes can be linked to produce an integrated modeling system to identify the optimal silvicultural regime for different end products.

At present, few empirical models to simulate growth and location of first-order branches along and around the stem have been reported (Grace et al. 1999). Others have recently evaluated approaches for predicting branch diameter growth, but without considering the complete growth process of branches (Briggs et al. 2002). Past and current research is heavily concentrated on modeling external branch characteristics from cross-sectional data (Maguire et al. 1988, Colin and Houllier 1991, Pukkala et al. 1992, Rohe and Maguire 1997, Mäkinen and Colin 1998, Meredieu et al. 1998, Maguire et al. 1999, Woollons et al. 2002, Turnblom and Becker 2002, Catchpole et al. 2002, Mäkinen et al. 2003a, Garber and Maguire 2005). In contrast, research on dynamic models has been limited mainly because of the scarcity of longitudinal data on branch development for different commercial tree species. Past studies of branch development have relied on information from dissected branches for modeling purposes (e.g. Mäkinen 1999).

This study aimed at developing a general modeling framework to simulate the growth of first-order branches and internal stem structure in relation to knots in loblolly pine trees. Particular importance is given to the search for empirical relationships and new modeling approaches to predict branch and knot development.

## 1.2 Objectives

The main objective of this research was to characterize through statistical models the development of first-order branches and knot formation for loblolly pine. The specific objectives were:

- (1) Study and model the structure of internal branches (e.g. knots) based on destructive analysis techniques (Chapter 3);
- (2) Characterize and predict the process of branch development and knot formation over time both along and around the stem using statistical models as a tool to understand the effect of silvicultural practices (Chapter 4);
- (3) Examine the effect of initial spacing and thinning intensity on branch diameter growth using simulation of individual-tree growth and first-order branch formation over time (Chapter 5).

### 1.3 Literature Cited

- Amateis, R.L., and H.E. Burkhart. 2005. The influence of thinning on the proportion of peeler, sawtimber, and pulpwood trees in loblolly pine plantations. *South. J. Appl. For.* 29:158-162.
- Amateis, R.L., P.J. Radtke, and G.D. Hansen. 2004. The effect of spacing rectangularity on stem quality in loblolly pine plantations. *Can. J. For. Res.* 34:498-501.
- Baldwin, V.C., Jr., K.D. Peterson, and D.R. Simmons. 1995. A program to describe the crown shape of loblolly pine trees. *Compiler* 13:17-19.
- Baldwin, V.C., Jr., and K.D. Peterson. 1997. Predicting the crown shape of loblolly pine trees. *Can. J. For. Res.* 27:102-107.
- Baldwin, V.C.Jr., K.D. Peterson, A. Clark III, R.B. Ferguson, M.R. Strub, and D.R. Bower. 2000. The effects of spacing and thinning on stand and tree characteristics of 38-year-old loblolly pine. *For. Ecol. Manage.* 137:91-102.
- Bridgwater, F.E. 1990. Shoot elongation patterns of loblolly pine families selected for contrasting growth potential. *For. Sci.* 36:641-656.
- Bridgwater, F.E., C.G. Williams, and R.G. Campbell. 1985. Patterns of leader elongation in loblolly pine families. *For. Sci.* 31:93-944.
- Briggs, D. 1996. Modeling crown development and wood quality. *J. For.* 94(12): 24-25.
- Briggs, D., E. Turnblom, O. Høibø, and S. Irmen. 2002. Relationship between branch diameter growth and stem growth in young coastal US Douglas-fir. P. 282-289 *in* Fourth Workshop Connection between silviculture and wood quality through modelling approaches and simulation softwares, Nepveu, G. (ed.). Harrison Hot Spring, B.C., Canada.
- Burkhart, H.E., R.L. Amateis, J.A. Westfall, and R.F. Daniels. 2004. PTAEDA 3.1: Simulation of individual tree growth, stand development and economic evaluation in loblolly pine plantations. Department of Forestry, Virginia Polytechnic Institute and State University. 23p.
- Catchpoole, K., I. Andrew, M.R. Nester, K. Harding, and B. Hogg. 2002. Development of branch models for use in a silvicultural decision support system. P. 406-414 *in* Fourth Workshop Connection between silviculture and wood quality through



- modelling approaches and simulation softwares, Nepveu, G. (ed.). Harrison Hot Spring, B.C., Canada.
- Clark III, A., and R.H. McAlister. 1998. Visual tree grading systems for estimating lumber yields in young and mature southern pine. *Forest Prod. J.* 48(10):59-67.
- Clark III, A., and R.F. Daniels. 2002. Modeling the effect of physiographic region on wood properties of planted loblolly pine in Southeastern United States. p. 54-60 *in* Fourth Workshop Connection between silviculture and wood quality through modelling approaches and simulation softwares, Nepveu, G. (ed.). Harrison Hot Spring, B.C., Canada.
- Clark III, A., J.R. Saucier, V.C. Baldwin, and D.R. Bower. 1994. Effect of initial spacing and thinning on lumber grade, yield, and strength of loblolly pine. *For. Prod. J.* 44 (11/12):14-20.
- Clark III, A., M. Strub, L. R. Anderson, H.G. Lloyd, R.F. Daniels, and J.H. Scarborough. 2004. Impact of early pruning and thinning on lumber grade yield from Loblolly pine. P. 199-204 *in* Proceedings of the 12<sup>th</sup> biennial southern silvicultural research conference, Connor, K.F. (ed.). USDA For. Serv. Gen. Tech. Rep. SRS-71. 594p.
- Colin, F., and F. Houllier. 1991. Branchiness of Norway spruce in north-eastern France: modeling vertical trends in maximum nodal branch size. *Ann. Sci. For.* 48:679-693.
- Daniels, R.F., and H.E. Burkhart. 1975. Simulation of individual tree growth and stand development in managed loblolly pine plantations. Virginia Polytechnic Institute and State University, Pub. FWS-5-75.69p.
- Daniels, R.F., R. He, A. Clark III, and R.A. Souter .2002. Modeling wood properties of planted loblolly pine from pith to bark and stump to pith. P. 238-245 *in* Fourth Workshop Connection between silviculture and wood quality through modelling approaches and simulation softwares, Nepveu, G. (ed.). Harrison Hot Spring, B.C., Canada.
- Doruska, P.F., and H.E. Burkhart. 1994. Modeling the diameter and locational distribution of branches within the crowns of loblolly pine trees in unthinned plantations. *Can. J. For. Res.* 24:2362-2376.
- Doruska, P.F., and J.E. Mays. 1998. Crown profile modeling of loblolly pine by nonparametric regression. *For. Sci.* 44:445-453.

- Dyer, M.E., and H.E. Burkhart. 1987. Compatible crown ratio and crown height models. *Can. J. For. Res.* 17:572-574.
- Garber, S.M., and D.A. Maguire. 2005. Vertical trends in maximum branch diameter in two mixed-species spacing trials in the central Oregon Cascades. *Can. J. For. Res.* 35:295-307.
- Gartner, B.L. 2005. Assessing wood characteristics and wood quality in intensively managed plantations. *J. For.* 103(2):75-77.
- Grace, J.C., D. Pont, and C.J. Goulding. 1999. Modelling branch development for forest management. *N. Z. J. For. Sci.* 29:391-408.
- Haygreen, J.G., and J.L. Bowyer. 1996. Forest products and wood science: an introduction. Third Edition, Iowa State University Press, Iowa. 484p.
- Hilpp, G.K., and M.H. Pelkki. 2003. Log grade prediction for standing Yellow-poplar trees in eastern Kentucky. *South. J. Appl. For.* 27:61-65.
- Lemieux, H., M. Beaudoin, and S.Y. Zhang. 2001. Characterization and modeling of knots in black spruce (*Picea Mariana*) logs. *Wood and Fiber Science* 33:465-475.
- Lemieux, H., M. Beaudoin, S.Y. Zhang, and F. Grondin. 2002. Improving structural lumber quality in a sample of *Picea mariana* logs sawn according to the knots. *Wood and Fiber Science* 34:266-275.
- Liu, J., H.E. Burkhart, and R.L. Amateis. 1995. Projecting crown measures for loblolly pine trees using a generalized thinning response function. *For. Sci.* 41:43-53.
- Maguire, D.A., and D.W. Hann. 1990. A sampling strategy for estimating past crown recession on temporary growth plots. *For. Sci.* 36:549-563.
- Maguire, D.A., D.W. Hann, and J.A. Kershaw, Jr. 1988. Prediction of branch diameter and branch distribution for Douglas-fir in Southwestern Oregon. P.1029-1036 in *Forest Growth Modeling and Prediction*, Ek, A.R. , S.R. Shifley and T.E. Burk (eds.). USDA For. Serv. Gen. Tech. Rep. NC-120. 1149p.
- Maguire, D.A., S.R. Johnston, and J. Cahill. 1999. Predicting branch diameters on second-growth Douglas-fir from tree-level descriptors. *Can. J. For. Res.* 29:1829-1840.
- Mäkinen, H. 1999. Growth, suppression, death, and self-pruning of branches of scots pine in southern and central Finland. *Can. J. For. Res.* 29:585-594.

- Mäkinen, H., and F. Colin. 1998. Predicting branch angle and branch diameter of scots pine from usual tree measurements and stand structural information. *Can. J. For. Res.* 28:1686-1696.
- Mäkinen, H., R. Ojansuu, P. Sairanen, and H. Yli-Kojola. 2003a. Predicting branch characteristics of Norway spruce (*Picea abies* (L.) Karst.) from simple stand and tree measurements. *Forestry* 76:525-546.
- Meredieu, C., F. Colin, and J.C. Hervé. 1998. Modeling branchiness of Corsica pine with mixed-effect models (*Pinus nigra* Arnold ssp. *Laricio* (Poiret) Maire). *Ann. Sci. For.* 55:359-374.
- Mora. 2003. Effects of early intensive silviculture on wood properties of loblolly pine. M.Sc. Thesis, North Carolina State University, Raleigh, NC. 70p.
- Mudano, J.E., H.L. Allen, and L.W. Kress. 1992. Stem and foliage elongation of young loblolly pine as affected by ozone. *For. Sci.* 38:324-335.
- Phillips, K.M. 2002. Modeling within-tree changes in wood specific gravity and moisture content for loblolly pine in Georgia. M.Sc. Thesis, University of Georgia, Athens, GA. 95p.
- Pinto, I., H. Pereira, and A. Usenius. 2003. Analysis of log shape and internal knots in twenty Maritime pine (*Pinus pinaster* Ait.) stems based on visual scanning and computer aided reconstruction. *Ann. For. Sci.* 60:137-144.
- Pinto, I., A. Usenius, T. Song, and H. Pereira. 2005. Sawing simulation of maritime pine (*Pinus pinaster* Ait.) stems for production of heartwood-containing components. *Forest Prod. J.* 55(4):88-96.
- Pukkala, T., J. Karsikko, and T. Kolström. 1992. A spatial model for the diameter of the thickest branch of Scot pine. *Silv. Fenn.* 26:219-230.
- Roeh, R.L., and D.A. Maguire. 1997. Crown profile models based on branch attributes in Coastal Douglas-fir. *For. Ecol. Manage.* 96:77-100.
- Schultz, R.I. 1997. The ecology and culture of Loblolly pine (*Pinus taeda* L.). U.S. Department of Agriculture, Forest Service, Southern Forest Experiment Station, New Orleans, Louisiana, Agricultural Handbook 713.
- Sharma, M., H.E. Burkhart, and R.L. Amateis. 2002. Spacing rectangularity effect of the growth of loblolly pine plantations. *Can. J. For. Res.* 32:1451-1459.

- Short, E.A., and H.E. Burkhart. 1992. Predicting crown-height increment for thinned and unthinned loblolly pine plantations. *For. Sci.* 38:594-610.
- Tasissa, G., and H.E. Burkhart. 1998. An application of mixed effects analysis to modeling thinning effects on stem profile of loblolly pine. *For. Ecol. Manage.* 103:87-101.
- Todoroki, C.L. 1997. Developments of the sawing simulation software AUTOSAW: linking wood properties, sawing, and lumber end-use. P. 241-247 *in* Second Workshop Connection between silviculture and wood quality through modelling approaches and simulation softwares, Nepveu, G. (ed.). Berg-en-Dal, South Africa.
- Turnblom, E., and G. Becker. 2002. Cross-validation of alternative branch models for Douglas-fir using geographically disparate data sources from Europe and the Northwest USA. P. 399-405 *in* Fourth Workshop Connection between silviculture and wood quality through modelling approaches and simulation softwares, Nepveu, G. (ed.). Harrison Hot Spring, B.C., Canada.
- Whiteside, I.D., M.D. Wilcox, and J.R. Tustin. 1977. New Zealand Douglas-fir timber quality in relation to silviculture. *N. Z. Journal of Forestry* 22: 24-45.
- Woollons, R.C., A. Haywood, and D.C. McNickle. 2002. Modeling internode length and branch characteristics for *Pinus radiata* in New Zealand. *For. Ecol. Manage.* 160:243-261.
- Yu, S., J.L. Chambers, Z. Tang, and J.P. Barnett. 2003. Crown characteristics of juvenile loblolly pine 6 years after application of thinning and fertilization. *For. Ecol. Manage.* 180:345-352.
- Zhang, Y., B.E. Borders, R.E. Will, and H. De Los Santos Posadas. 2004. A model for foliage and branch biomass prediction for intensively managed fast growing loblolly pine. *For. Sci.* 50:65-80.

# Chapter 2

## Literature Review

### 2.1. Introduction

Current research on empirical models focuses heavily on developing models to predict external branch characteristics rather than modeling dynamics of branch structure and knot formation. Studies of branch dynamics are limited by the scarcity or absence of longitudinal data on branch development (Mäkinen 1999). However, dissection techniques have been developed to recover information on branch dynamics as well as knot structure (Fujimori 1993, Mäkinen 1999, Grace et al. 1999).

Process-oriented approaches (e.g. Cochrane and Ford 1978, Ford and Ford 1990, Ford et al. 1990) and branch architecture models (e.g. Honda 1971, Burk et al. 1983, Remphrey and Powell 1984, Kurth and Landwert 1995) have been proposed for modeling branching structure. Nevertheless, given the objectives of this study and data available, this review focuses on empirical approaches.

In the following sections the different approaches utilized for modeling external branch characteristics, branch dynamics and knot structure are discussed.

### 2.2 Modeling external branch characteristics

A number of approaches have been reported for modeling branch characteristics. They can be broadly grouped in six different groups:

- (i) Modeling branch index
- (ii) Modeling maximum branch diameter
- (iii) Modeling mean maximum branch diameter near base of live crown
- (iv) Modeling vertical trend of branch characteristics

- (v) Modeling internode length and
- (vi) Modeling distribution of branches along and around the stem.

A common feature of the equations or system of equations proposed is that they rely on cross-sectional data (e.g. Maguire et al. 1991, Doruska and Burkhart 1994, Mäkinen and Colin 1998).

### ***Modeling branch index***

Because of the impact of branch size on timber grade a series of indexes relating these two variables were evaluated by Whiteside (1982). The best index was found to be the arithmetic mean diameter of the largest four branches for a specified log length, one from each quadrant. This index is known as Branch Index (BI) and it has been commonly used to evaluate the effects of branch size on log grading and value in different tree species (Bier 1986, Maguire et al. 1991, DeBell and Gartner 1997). Inglis and Cleland (1982) developed, for thinned radiata pine (*Pinus radiata* D. Don) plantations in New Zealand, a model for predicting a mean BI at stand-level to any 5.5 m logs located in the lower 17m of the tree bole. They proposed the following equation

$$\overline{BI} = \beta_1 SI + \beta_2 \frac{D_{20}}{SI} + \beta_3 HC + \beta_4 \frac{1}{HTT} + \beta_5 + \varepsilon , \quad (2.1)$$

where  $SI$  = site index,  $D_{20}$  = mean DBH of the stand at age 20,  $HC$  = log height class and  $HTT$  = dominant mean height at time of last thinning. This study showed that the BI could be predicted with reasonable accuracy, in particular for the first three 5.5m log lengths. However, at present the use or development of an equation similar to (2.1) has two major limitations. First, the relationship between branch index and lumber grade is only valid for a given sawing process, which makes this index inflexible for changes in standards of utilization (Grace et al. 1999). Second, no information about location of branches is obtained to facilitate linkage with existing sawing simulators (Woollons et al. 2002).

### ***Modeling maximum branch diameter***

Others studies have focused on evaluating the impact of stand structure on the maximum branch diameter reached by individual trees. Pukkala et al. (1992) studied the effect of spatial distribution of trees on branch growth and developed an equation to predict the maximum branch diameter ( $BD_{\max}$ ) for Scots pine (*Pinus sylvestris* L.) trees. The predictor variables included stand age, basal area and a distance-dependent competition index. In order to account for within- and between-stand residual variation, the model was fitted using mixed-effects modeling techniques (Lappi 1986). Subsequently, they applied the model on simulated stands and examined the effects of stand age, density and spatial distribution of trees (regular, poisson and clustered) on the mean maximum branch diameter. It was concluded that the mean maximum branch diameter in a stand decreases with increasing aggregation of trees and increasing stand density. For the same tree species, Mäkinen and Colin (1998) concluded that spatial information was a significant variable in models developed to predict the vertical trend of branch diameter and branch angle. However, spatial information improved only slightly the accuracy of the models when it was included.

Even though, the model proposed by Pukkala et al. (1992) proved to be useful to evaluate the effect of spatial arrangement of trees on maximum branch diameter, its inclusion in a growth and yield simulation system with the aim of quantifying the effect of branch size on wood quality is limited. The main reason is that it does not provide information on number and location of branches.

### ***Modeling mean maximum branch diameter near base of live crown***

Maguire et al. (1988) developed a nonlinear equation to estimate mean maximum branch diameter for whorls located near the crown base using tree-level variables for Douglas fir (*Pseudotsuga menziesii* (Mirb.) Franco).

$$BD = \beta_1 DINC^{\beta_2} D^{\beta_3} H^{\beta_4} \exp(\beta_5 H / D) + \varepsilon , \quad (2.2)$$

where  $BD$  = mean maximum branch diameter for an annual whorl near the crown base,  $DINC$  = depth into crown (total height-branch height within the crown),  $D$  = diameter at breast height and  $H$  = total tree height. Afterward, this model was extended in order to include the effects of stand density and site index (Maguire et al. 1991):

$$\ln(BD) = \beta_0 + \beta_1 \ln(DINC) + \beta_2 \ln(D) + \beta_3 \ln(RD) + \beta_4 SI + \varepsilon, \quad (2.3)$$

where  $RD$  = relative density (Curtis 1982) and  $SI$  = site index. Both equations assumed that the trend of the mean maximum branch diameter is monotonic increasing with distance into the crown from the tip. Probably, the main limitation of these studies was the reduced number (one to four per tree) and location of branches (near to crown base) used to develop the equations. Thus, the vertical trend of branch diameters could not be adequately investigated.

Maguire et al. (1999) refitted Equation [2.3] to another Douglas-fir data set, but stand density and site index were not significant (Maguire et al. 1999). Contrarily, Mäkinen and Colin (1998), using an extensive data set from the central and southern Finland, found that a distance-dependent competition index was a significant variable for predicting the vertical trend of branch diameters for Scots pine. Those models including only tree-level variables were slightly less accurate than those including a competition index. As mentioned above, Pukkala et al. (1992) also found that a distance-dependent competition index was a significant predictor variable to estimate maximum branch diameter. Mäkinen and Colin (1998) concluded that site index was not significant when modeling the vertical trend in branch diameter.



### ***Modeling the vertical trend of branch characteristics***

During the last decades, the most common approach to study branch structure has been to model the vertical trend of branch characteristics. Generally, branch characteristics are modeled within the live crown including the vertical trend in maximum or mean branch diameter, branch inclination and branch length. The approaches used include the development of individual equations for each branch characteristic or the development of a system of equations to model simultaneously different branch characteristics. Because of the hierarchical structure of the branch data (-stand, -plot, -tree and -whorl) some authors have utilized mixed-effects modeling techniques (e.g. variance component model).

Empirical observations in different tree species support the idea that the maximum branch diameter is located somewhat above the base of the live crown. Thus, the assumption of a monotonic increasing trend in branch diameter along the live crown assumed in some models has proved not to be valid (Maguire et al. 1988, Maguire et al. 1991). This finding has been confirmed by Colin and Houllier (1991) for Norway spruce (*Picea abies* (L.) Karst.), Maguire et al. (1994), Roeh and Maguire (1997) and Maguire et al. (1999) for Douglas-fir, Mäkinen and Colin (1998) for Scots pine and Gilmore and Seymour (1997) for *Abies balsamea* (L.) Miller. After studying the crown structure for *Pinus sylvestris*, Schöpf (1954) concluded that the maximum branch diameter is located near the level of maximum extension of the crown. On the other hand, Kershaw et al. (1990) and Fujimori (1993) stated that the location of the maximum branch diameter can be explained by the longevity of the branches at the crown base.

Under the mentioned constraint, segmented polynomial regression and variable-exponent equations have been proposed to model more realistically the vertical trend of branch diameters. Both approaches were applied previously in forestry for modeling stem profiles (Max and Burkhart 1976, Kozak 1988, 1997). Colin and Houllier (1991, 1992) proposed a segmented polynomial for Norway spruce with a join point at the height of the largest branch diameter for each tree. The proposed model was first fit to each

individual tree. Then, a more general model was obtained relating estimated parameters to tree-level variables (Colin and Houllier, 1992)

$$\begin{aligned}
 BD &= \lambda + \alpha X + \beta X^2 && \text{if } X < \xi \\
 &= \lambda + \alpha \xi + \beta \xi^2 + \gamma (X - \xi)^2 && \text{if } X \geq \xi
 \end{aligned} \tag{2.4}$$

were  $X$  = relative distance of a branch to the top of the tree and  $\lambda$ ,  $\alpha$ ,  $\beta$ ,  $\gamma$  and  $\xi$  are parameters estimated as functions of other variables. Maguire et al. (1999) used a different approach for Douglas-fir. They constrained a variable-exponent equation to estimate branch diameter as zero at tree tip and predict maximum branch diameter at a given relative height within the live crown. Because multiple measurements on the same individual are taken the final equation was fit using mixed-effects modeling techniques. The form of the variable-exponent model was

$$BD = (\lambda_1 CW^{\lambda_2} + \delta_i) W^c + \varepsilon ,$$

where  $BD$  = branch diameter,  $CW$  = crown width,  $Z = h / CL$ ,  $W = 1 - Z^{0.5}$ ,  $h$  = height of the whorl above crown base,  $CL$  = crown length,  $c = \lambda_3 Z^{\lambda_4}$ ,  $\lambda_i$  = fixed-effects parameter ( $i=1, \dots, 4$ ) and  $\delta_i$  = random-effects parameter. Two additional equations were necessary to estimate crown width ( $CW$ )

$$CW = MCW * CR^{\beta_0 CL + \beta_1 (D/H)}$$

and maximum crown width ( $MCW$ )

$$MCW = \alpha_0 + \alpha_1 D + \alpha_2 D^2$$

Recently, Garber and Maguire (2005) utilized this model as baseline to study the influence of spacing and species composition on the vertical trend in maximum branch diameter in four commercial tree species in Oregon, U.S. In this study, most of the variability in maximum branch diameter was accounted by tree-level variables. However,

models that considered additional variables representing spacing and species composition were superior.

Another equation form for modeling maximum branch diameter was proposed by Wobst (1995) for Douglas-fir and Schmidt (2001) for different tree species in Germany. Turnblom and Becker (2002) compared the models proposed by Wobst (1995) and Maguire et al. (1999) using data for Douglas-fir from Europe (Germany) and Northwest USA (Oregon). They concluded that both equations adequately describe the vertical trend in maximum branch diameter in both regions.

A system of equations for modeling simultaneously the vertical trend of mean basal branch diameter, branch angle of origin, branch length and crown radius for Douglas-fir was developed by Roeh and Maguire (1997). The vertical trend of simulated branch characteristics for different tree sizes using individual equations is presented in Figure 2.1. The average branch diameter and branch length increase from the tree top reaching a maximum over the crown base. Similarly, as observed in other studies, the branch angle increases monotonically from the tree top to crown base (Colin and Houllier 1991, Mäkinen and Colin 1998).

Roeh and Maguire (1997) used a nonlinear three-stage least squares (N3SLS) procedure to fit a system of four equations in order to account for the correlation of error terms across them. However, during the fitting process a high number of parameters of the original individual equations were found to be non significant when considered in a system of equations. The final system of equations reduced to the following form:

$$BD = s_1 DINC + s_2 DINC^2 + s_3 D DINC^2$$

$$VA = s_4 [1 - \exp(s_5 DINC)]^{s_6 BD_i}$$

$$BL = \exp(s_7) DINC^{s_8} \exp(s_9 DINC) BD_i^{s_{10}}$$

$$CR = BL[\pi \sin(VA/180)]$$

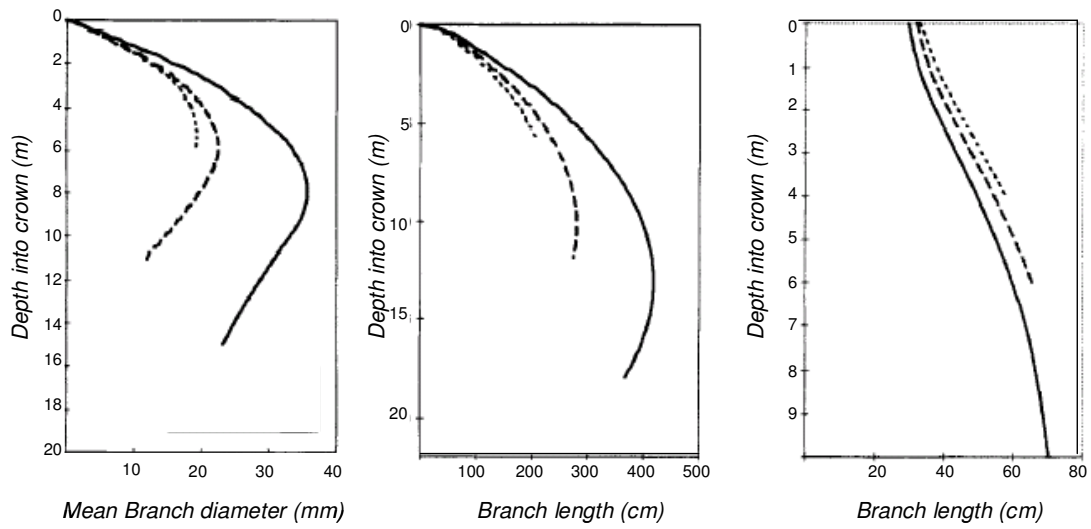


**Figure 2.1.** Simulated vertical trend of branch characteristics for Douglas-fir trees (Adapted from Roeh and Maguire 1997).

Meredieu et al. (1998) accounted for within- and between-individual variability in branch characteristics when applying mixed-effects modeling techniques for Corsica pine (*Pinus nigra* Arnold ssp. Laricio (Poiret) Maire) in France. The modeled characteristics were branch length, angle of insertion and branch diameter and the predictor variables were limited by those attributes usually provided by a tree-level growth and yield simulator. In comparison to Roeh and Maguire (1997) they modeled different branch characteristics, but using individual equations for each of them. For instance, the mixed-effects model proposed for predicting the vertical trend in branch length (*BL*) has the following form

$$BL_{ij} = (A_0 + \alpha_{0i}) + (A_1 + \alpha_{1i}) DFA_{ij} + (A_2 + \alpha_{2i}) DFA_{ij}^2 + A_3 DFA_{ij} DBH_i + \varepsilon_{ij}$$

where *DFA* = distance from the apex,  $A_i$  = fixed-effect parameters ( $i=0,\dots,3$ ) and  $\alpha_i$  = random-effect parameters ( $i=0,\dots,2$ ). Under this modeling framework the distribution of the random-effect parameters are assumed to be multivariate distributed

$$\boldsymbol{\alpha} \sim \text{MVN} \left( \begin{pmatrix} 0 \\ 0 \\ 0 \end{pmatrix}, \begin{pmatrix} \text{Var}(\alpha_0) & \text{Cov}(\alpha_0, \alpha_1) & \text{Cov}(\alpha_0, \alpha_2) \\ \text{Cov}(\alpha_0, \alpha_1) & \text{Var}(\alpha_1) & \text{Cov}(\alpha_1, \alpha_2) \\ \text{Cov}(\alpha_0, \alpha_2) & \text{Cov}(\alpha_1, \alpha_2) & \text{Var}(\alpha_2) \end{pmatrix} \right).$$

During the simulation process Meredieu et al. (1998) generated stochastic estimates of random-effects sampling from this multivariate distribution. They also noticed that the residuals between the branch diameter and branch angle equations were negatively correlated and utilized this correlation to derive an empirical variance-covariance structure of residuals from both equations. The variance-covariance relationships allowed simulation of stochastic variability around the mean profiles of diameter and angle by taking the correlation of the residuals into account.

Another modeling approach that recognizes the hierarchical structure of the data was utilized by Mäkinen and Colin (1998). They used a variance component model approach (Searle et al. 1992) when predicting the vertical trend in branch diameter and branch angle for Scots pine in southern and central Finland. During the model development they utilized the three-stage least square (3SLS) method proposed by Borders (1989). The branch angle (*BRA*) and branch diameter (*BRD*) were modeled using the following equations

$$\log(BRA_{spjk}) = a_0 + a_1 DBH_{spj} + a_2 \log(whorl_{spj}) + a_3 DBH_{spj} \log(whorl_{spj}) + u_{spj} + \varepsilon_{spjk}$$

$$\log(BRD_{spjk}) = d_0 + d_1 DBH_{spj} + d_2 CLR_{spj} + d_3 whorl_{spj} + d_4 \log(whorl_{spj}) + d_5 BRA_{spjk} + u_{spj} + \varepsilon_{spjk}$$

where  $whorl_{spj}$  = whorl number from the stem apex, CLR = relative crown length, and  $u_{spj}$  = random tree error  $\sim N(0, \sigma_u^2)$ . Under this approach, it was possible to separate the stand-, plot- and tree-level variation in the dependent variables. As in other studies, they concluded that reasonable prediction of branch characteristics can be obtained using only tree dimensions as predictor variables (Maguire et al. 1999, Colin and Houllier 1991, Colin and Houllier 1992, Meredieu et al. 1998).

Using the same modeling approach, Mäkinen and Colin (1999) developed equations to predict the number of branches in a new whorl, the probability of a branch being alive and self-pruning of branches below the crown base for Scots pine trees (Figure 2.2). As before, the inclusion of variables representing stand density and spatial arrangement of neighboring trees reduced the predictive capability of the equations only slightly. Thus, detailed information about the past development and current conditions at stand-level are not required. Site index was not a significant predictor variable in any of the equations.

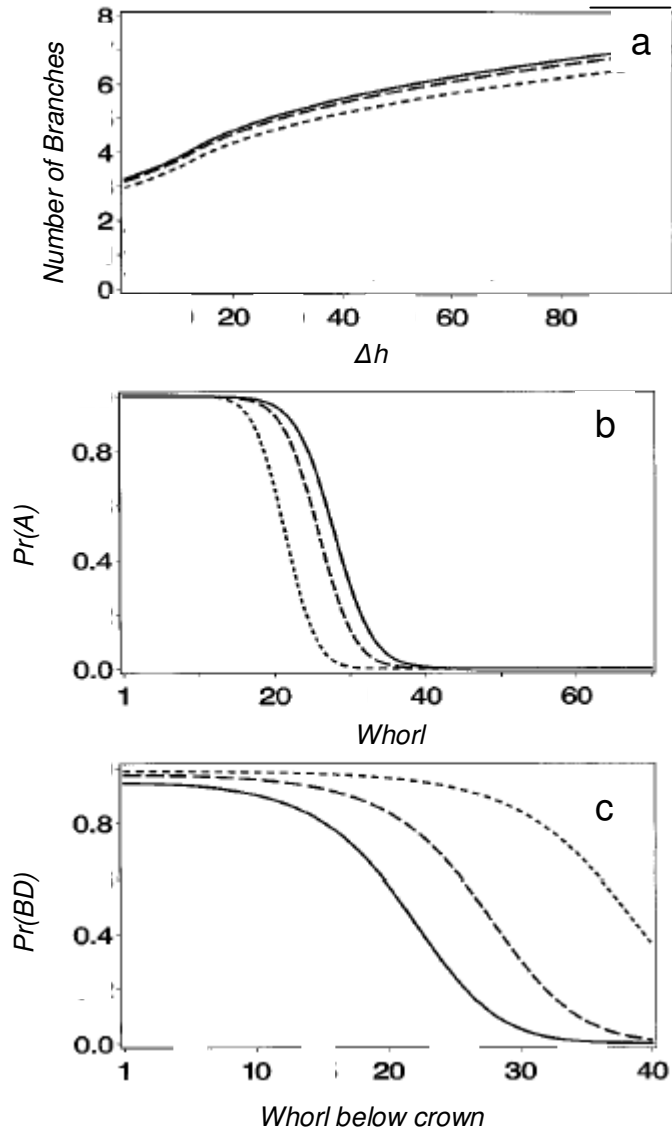


**Figure 2.2.** Simulated branch characteristics for trees of different social status (a) predicted number of branches in a new whorl, (b) probability of a branch to be alive and (c) proportion of the actual number of branches on a whorl to the predicted initial number below the crown, where  $\Delta h$  is the height increment and whorl is the whorl number (Adapted from Mäkinen and Colin 1999).

Development of individual equations for different branch characteristics without considering the hierarchical data structure have continued being reported. Catchpoole et al. (2002) developed individual equations to model height to the lowest live branch, height to the lowest live whorl, height to the lowest dead branch, number of branches per whorl, mean branch diameter, maximum branch diameter and mean branch angle for Caribbean pine (*Pinus caribaea* var. *hondurensis*) in Australia. The authors concluded that despite the effort dedicated to developing static relationships, there is still not enough detail in models of branch characteristics to facilitate linkage to a sawing simulator.

Three different methods were proposed by Mäkinen and Mäkelä (2003) to model branch diameter along the stem for Scots pine. They used a variance component model and applied multivariate models to fit the equations simultaneously. The first method predicted basal area of the largest and smallest live branch in each whorl, assuming that the total number of branches and total basal area for each whorl was known. The diameter of the other branches contained in the whorl are obtained by drawing a random number from a uniform distribution and adjusting their diameter estimates to make the sum of individual branches equal to the total basal area of the whorl. The second method for a given whorl predicted the basal area of the thickest branch and then assigned the basal area for the other branches as a percentage of the thickest branch. The third method predicted in each whorl the basal area for each branch 50 times generating random variation into the random parameters. After each simulation, the predicted basal area of the smallest and largest branches is selected to compute the mean and standard deviation.

The equations of Mäkinen and Mäkelä (2003) were incorporated into a process-based tree model (Mäkelä 1997, Mäkelä et al. 1997). The combined process-based model was called PipeQual (PIPE model as basis for wood QUALity predictions) and it was evaluated to predict the 3D geometry of the stem and its internal knots (Mäkelä and Mäkinen 2003).



Mäkinen et al. (2003a, 2003b) developed generalized linear variance component models for external branch characteristics for Norway spruce and planted silver birch (*Betula pendula* Roth.). The branch characteristics modeled for both tree species were crown ratio, self-pruning ratio (i.e. height of the lowest dead branch divided by the height of the crown base), number of living branches along the stem, total number of branches, diameter of the thickest branch, diameters of the smallest branches and branch angle. For each model, most of the variation was explained using tree-level variables and only slight improvements were observed when including stand-level variables.

### ***Modeling internode length***

The effect of branches on wood quality can be addressed by modeling the internode length. This variable is important, because it determines the volume of clearwood that can be obtained from unpruned logs. At the stand-level, Grace and Carson (1993) developed a model to predict the stand mean internode length for radiata pine plantations in New Zealand. They defined the internode length as the vertical distance between the top of one whorl and the base of the next higher whorl (Figure 2.3). The predictor variables included mean annual rainfall, altitude, latitude and level of genetic improvement.

Woollons et al. (2002) developed a model for the same tree species to predict internode length, number of branches in each branch cluster (whorl) and the size of each branch below the green crown at age 20. They found that including the diameter of the largest branch in the first whorl occurring above 2 m (branch factor BF) improved the predictive capability of the equations. The modeling approach for all variables was based on a sampling distribution approach. Stochastic simulation was applied because of the difficulty in finding adequate relationships among the variables to construct deterministic equations. In this study internode length and the number of branches per whorl were found to be independent of tree size, site index and stand density.

In both the Grace and Carson (1993) and Woollons et al. (2002) the application of the proposed models is intended for plantations close to the rotation age.

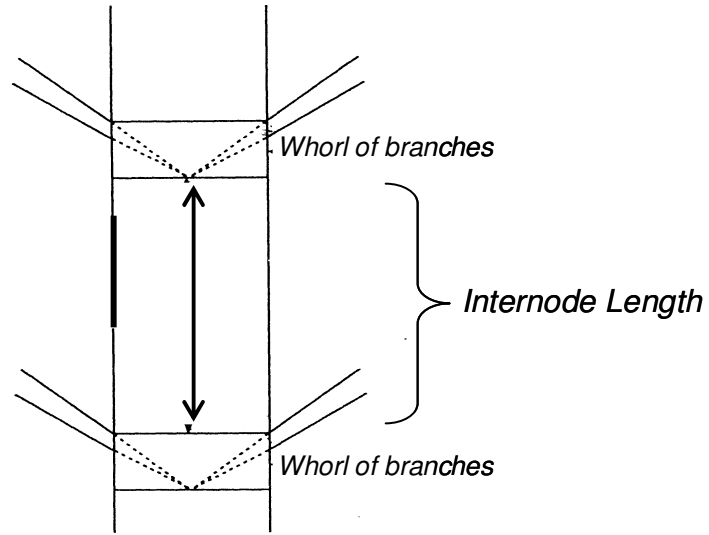


**Figure 2.3.** Internode length (Adapted from Grace and Carson 1993).

### ***Modeling the distribution of branches along and around the stem***

Even though, one of the most important requirements in terms of wood quality is to know the location of branches along and around the stem, very few studies have been reported. Maguire et al. (1994) presented a modeling approach to permit a more detailed description of the location and size of first-order branches along the stem before crown-closure for Douglas-fir trees (4 to 7 year old). They developed a system of individual equations for predicting within each annual shoot the total number of branches, relative frequency of branches, relative branch diameter, and maximum branch diameter (Figure 2.4). Different parametric models were tested to model the relative frequency of branches within an annual shoot, however, none was sufficiently flexible to model the observed distribution. Therefore, the overall empirical distribution was used to estimate the relative frequency of branches (Figure 2.4b). The relative branch diameter (e.g. the ratio of branch diameter to maximum branch diameter within an annual shoot) was modeled using a reverse Weibull cumulative probability function (Figure 2.4c). A segmented polynomial model similar to Colin and Houllier (1991) was used to model maximum branch diameter within the live crown (Figure 2.4d). The model was based on a quadratic-quadratic segmented model and had the following form

$$BD_{\max} = b_0 + b_1 X1 + b_2 DBH X1 + b_3 DBH X2 + b_4 HT X1 + b_5 HT X2 + b_6 DINC_{rel} X3$$

$I = 0$  if  $DINC \leq K$  or  $I = 1$  if  $DINC > K$ .

where  $X1 = DINC$ ,  $X2 = DINC^2$ ,  $X3 = I(K^2 - 2K DINC + DINC^2)$  and  $K = 0.1 CL$ . The location of the join point ( $K$ ) was selected from a set of possible values  $\{0.1, 0.2, \dots, 0.9\}$  comparing their effect on the mean square error.

The location of branches around the stem was not addressed in Maguire et al. (1994). However, they indicated that branches were regularly dispersed around of the stem. Therefore, their model can be expanded by assigning branch azimuths consistent with a regular arrangement.

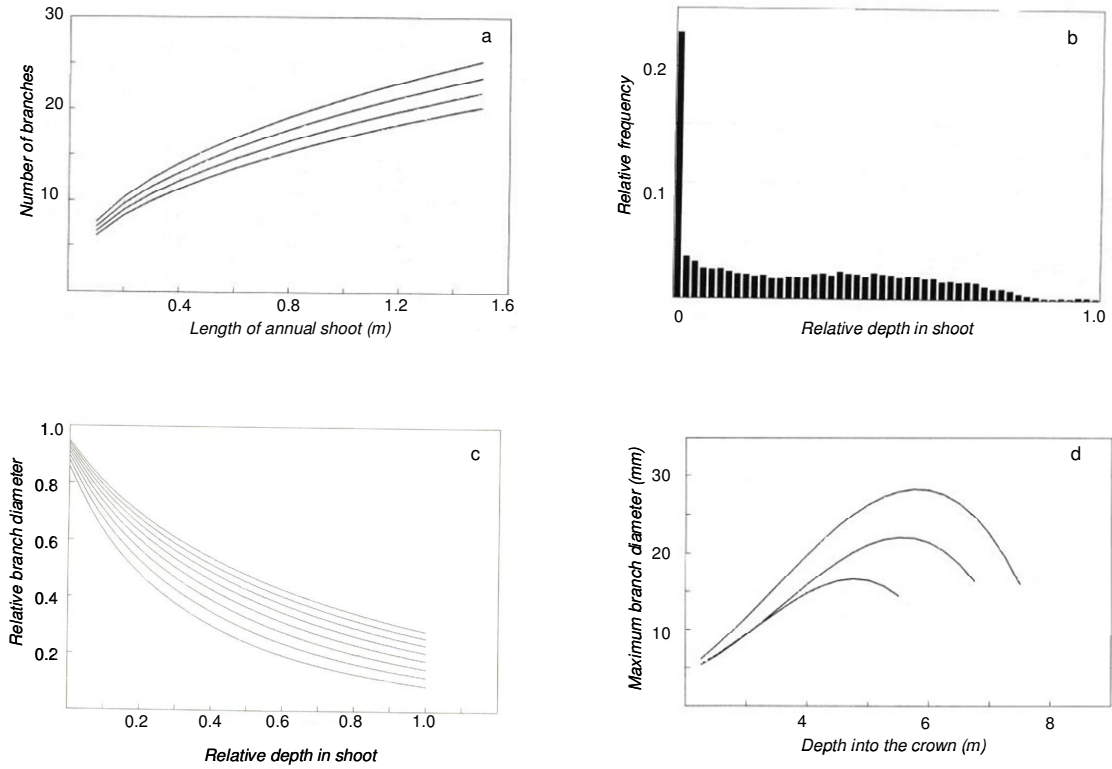


**Figure 2.4.** Simulation of branch characteristics for Douglas-fir trees (a) prediction of number of branches as function of shoot length, (b) empirical relative frequency of branches across relative depth into annual shoot, (c) prediction of relative branch diameter and relative depth into annual shoot, and (d) predicted vertical trend of maximum branch diameter (Adapted from Maguire et al. 1994).

Doruska and Burkhart (1994) modeled the diameter and locational distribution of branches within the crown, both along and around the bole, for loblolly pine (*Pinus taeda* L.) trees from unthinned plantations. The system of equations and algorithms permitted prediction within the live crown of the total number of whorls and branches, location of whorls along the stem, number of branches per whorl, branch diameters, and location of branches around the stem (azimuth). The total number of whorls ( $N_w$ ) and total number of branches ( $N_b$ ) are estimated using a two-equation system

$$N_w = b_0 + b_1 D + b_2 CL$$

$$N_b = b_0 + b_1 N_w$$

where  $D = \text{DBH}$  and  $CL = \text{crown length}$ . The location of the predicted total number of whorls assumed an equidistant yearly growth from crown base to tip and equal number of whorls per year. Afterward, for each growing season, the internode length was assigned according to data reported by Bridgewater et al. (1985).

The number of branches per whorl was predicted using the empirical distribution of the entire data set and assigned randomly to each whorl, constrained by the total number of branches predicted ( $N_b$ ). The diameters for each branch are allocated according to three equations to predict the minimum, maximum, and mean branch diameter per whorl. The mean branch diameter within a whorl ( $\overline{WD}$ ) was predicted as a function of DBH and relative whorl height ( $RWH = H_w/H$ , where  $H_w$  is the height of the whorl), using the following expression

$$\overline{WD} = b_0 + b_1 D + b_2 RWH^2$$

and the minimum and maximum branch diameter using the same equation form:

$$W_i = b_0 + b_1 D + b_2 RWH .$$

Finally, the azimuth of each branch within a whorl is assigned by an algorithm depending on the number of branches.

In this study the branching patterns around the bole were examined using circular statistics. A uniform or regular distribution of branches around the bole on a tree basis was found to be appropriate after statistical analysis using a Rayleigh test (Batschelet 1981). It meant that the branch azimuths were not heavily concentrated around a mean angle on a whole tree basis. However, a strong positive correlation between branch azimuths was found between consecutive whorls with the same number of branches.

### **2.3 Modeling branch development and dynamics**

The lack of longitudinal data from permanent plots has resulted in little work on modeling branch development being conducted. Existing studies of crown dynamics have relied on cross-sectional data. However, research has shown that information on branch growth and crown dynamics can be accurately recovered with destructive sampling of branches (Maguire and Hann 1987, Maguire and Hann 1990, Fujimori 1993). Some of the proposed dissection techniques are presented in Figure 2.5.

Using the dissection technique reported by Fujimori (1993), Mäkinen (1999) studied the dynamics of branch growth, suppression, death, natural pruning and knot formation for Scots pine trees. Using the same data, Mäkinen and Colin (1999) developed equations to model the number of new branches, probability of a branch being alive and the proportion of dead branches in the whorls below the crown base (self-pruning).

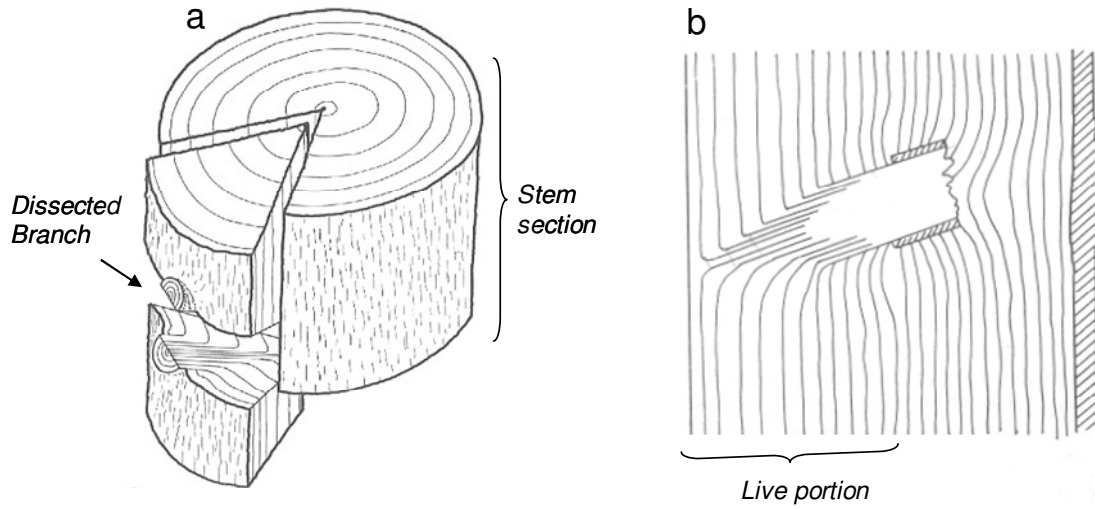


**Figure 2.5.** Dissection techniques proposed by (a) Maguire and Hann (1987) for Douglas-fir and (b) Fujimori (1993) for hinoki cypress (Adapted from Maguire and Hann 1987 and from Fujimori 1993).

Grace et al. (1999) used dissected branch data to model branch development over time for radiata pine plantations in New Zealand. They modeled the occurrence of branch clusters (whorls) within an annual growing season (annual shoot), and the diameter growth of branches at the point of attachment to the tree stem. They attempted, unsuccessfully, to predict branch diameter increment from current branch diameter and branch age. Consequently, they alternatively developed a model to predict branch diameter at any age as a function of branch age and maximum diameter attained by the branch.

The relationship between radial increment of the largest branches and stem growth at the same tree height was studied by Briggs et al. (2002). They proposed a related rates model to determine the relationship between the rate of growth in branches ( $dX/dt$ ) and the stem ( $dY/dt$ ). The relationship between rates of growth was as follows:

$$k = \left( \frac{1}{Y} \frac{dY}{dt} \right) \bigg/ \left( \frac{1}{Y} \frac{dX}{dt} \right).$$

The parameter  $k$  for each sample branch was modeled using a quadratic equation as a function of physiological branch age. Subsequently, the parameters of the quadratic equations were modeled as functions of stand variables. The relationships found were considered promising. However, before initiating the simulation using this technique, the stem diameter and the branch diameter at the end of the first growing season need to be known.

## **2.4 Measurement and modeling of knot shape**

Even though knots are important in determining wood quality, few studies have characterized knot morphology within the tree stem (e.g. Lemieux et al. 1997a). The different approaches to gathering data on knots can be subdivided in non-destructive and destructive techniques. The non-destructive techniques involve the use of ultrasound, electromagnetic and nuclear magnetic resonance. Internal log structure has been studied in *Picea abies* and *Pinus silvestris* using computer tomography (Oja 1997, Moberg 2000,



2001). The use of non-destructive techniques has shown promising advances. However, the application of these techniques requires the use of sophisticated and expensive instruments. Additionally, a semi-automatic data processing is required to identify and classify internal stem characteristics accurately.

On the other hand, destructive dissection techniques have been proposed to extract information on knot geometry. A comprehensive review of the most common destructive dissection techniques is given by Lemieux (1995). The three destructive dissection techniques described in this study are: (i) the flitch method, (ii) the disk method and (iii) the peeling method. These methods are presented in Figure 2.6 for illustration purposes.

The ‘flitch method’ consists of breaking down a log into longitudinal sections or flitches maintaining the same thickness (Figure 2.6a). The angle of the sawing plane with respect to each knot will determine the geometrical shape that will be exposed for measurement. In Figure 2.6a, the knot A is cut parallel to the sawing plane and because the knot is contained in the section no information on knot geometry can be obtained. Contrarily, knot B is cut perpendicular to the sawing plane, thus information on knot geometry can be obtained. Hence, the ‘flitch method’ is not completely suitable to recover geometrical information for all knots.

The ‘disk method’ consists in making transversal cuts throughout the length of the log (Figure 2.6b). The thickness of the cuts can result in some knots being contained in the disk, without the possibility of recovering information. Operationally is very difficult to maintain consistence both in the thicknesses of the disk and the perpendicular position with respect to the log pith. Also, each disk needs to be referenced to an external axis to maintain a common reference among the disks.

In the ‘peeling method’ each log is cut in a continuous veneer with a wide sharp knife (Figure 2.6c). In comparison to the other two methods, no loss of wood is produced because of cutting as opposed to sawing. The application of this method was described by Park (1983) to characterize logs for the optimization of the peeling process.

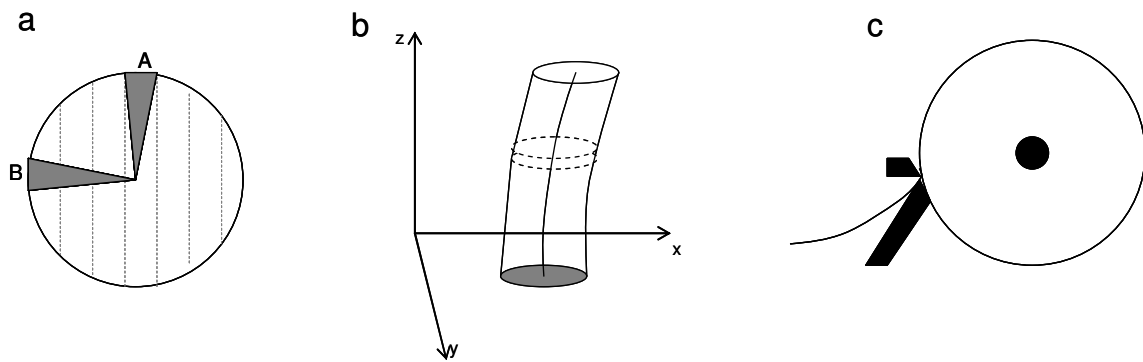


**Figure 2.6.** Dissection techniques used to study knot geometry (a) flicht method, (b) disk method and (c) peeling method.

The veneer obtained represents a tangential-longitudinal (L-T) profile of the log internal morphology (Lemieux et al. 1997b). Thus, each knot is cut at each rotation of the peeler and the complete radial-tangential profile for each knot can be recovered. Some of the shortcomings are the loss of external wood before the log becomes cylindrical during the process. As a result the external knot part can not be characterized as well as the initial part that resides in the residual cylinder. Factors such as the elliptical form of the cross-section of a log and eccentricity of the log pith can produce measurement errors. Even though the application of this method requires adequate facilities and equipment it has been considered as one of the most promising destructive methods to recover information on log shape and internal stem structure (Pinto et al. 2003, 2005).

Another dissection method was proposed by Lemieux et al. (2001) to study the geometry of knots. The method consists in extracting sample knots from a log section and making radial-tangential cuts to expose the knot (Figure 2.7). This method permits the recovery of information on the geometry of selected knots using a band saw, and provides information similar to that of the 'peeling method'.

An accurate mathematical representation of knot shape and structure is important to better understand and evaluate the effect of knots on the quality of sawn timber. In sawing simulation, knots have been represented as 3D entities assuming geometrical shapes. Sawing simulators as SEESAW (García 1987) and SIMQUA (Leban and Duchanois 1990) represent the shape of knots as cones. In AUTOSAW the live portion of a knot is represented by a cone and the dead portion, attached to the end of the cone, is represented by a cylinder (Todoroki 1996). Samson et al. (1996) proposed the only mathematical model able to represent a variety of knot shapes. This model considers three different zones from the stem-pith to the bark (Figure 2.8). The first zone is represented by a nonlinear (cubical) portion, the second zone by a linear portion and the third zone by a half ellipsoid to describe the healing over area after pruning. Despite its high flexibility, the main shortcoming is the large number of parameters required to represent a knot (i.e. 17 parameters). A simplified version of this model has been used to smooth data from dissected knots (Lemieux et al. 1997b).

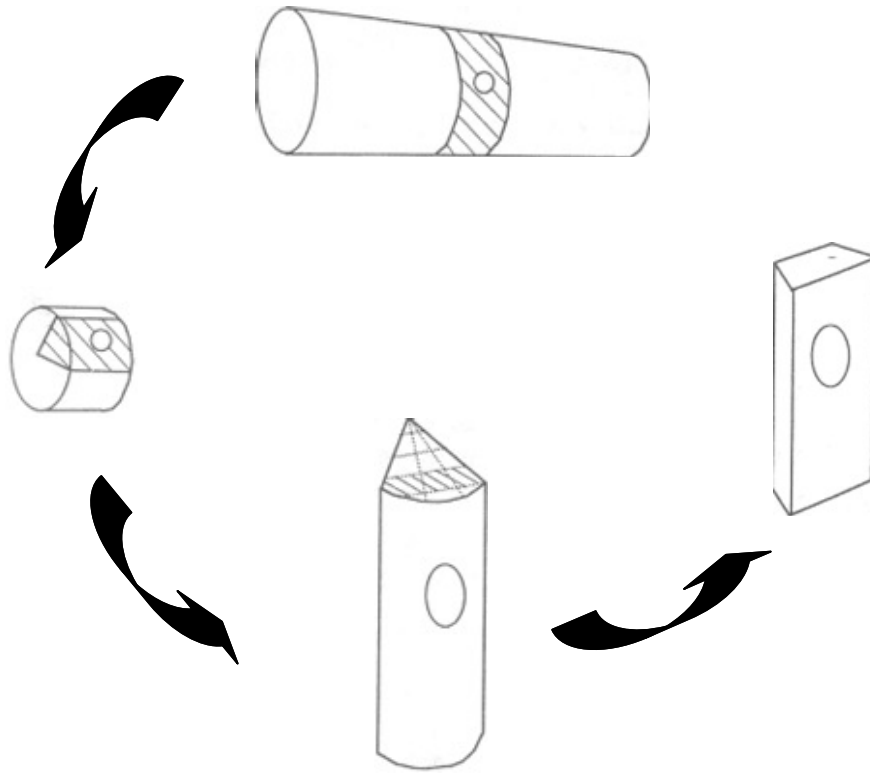


**Figure 2.7.** Dissection technique utilized to study the morphology of knots (Adapted from Lemieux et al. 2001).

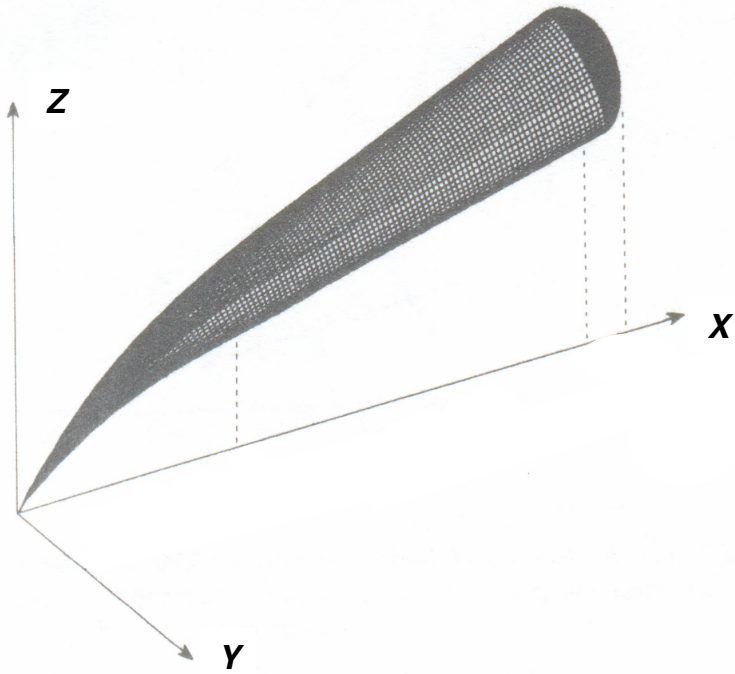


**Figure 2.8.** Representation of knot shape (Adapted from Samson et al. 1996).

## 2.5 Conclusions

Most of the past research on modeling tree branches has concentrated in predicting external branch characteristics within the tree crown. Among the branch characteristics modeled are branch diameter (mean and maximum), branch inclination and branch length. Due to the relationships among branch characteristics, systems of equations have been proposed and parameters estimated using restricted multi-stage least squares. Also, because of the hierarchical structure of the data mixed-effects models have been specified. In general, studies have shown that the vertical trend of branch diameter inside the crown and other branch characteristics can be modeled using only tree-level variables. The inclusion of distance-dependent competition indexes has been found to be not significant or the predictive capability of a model has been not greatly improved. This lack of statistical significance could indicate that the effects of competition are accounted indirectly through tree size. Furthermore, the inclusion of site index as another predictor variable has been inconclusive, where in most cases it has been found to be not significant. Even though models to predict external branch characteristics can be incorporated into a simulation system they can produce inconsistent predictions of branch characteristics over time.

Only one model has been reported for loblolly pine that describes the branch structure along and around the stem. However, it permits the modeling of branches only at one point in time and prediction of external branch characteristics is limited to the crown. Again, the method will probably produce inconsistent predictions over time and it lacks detail for internal stem characteristics in relation to knots.

Models to predict branch development and its dynamics over time are currently lacking for the most important commercial tree species, including loblolly pine. The main reason given is the scarcity of longitudinal measurements of branch characteristics on standing trees. However, for some tree species data similar to what might be obtained by remeasurements over time have been obtained through destructive analysis of sample branches. Different dissection techniques and technological advances have been proposed for measuring internal knots. The study of knot shape has involved using dissection of

branches. Among them, the peeling method and a radial/tangential dissection of knots have been more commonly utilized. On the other hand, a longitudinal/radial dissection of branches permits the recovery of information on branch growth (Fujimori 1993, Grace et al. 1999). Based on morphological characteristics of ring growth, the time a branch was alive can be also determined. Initial tests performed in this study to determine the most convenient dissection technique indicated that a longitudinal/radial dissection can be very difficult to perform when applied in knots (branches) located under the live crown.

Only one model has been proposed to represent accurately the knot shape. However, the great number of parameters required to represent the knots make it difficult to utilize this model in a simulation system. The main utility of a reduced expression of this model has been to smooth knot data. A dynamic simulation system requires maintaining spatial information of the location of branches and internal knots structure along the stem. Thus, a simpler representation is probably required for implementation in a simulation framework.

## **2.6 Literature cited**

- Batschelet, E. 1981. Circular statistics in biology. Academic Press, London.
- Bier, H. 1986. Log quality and the strength and stiffness of structural timber. *N.Z.J. For. Sci.* 16:176-186.
- Borders, B.E. 1989. Systems of equations in forest stand modeling. *For. Sci.* 35:548-556.
- Bridgwater, F.E., C.G. Williams, and R.G. Campbell. 1985. Patterns of leader elongation in loblolly pine families. *For. Sci.* 31:93-944.
- Briggs, D. 1996. Modeling crown development and wood quality. *J. For.* 94(12):24-25.
- Briggs, D., E. Turnblom, O. Høibø, and S. Irmen. 2002. Relationship between branch diameter growth and stem growth in young coastal US Douglas-fir. P. 282-289 *in* Fourth Workshop Connection between silviculture and wood quality through modelling approaches and simulation softwares, Nepveu, G. (ed.). Harrison Hot Spring, B.C., Canada.

- Burk, T.E., N.D. Nelson, and J.G. Isebrands. 1983. Crown architecture of short-rotation, intensively cultured *Populus*.III: a model of first-order branch architecture. *Can. J. For. Res.* 13:1107-1116.
- Catchpoole, K., I. Andrew, M.R. Nester, K. Harding and B. Hogg. 2002. Development of branch models for use in a silvicultural decision support system. P. 406-414 *in* Fourth Workshop Connection between silviculture and wood quality through modelling approaches and simulation softwares, Nepveu, G. (ed.). Harrison Hot Spring, B.C., Canada.
- Cochrane, L.A., and E.D. Ford. 1978. Growth of a sitka spruce plantation: analysis and stochastic description of the development of the branching structure. *Journal of Applied Ecology* 15:227-244.
- Colin, F. and F. Houllier. 1991. Branchiness of Norway spruce in north-eastern France: modeling vertical trends in maximum nodal branch size. *Ann. Sci. For.* 48:679-693.
- Colin, F. and F. Houllier. 1992. Branchiness of Norway spruce in north-eastern France: predicting the main crown characteristics from usual tree measurements. *Ann. For. Sci.* 49:511-538.
- Curtis, R.O. 1982. A simple index of stand density for Douglas-fir. *For. Sci.* 28:92-94.
- DeBell, J.D., and B.L. Gartner. 1997. Stem characteristics on the lower log of 35-year-old western redcedar grown at several spacings. *Western J. Appl. For.* 12:9-15.
- Doruska, P. F. and H. E. Burkhart. 1994. Modeling the diameter and locational distribution of branches within the crowns of loblolly pine trees in unthinned plantations. *Can. J. For. Res.* 24:2362-2376.
- Doruska, P.F., and J.E. Mays. 1998. Crown profile modeling of loblolly pine by nonparametric regression. *For. Sci.* 44:445-453.
- Ford, R., and E.D. Ford. 1990. Structure and basic equations of a simulator for branch growth in the pinaceae. *J. Theor. Biol.* 146:1-13.
- Ford, E.D., A. Avery, and R. Ford. 1990. Simulation of branch growth in the *Pinaceae*: interactions of morphology, phenology, foliage productivity, and the requirement for structural support, on the export of carbon. *J. Theor. Biol.* 146:15-36.
- Fujimori, T. 1993. Dynamics of crown structure and stem growth based on knot analysis of a hinoki cypress. *For. Ecol. Manage.* 56:57-68.



- Garber, S.M., and D.A. Maguire. 2005. Vertical trends in maximum branch diameter in two mixed-species spacing trials in the central Oregon Cascades. *Can. J. For. Res.* 35:295-307.
- García, O. 1987. A visual sawing simulator. Part II: The SEESAW computer program. P. 107-116 *in* Proceedings of the conversion planning conference, Kininmonth J.A. (ed.). Ministry of Forestry, FRI Bulletin No. 128.
- Gilmore, D.W., and R.S. Seymour. 1997. Crown architecture of *Abies balsamea* from four canopy positions. *Tree Physiol.* 17:71-80.
- Grace, J.C., and M.J. Carson. 1993. Prediction of internode length in *Pinus radiata* stands. *N. Z. J. For. Sci.* 23:10-26.
- Grace, J.C., D. Pont, and C.J. Goulding. 1999. Modelling branch development for forest management. *N. Z. J. For. Sci.* 29:391-408.
- Honda, H. 1971. Description of the form of trees by parameters of the tree-like body. *J. Theor. Bio.* 31:331-338.
- Inglis, C.S. and M.R. Cleland. 1982. Predicting final branch size in thinned radiata pine stands. *N.Z. For. Serv. FRI Bull. No 3.* 9p.
- Kershaw, J.A., D.A. Maguire, and D.W. Hann. 1990. Longevity and duration of radial growth in Douglas-fir branches. *Can. J. For. Res.* 20:1690-1695.
- Kozak, A. 1988. A variable-exponent taper equation. *Can. J. For. Res.* 18:1363-1368.
- Kozak, A. 1997. Effects of multicollinearity and autocorrelation on the variable-exponent taper functions. *Can. J. For. Res.* 27:619-629.
- Kurth, W., and D. Lanwert. 1995. Biometrische Grundlage für ein dynamisches Architekturmodell der Fichte (*Picea abies* (L.) Karst.). *Allgemeine Forst- und Jagdzeitung* 166:177-184.
- Lappi, J. 1986. Mixed linear models for analyzing and predicting stem form variation of Scots pine. *Communicationes Instituti Forestalis Fenniae* 134. 69p.
- Leban, J.M., and G. Duchanois. 1990. SIMQUA: un logiciel de simulation de la qualité des bois. *Ann. Sci. For.* 47:483-493.
- Lemieux, H. 1995. Morphological characterization of knots in Norway spruce logs. M.Sc. Thesis, Université Laval. Canada. 110p.

- Lemieux, H., M. Samson, and A. Usenius. 1997a. Shape and distribution of knots in a sample of *Picea abies* logs. *Scand. J. For. Res.* 12:50-56.
- Lemieux, H., A. Usenius, and M. Samson. 1997b. A method for the characterization of knots in logs. *Forest Prod. J.* 47(2):57-62.
- Lemieux, H., M. Beaudoin, and S.Y. Zhang. 2001. Characterization and modeling of knots in black spruce (*Picea mariana*) logs. *Wood and Fiber Science* 33:465-475.
- Maguire, D.A., and D.W. Hann. 1987. A stem dissection technique for dating branch mortality and reconstruction past crown recession. *For. Sci.* 33:858-871.
- Maguire, D.A., D.W. Hann, and J.A. Kershaw, Jr. 1988. Prediction of branch diameter and branch distribution for Douglas-fir in Southwestern Oregon. P.1029-1036 *in* *Forest Growth Modeling and Prediction*, Ek, A.R. , S.R. Shifley and T.E. Burk (eds.). USDA For. Serv. Gen. Tech. Rep. NC-120. 1149p.
- Maguire, D.A., J.A. Kershaw, Jr., and D.W. Hann. 1991. Predicting the effects of silvicultural regime on branch size and crown wood core in Douglas fir. *For. Sci.* 37:1409-1428.
- Maguire, D.A., M. Moeur and W.S. Bennett. 1994. Models for describing basal diameter and vertical distribution of primary branches in young Douglas-fir. *For. Ecol. Manage.* 63:23-55
- Maguire, D.A., S.R. Johnston and J. Cahill. 1999. Predicting branch diameters on second-growth Douglas-fir from tree-level descriptors. *Can. J. For. Res.* 29:1829-1840.
- Mäkelä, A. 1997. A carbon balance model of growth and self-pruning in trees based on structural relationships. *For. Sci.* 43:7-24.
- Mäkelä, A., Pavanninen, and V-P. Ikonen. 1997. An application of process based modeling to the development of branchiness in Scots pine. *Silv. Fenn.* 31:369-380.
- Mäkelä, A., and H. Mäkinen. 2003. Generating 3D sawlogs with a process-based growth model. *For. Ecol. Manage.* 184:337-354.
- Mäkinen, H. 1999. Growth, suppression, death, and self-pruning of branches of scots pine in southern and central Finland. *Can. J. For. Res.* 29:585-594.
- Mäkinen, H. and F. Colin. 1998. Predicting branch angle and branch diameter of scots pine from usual tree measurements and stand structural information. *Can. J. For. Res.* 28:1686-1696.

- Mäkinen, H., and F. Colin. 1999. Predicting the number, death, and self-pruning of branches in scots pine. *Can. J. For. Res.* 29:1225-1236.
- Mäkinen, H., and A. Mäkelä. 2003. Predicting basal area of scots pine branches. *For. Ecol. Manage.* 179:351-362.
- Mäkinen, H., R. Ojansuu, P. Sairanen and H. Yli-Kojola. 2003a. Predicting branch characteristics of Norway spruce (*Picea abies* (L.) Karst.) from simple stand and tree measurements. *Forestry* 76:525-546.
- Mäkinen, H., R. Ojansuu and P. Niemistö. 2003b. Predicting external branch characteristics of planted silver birch (*Betula pendula* Roth.) on the basis of routine stand and tree measurements. *For. Sci.* 49:301-317.
- Max, T.A., and H.E. Burkhart. 1976. Segmented polynomial regression applied to taper equations. *For. Sci.* 22:283-289.
- Meredieu, C., F. Colin, and J-C. Hervé. 1998. Modeling branchiness of Corsica pine with mixed-effect models (*Pinus nigra* Arnold ssp. *Laricio* (Poiret) Maire). *Ann. For. Sci.* 55:359-374.
- Moberg, L. 2000. Models of internal knot diameter for *Pinus sylvestris*. *Scand. J. For. Res.* 15:177-187.
- Moberg, L. 2001. Models of internal knot properties for *Picea abies*. *For. Ecol. Manage.* 147:123-138.
- Oja, J. 1997. A comparison between three different methods of measuring knot parameters in *Picea abies*. *Scand. J. For. Res.* 12:311-315.
- Pinto, I., Pereira A., and A. Usenius. 2003. Analysis of log shape and internal knots in twenty Maritime pine (*Pinus pinaster* Ait.) stems based on visual scanning and computer aided reconstruction. *Ann. For. Sci.* 60:137-144.
- Pinto, I., A. Usenius, T. Song, and H. Pereira. 2005. Sawing simulation of maritime pine (*Pinus pinaster* Ait.) stems for production of heartwood-containing components. *Forest Prod. J.* 55(4):88-96.
- Pukkala, T., J. Karsikko, and T. Kolström. 1992. A spatial model for the diameter of the thickest branch of Scot pine. *Silv. Fenn.* 26:219-230.

- Remphrey, W.R., and G.R. Powell. 1984. Crown architecture of *Larix laricina* saplings: quantitative analysis and modelling of (non-sylleptic) order 1 branching in relation to development of the main stem. *Can. J. Bot.* 62:1904-1915.
- Roeh, R. L., and D. A. Maguire. 1997. Crown profile models based on branch attributes in Coastal Douglas-fir. *For. Ecol. Manage.* 96:77-100.
- Samson, M., I. Bindzi and L.M. Kamoso. 1996. Représentation mathématique des noeuds dans le tronc des arbres. *Can. J. For. Res.* 26:159-165.
- Schmidt, M. 2001. Prognosemodelle für ausgewählte Holzqualitätsmerkmale wichtiger Baumarten. Dissertation, University of Göttingen, Germany. 302p.
- Schöpf, J. 1953. Untersuchungen über Astbildung und Astreinigung der Selber Kiefer. *Forstwiss. Centralbl.* 73:275-290.
- Searle, S.R., G. Casella, and C.E. Mc Gulloch. 1992. Variance components. Wiley, New York.
- Todoroki, C.L. 1996. Developments of the sawing simulation software AUTOSAW: linking wood properties, sawing, and lumber end-use. P. 241-247 in *Second Workshop Connection between silviculture and wood quality through modelling approaches and simulation softwares*, Nepveu, G. (ed.). Berg-en-Dal, South Africa.
- Turnblom, E., and G. Becker. 2002. Cross-validation of alternative branch models for Douglas-fir using geographically disparate data sources from Europe and the Northwest USA. P. 399-405 in *Fourth Workshop Connection between silviculture and wood quality through modelling approaches and simulation softwares*, Nepveu, G. (ed.). Harrison Hot Spring, B.C., Canada.
- Vestøl, G., O.A. Høibø, D.E. Molteberg and H.J. Sundby. 1997. Modelling knottiness and knot characteristics of Norway spruce (*Picea abies* (L.) Karst.) – differences in the distribution of sound and dead knots between suppressed and dominant trees. P. 40-44 in *Second Workshop Connection between silviculture and wood quality through modelling approaches and simulation softwares*, Nepveu, G. (ed.). Berg-en-Dal, South Africa.
- Whiteside, I. 1982. Predicting radiata pine gross sawlog values and timber grades from log parameters. New Zealand Forest Service, Forest Research Institute FRI Bulletin No 4. 33p.

- Wobst, J. 1995. Auswirkungen von Standortsgüte und Durchforstungsstrategien auf verwertungsrelevante Holzeigenschaften von Douglasie. Dissertation, University of Göttingen, Germany. 210p.
- Woollons, R.C., A. Haywood, and D.C. McNickle. 2002. Modeling internode length and branch characteristics for *Pinus radiata* in New Zealand. *For. Ecol. Manage.* 160:243-261.

## Chapter 3

### A Simple Model to Represent Knots in Simulated Loblolly pine Trees

---

**ABSTRACT.** The shape and structure of branches attached internally to the stem (knots) for loblolly pine (*Pinus taeda* L.) trees were modeled. Data on knot shape were obtained from the dissection of branches taken from 34 sample trees (22 years old) growing under ten different initial spacings. A total of 341 branches located below the live crown were dissected in the radial/tangential (R/T) plane. Afterwards, a procedure was implemented to reconstruct the branch diameter perpendicular to the branch pith. This information was used to develop a model for representing knot shape, which assumed that the live portion of a knot can be modeled by a one-parameter equation and the dead portion by assuming a cylindrical shape. To study the variability in shape of individual knots (live portion), the model was fitted to 218 branch profiles using nonlinear mixed-effects modeling techniques. A graphical analysis indicated that the random-effects parameter was related to branch diameter. Thus, branch diameter was included as a predictor variable in order to reduce between-individual variability in knot shape. Reconstructed knots with smaller diameters were more cylindrical; those with larger diameters presented a more parabolic or conical shapes. Analytical expressions were derived for estimating the volume of knots (live/dead portions) for three types of branch conditions on simulated trees: (i) live branches, (ii) non-occluded dead branches and (iii) occluded dead branches. The knot model assumes a substantial simplification of branch morphology, but should be useful for representing knots as 3D entities in individual-tree growth and yield simulation systems.

---

**Keywords.** wood quality, tree-level growth model, knot shape, loblolly pine.

### 3.1 Introduction

A knot represents the internal attachment of first-order branches to the tree stem (Lemieux et al 2001). Knot frequency, size and location along and around the stem are determined by both the crown and branch dynamics. Silvicultural decisions such as initial planting density and spacing (Clark et al. 1994, Sharma et al. 2002, Amateis et al. 2004), thinning (Baldwin et al. 2000), pruning (Clark et al. 2004) and fertilization (Yu et al. 2003) have important effects on the size of branches and thus on knot dimensions. Clark and McAlister (1998) developed a new tree grading system for southern pines based on the number and size of branches in the lower part of the bole. They found that the inclusion of branch variables improved the prediction in expected lumber grade yield. Furthermore, size and location of knots are important characteristics for determining grade of solid wood products such as dimension lumber (Haygreen and Bowyer 1996).

From a wood quality perspective knots are considered defects that reduce the value of the raw material, because they decrease the strength and stiffness of wood intended for structural uses (Whiteside et al. 1977, Briggs 1996, Gartner 2005). Their effect on mechanical properties is due to the interruption of continuity and change in the direction of wood fibers (Grace et al. 1999). Despite their importance in determining wood quality, first-order branch development and knots have not been thoroughly studied in loblolly pine (*Pinus taeda* L.). The study of branch development and knot formation can permit construction of predictive models for these variables and enhance the capability of individual-tree growth and yield simulation systems.

In a simulation framework knots need to be represented as 3D-entities. Generally, external information of branches such as diameter, azimuth, location in a log, and angle of inclination are used to project knots internally assuming a certain geometric shape (e.g. Barbour et al. 2003). Sawing simulators as SEESAW (García 1987) and SIMQUA (Leban and Duchanois 1990) represent the shape of knots contained in logs as cones. In contrast, in AUTOSAW the live portion of a knot is represented with a cone and the dead portion, attached to the end of the cone, is represented with a cylinder (Todoroki 1996). An analytical system of equations to describe the geometry of a large variety of knot

shapes was reported by Samson et al. (1996). However, despite the flexibility of this system, the complexity and amount of parameters (i.e. 17 parameters) required to represent knots makes the implementation of this model unfeasible for most practical applications. Lemieux et al. (1997) reported on a reduced expression of this model that was used to smooth knot data for Norway spruce (*Picea abies* (L.) Karst).

The inclusion of knots in individual-tree growth and yield simulation requires a simpler representation of knots and the capability of maintaining spatial information (3D) of their internal location along the stem. This research presents the development of a model for representing the internal knot shape and structure, which is part of a dynamic branch component model currently linked to PTAEDA3.1 (Burkhart et al. 2004). The specific objectives of this research were to (i) recover information on knot shape using a destructive analysis technique, (ii) characterize the shape and structure (live/dead portion) of knots using a mathematical model, and (iii) from the developed knot model derive analytical expressions to predict the volume of individual knots.

## **3.2 Data**

### **3.2.1 Loblolly pine spacing trial**

In 1983, spacing trials were established at four locations by the ‘Loblolly Pine Growth and Yield Research Cooperative’ on site prepared-areas in Virginia and North Carolina. Two of these trials were situated in the Atlantic Coastal Plain and two in the Appalachian Piedmont region. The experimental design selected for this spacing study was the nonsystematic design presented by Lin and Morse (1975). The study consists of three replications at each location. In each replication spacing levels of 4 ft (1.2 m), 6 ft (1.8 m), 8 ft (2.4 m) and 12 ft (3.6 m) were assigned randomly both in rows and columns. Each row and column was composed for seven measurement trees. Thus, the intersection of rows and columns defined a plot with 49 measurement trees. The result was a factorial arrangement of 16 treatments with an equal number of trees per plot, but different plot sizes and shapes (see Sharma et al. 2002). In addition, each plot was surrounded by three



rows of guard trees. More details on the experimental design used in this long-term study can be found in Amateis et al. (1988).

Growing stock planted at each location was genetically improved 1-0 loblolly pine seedlings from a single nursery. During the first three years after planting, both herbaceous and woody competing vegetation was controlled. From establishment to age 5 the diameter at groundline was measured annually. Beginning at age 5 the diameter at breast height (dbh) was measured annually. Through age 10, total tree height, height to live crown, and crown width were measured annually for all trees. Measures of crown width were carried out until age 12. Categorical tree condition of each individual tree was also recorded. After age 10, total tree height and height to live crown were measured bi-annually, while dbh and tree condition were measured annually.

### **3.2.2 Collection of branch data**

Data for this research were obtained from the loblolly pine spacing study located near Appomattox, Virginia (Piedmont region). During the dormant season of 2004-2005, at stand age 22 years old, 34 trees were selected for comprehensive measurements of whorl characteristics and sampling of whorl sections (Table 3.1). Trees with a single stem and no record of visible broken top were selected. The main goal was to collect data to model the morphology of knots and the dynamics of first-order branches. Among the branch characteristics of interest were number of branches per whorl, branch orientation around the stem (azimuth), angle of insertion with respect to the stem pith (inclination) and diameter growth. Additional information on whorl number and location within growing seasons was available from field measurements and past measurements on crown recession. Trees were selected from ten different initial spacings (Table 3.1).

Before each tree was felled, dbh outside bark at 4.5 ft (1.37 m) was measured using a caliper and a vertical line on the within row side of the stem was marked to an approximate height of 6.5 ft (2 m). Once the tree was on the ground, this line was extended along the length of the stem. This line served as a reference (azimuth zero degree) for determining the orientation of the sampled whorl sections. For each sample

tree the stump height (cm) and distance from stump height to tree tip (m) were measured. For each visible whorl the following variables were measured: (i) height above ground (m), (ii) diameter outside bark (cm), (iii) status, and (iv) number of visible branches or branch stubs in each whorl. The status of each whorl was visually categorized as: live, sound, decayed or knot. After that, a number of whorl sections was chosen from each sample tree for subsequent laboratory dissection (Table 3.1). Each whorl section was labeled for identification and marked on its bottom surface with the position of the reference line. A total of 217 whorl sections was collected in the field from the sample trees.

### **3.3 Methods**

#### **3.3.1 Dissection and measurement of knots**

A dissection technique similar to that reported by Lemieux et al. (2001) was used in this study to collect information on knot shape. Before dissection each whorl was dried, debarked and when necessary trimmed to fit on the band saw. After that, the sample whorl preparation procedure included: (i) identifying and labeling each visible branch proceeding clockwise from the reference line, (ii) marking the largest branch and possibly a second branch on the opposite side of the stem, and (iii) marking the top of the whorl section with the horizontal direction (azimuth) from the pith to bark of each branch identified in (i). From the 217 whorl sections only 198 whorl sections were suitable for dissection, because some sample sections could not be identify or were missing. Only one branch was selected from 42 whorl sections and two branches from 156 whorl sections, for a total of 354 dissected knots. In addition, a disk was cut from the top and used to determine branch azimuth with a protractor and ring width to the nearest 0.002 mm in the direction of branches selected for dissection. Ring width was measured using Velmex<sup>TM</sup> tree ring measurement system. Only 341 knots proved suitable for measurement of ring width, providing the final sample size for this study.

**Table 3.1.** Location of sampled whorl sections along the stem for the selected trees, where DBH is diameter at breast height and H is total tree height.

| Sample Tree | Spacing (ft x ft) | Tree            | DBH (inches) | H (feet) | Stem height (feet) of sampled whorls |       |       |       |       |       |       |       |  |
|-------------|-------------------|-----------------|--------------|----------|--------------------------------------|-------|-------|-------|-------|-------|-------|-------|--|
|             |                   |                 |              |          | 1                                    | 2     | 3     | 4     | 5     | 6     | 7     | 8     |  |
| 1           | 4 x 4             | 27              | 4.2          | 46.9     | 4.9†                                 | 10.8  | 13.5  | 20.0  | 24.3  |       |       |       |  |
| 2           |                   | 29              | 7.5          | 61.7     | 3.4‡                                 | 7.5   | 14.8  | 18.4  | 23.5  | 31.0† |       |       |  |
| 3           |                   | 39              | 5.3          | 52.8     | 3.9†                                 | 8.7†  | 9.4†  | 10.2† | 19.2  | 20.7  | 23.1  | 27.2  |  |
| 4           |                   | 43              | 4.8          | 53.3     | 8.7                                  | 12.0  | 17.9  | 24.8  | 25.4  | 31.3  |       |       |  |
| 5           | 4 x 6             | 33              | 5.6          | 61.7     | 2.3†                                 | 8.0   | 8.9   | 10.2† | 17.9  | 21.0  | 21.7  | 23.1  |  |
| 6           |                   | 41              | 7.5          | 61.7     | 9.2                                  | 16.2  | 17.1‡ | 26.4  | 27.2  | 35.6  | 36.4  |       |  |
| 7           |                   | 42              | 4.9          | 56.4     | 5.9                                  | 8.2   | 9.0   | 9.5   | 22.5  | 29.7  | 30.7  |       |  |
| 8           | 4 x 8             | 14              | 6.3          | 59.1     | 4.6‡                                 | 12.5  | 21.0  | 22.3  | 24.0  | 25.9  |       |       |  |
| 9           |                   | 32              | 7.8          | 63.6     | 2.3                                  | 8.7   | 16.1  | 20.9  | 22.1  | 24.0  | 30.8  |       |  |
| 10          | 4 x 12            | 22              | 7.0          | 62.0     | 3.4                                  | 8.2   | 9.4   | 10.5  | 11.3† | 26.6  | 27.9† | 28.9  |  |
| 11          |                   | 36              | 10.0         | 63.6     | 4.4†                                 | 5.1†  | 19.7  | 20.7‡ | 25.6  | 26.4  | 36.7‡ | 59.1  |  |
| 12          |                   | 39              | 4.8          | 47.9     | 6.4                                  | 11.8  | 18.0  | 18.7  | 26.6  | 32.6  |       |       |  |
| 13          | 6 x 8             | 19              | 9.7          | 61.7     | 12.8                                 | 18.6  | 23.6  | 39.7  |       |       |       |       |  |
| 14          |                   | 49              | 6.3          | 60.1     | 5.3                                  | 12.9  | 22.6  | 31.4  |       |       |       |       |  |
| 15          | 8 x 4             | 2               | 6.3          | 62.3     | 3.3‡                                 | 9.5†  | 11.3  | 13.1† | 19.2  | 28.9  | 31.8  |       |  |
| 16          |                   | 14              | 6.2          | 65.6     | 4.3†                                 | 11.2† | 12.8† | 19.4  | 21.7† | 23.3† | 32.5  | 36.7  |  |
| 17          |                   | 17              | 7.9          | 67.6     | 3.0                                  | 11.5† | 13.8† | 14.9† | 20.8  | 23.1† | 25.1† | 35.1  |  |
| 18          | 8 x 6             | 9               | 8.8          | 66.3     | 8.2                                  | 14.1† | 24.6  | 33.5  | 42.0  | 43.0  |       |       |  |
| 19          |                   | 40              | 6.2          | 63.3     | 1.8†                                 | 3.4‡  | 9.8†  | 18.9  | 26.6  | 27.6  | 34.8  |       |  |
| 20          |                   | 41              | 4.5          | 51.5     | 3.5                                  | 6.6†  | 10.7  | 17.4  | 24.0  | 29.4  | 33.6† |       |  |
| 21          | 8 x 8             | 5               | 10.1         | 68.6     | 7.5†                                 | 17.1  | 18.4  | 27.7  | 28.9  | 31.7† |       |       |  |
| 22          |                   | 19              | 6.9          | 60.4     | 6.1                                  | 10.2  | 16.1  | 18.2  | 20.2† | 30.3  | 33.8  | 35.4  |  |
| 23          |                   | 25              | 7.0          | 60.7     | 5.2                                  | 7.7‡  | 8.4‡  | 9.5‡  | 23.8‡ | 24.4† | 26.2  |       |  |
| 24          | 8 x 12            | 22              | 5.5          | 52.8     | 4.6                                  | 9.5   | 18.7  | 22.6  | 24.0  | 25.8† | 26.6  | 30.8† |  |
| 25          |                   | 34              | 7.0          | 50.5     | 4.0                                  | 9.4   | 18.5  | 20.5  | 22.5  | 23.6  | 30.7  |       |  |
| 26          |                   | 46              | 10.4         | 66.6     | 9.2                                  | 14.1  | 21.7  | 30.7  | 32.5  | 34.1  |       |       |  |
| 27          | 12 x 6            | 20 <sup>a</sup> | 10.4         | 66.8     | 4.1‡                                 | 10.3‡ | 12.3† | 13.3‡ | 21.5  | 29.4  |       |       |  |
| 28          |                   | 29              | 9.8          | 61.0     | 6.1                                  | 11.8  | 23.8  | 25.3  | 26.6  | 40.0  |       |       |  |
| 29          |                   | 36              | 9.8          | 64.6     | 3.4†                                 | 4.3   | 5.9   | 13.1  | 27.2  | 36.4  | 40.8† |       |  |
| 30          | 12 x 8            | 40              | 7.1          | 59.8     | 7.7                                  | 13.7  | 25.3  | 30.4  |       |       |       |       |  |
| 31          |                   | 48              | 10.0         | 68.2     | 3.6‡                                 | 12.5  | 19.5  | 26.4  | 29.7  |       |       |       |  |
| 32          | 12 x 12           | 1 <sup>a</sup>  | 11.8         | 66.9     | 3.6†                                 | 10.5† | 19.7  | 26.2  | 38.1  |       |       |       |  |
| 33          |                   | 18              | 8.1          | 57.4     | 8.4†                                 | 9.5   | 19.0  | 28.5† | 35.9‡ |       |       |       |  |
| 34          |                   | 20              | 11.7         | 67.6     | 6.6‡                                 | 14.3‡ | 26.9  | 35.8‡ |       |       |       |       |  |

<sup>a</sup> Trees from replicate two, all others sampled from replicate one

† Whorl samples with only one branch dissected

‡ whorl samples not dissected.

The sequence of cuts performed on each sample branch is presented in Figure 3.1. The distance between faces of consecutive slices from bark to pith was approximately 5 mm with 3mm thicknesses and 2 mm of kerf. In each slice the distance from the bottom of the whorl section to the top, pith and bottom the knot was measured (vertical direction). Using the pith of the branch as a reference another diameter measurement of the knot was made in the horizontal direction.

### 3.3.2 Reconstruction of knot profiles

The dissection procedure allowed measurement of knot diameters in the radial/tangential (R/T) plane. However, these measurements were not perpendicular to the main branch axis. A procedure was implemented to reconstruct the “true” branch diameters at a given branch age. It was necessary to determine the number of years a branch was alive. The height of the whorl was used to determine the tree age when the whorl was created. Data on crown recession was used to estimate the number of years a branch was alive. This information was used in conjunction to the ring width measurements to estimate the stem diameters during the period a branch was alive. Given this information the radial measurements of dissected branches (bark to pith) was referenced to actual stem radii. In Figure 3.2a, line **B** represents the radius of the stem and line **A** represents the radius of the stem at the estimated time of branch death. For this example, the branch was determined to be alive for a period of 10 years given the crown recession data. Correspondingly, line **A** denotes the radial extent of the first 10 ring measured from the pith. The measurements taken on each knot were smoothed by fitting a growth curve to the diameter measurements and a linear regression curve to the branch pith (Figure 3.3). The growth curve was a modified Weibull equation (Yang et al. 1978),

$$y = \alpha(1 - \exp(-\beta x^\gamma)), \quad (3.1)$$

where  $y$  is the measured branch diameter parallel to the stem pith in mm,  $x$  is the knot length in mm and  $\alpha$ ,  $\beta$  and  $\gamma$  are estimated parameters. We assumed  $\gamma=1$  in order to reduce the number of estimated parameters (exponential equation).

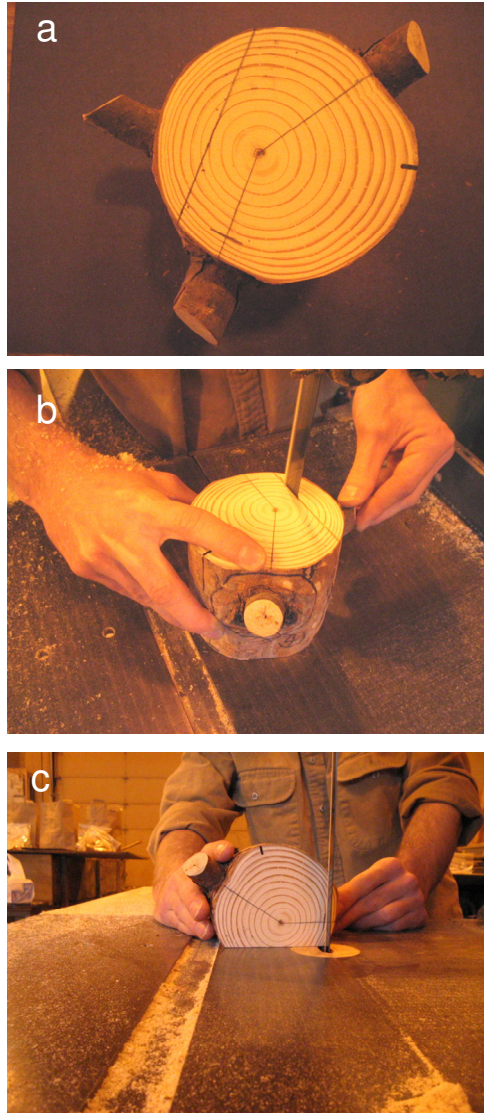


**Figure 3.1.** Procedure used for dissecting branches: (a) identification of target branches, (b) tangential cut for consistent positioning of the sample on the band saw and (c) sawing branch into approximately 3 mm slices parallel to stem pith.

To recover information on the live portion of a knot, the growth curve was fit only to points located to the left of line **A** (Figure 3.3a). Only branch samples with a minimum of five points to the left of line **A** were considered as adequate for this curve fitting and subsequent analyses. A total of 233 knot samples fulfilled this condition. Of the 233 samples, 15 did not converge when fitting the exponential function and were not used in subsequent analysis.

Fitting a linear regression equation to branch pith points provided information on the inclination angle of branches with respect to the stem pith (Figure 3.3b). Because this procedure assumed that the angle of inclination of branches is constant over time, a statistical analysis was applied to adequately test this observation. The statistical analysis involved fitting a quadratic model and testing for the significance of the quadratic term.

The growth curve permitted interpolation of the branch diameters in the R/T plane (parallel to the stem pith) for each age (Figure 3.2b). The reconstruction permitted recovery of increasing diameter with branch age. However, it assumed that the branch pith passed through the center of the branch. Based on the smoothed branch profile and location of interpolated points, the branch diameter for a given age perpendicular to branch pith was derived (Figure 3.2c). For each age, the calculation consisted of fixing the top point and passing a perpendicular line through the branch pith. Then, the intersection of this line with the bottom line of the smoothed branch profile defined the lower part of the branch for a given age. These reconstructed branch profiles were used later as basic information for modeling knot shape.

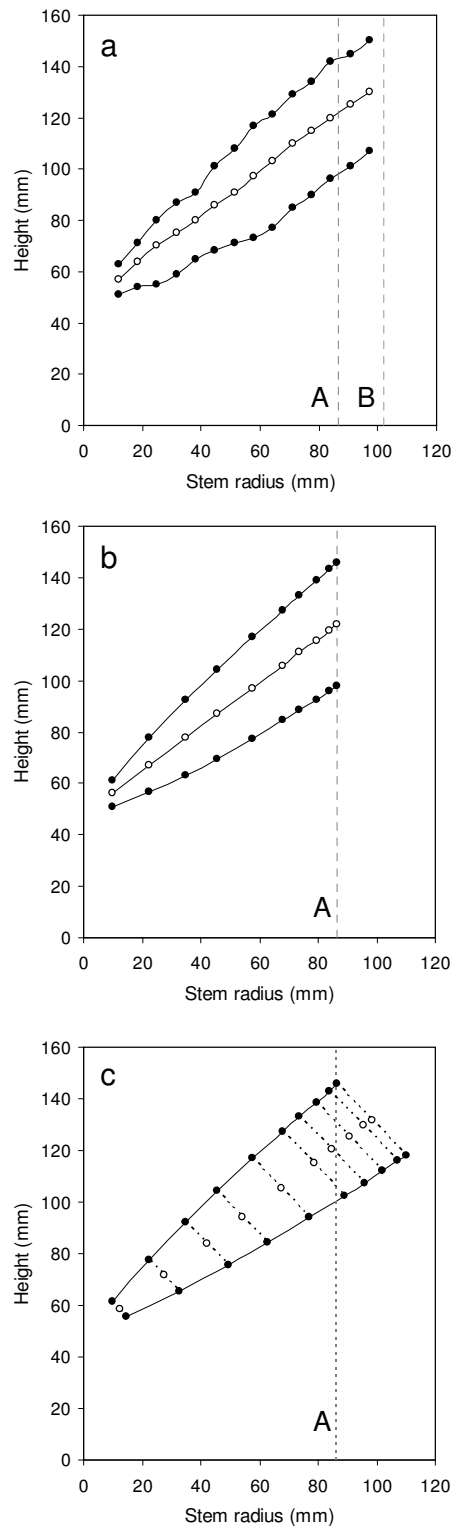


**Figure 3.2.** Reconstruction of knot profiles (a) measured branch profile, (b) smoothed branch profile with interpolated branch diameters at a given branch age in the R/T plane and (c) smoothed branch profile with branch diameters perpendicular to branch pith.

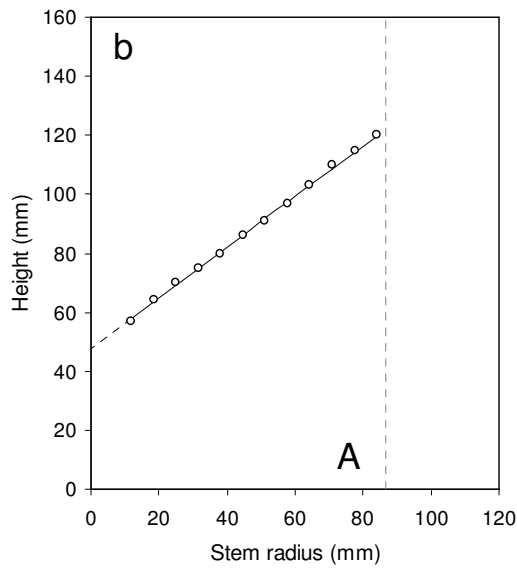
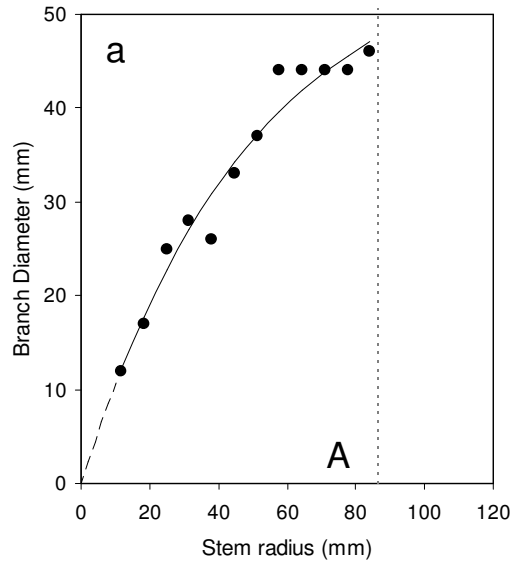


**Figure 3.3.** Smoothing of branch measurements (a) fitting a growth curve to the diameter measurements of a dissected branch, and (b) linear regression through the branch pith.



### 3.3.3 Model development

Past research modeled knot geometry by projecting internal branches as cones (García 1987, Leban and Duchanois 1990) or assuming the live portion was a cone and the dead portion a cylinder (Todoroki 1996). Here, we considered that the live portion of a knot can be modeled with a simple mathematical equation and the dead portion assuming a cylindrical shape. An additional assumption was that knots (not external branches) produced in fast-growing plantations have an insignificant curvature e.g constant inclination from pith to bark. A simple equation to model the live portion of a knot is (e.g. Husch et al. 2003)

$$\frac{r_{(l)}^2}{R^2} = \kappa \left( \frac{l}{L} \right)^\beta \quad 0 \leq l \leq L, \quad (3.2)$$

where  $r_{(l)}$  is the radius (mm) of the live portion of a knot at length  $l$  (mm),  $R$  is the maximum radius (mm) of the live portion of a knot,  $L$  is the total length (mm) of the live portion of a knot,  $\kappa$  is the taper parameter and  $\beta$  is the shape parameter. If  $\beta=1, 2$  or  $3$  the geometrical shape generated by equation (3.2) is a paraboloid, cone, or neiloid, respectively. The model of the live portion of a knot meets two conditions:  $r_{(l)} = 0$  when  $l=0$  and  $r(l)=R$  when  $l=L$ . The first condition is imposed by the model and the second condition can be met by making  $\kappa = 1$ . Therefore, the final model can be expressed as

$$r_{(l)}^2 = R^2 \left( \frac{l}{L} \right)^\beta \quad 0 \leq l \leq L. \quad (3.3)$$

Thus, knowing the total length of the live portion of a knot ( $L$ ) and its maximum radius ( $R$ ) it is possible to estimate the branch radius  $r_{(l)}$  at any point inside the stem. Additionally, the volume of this portion of a knot can be estimated by applying integral calculus

$$V = \pi R^2 \int_0^L \left(\frac{l}{L}\right)^\beta dl. \quad (3.4)$$

It should be noted that the shape of the live part of a knot is determined by only one parameter ( $\beta$ ), and the equation is highly tractable mathematically. A similar formulation (equation 3.2) has been adopted when modeling stem form profiles (e.g. Kozak 1988).

### 3.3.4 Volume estimate for branches internally attached to the stem

A practical implementation of a knot model required derivation of a series of expressions to estimate the volume of branches attached internally to the stem (knots). The calculation of volume for the live and dead portions of any given knot was also considered. The following sections develop volume estimates for three types of branch conditions: (i) live branches, (ii) non-occluded dead branches and (iii) occluded dead branches (Figure 3.4).

#### *Knot volume for a live branch*

Determination of the spatial location of a live knot and its dimensions (diameter and length) required the coordinates of the branch origin  $O = (X_O, Y_O, Z_O)$ , branch inclination ( $\alpha$ , vertical angle in degrees with respect to stem pith), branch azimuth ( $\theta$ , horizontal angle in degrees), branch diameter ( $2R = |\overline{SP}|$ , Figure 3.4a) and stem radius  $r$  at the point where the branch pith arises  $M = (X_M, Y_M, Z_M)$ . Branches from the same whorl were assumed to have the same origin  $O$ . The origin was located in the center of the stem pith at a given height ( $Z_O$ ) above the ground, so the values for  $X_O$  and  $Y_O$  were equal to zero e.g.  $O = (0, 0, Z_O)$ .

Internal knot length was the Euclidian distance  $|\overline{OM}|$  between the point  $(0,0,Z_O)$  and the point  $M$  where the branch pith arises  $(X_M, Y_M, Z_M)$ . The coordinates for point  $M$  and subsequent knot length were calculated using the branch inclination ( $\alpha$ ), branch azimuth ( $\theta$ ) and the stem radius  $r$  at the height where a branch arises by using a taper equation. Thus, the coordinates where the branch pith arises from the stem were determined from the following relationships:

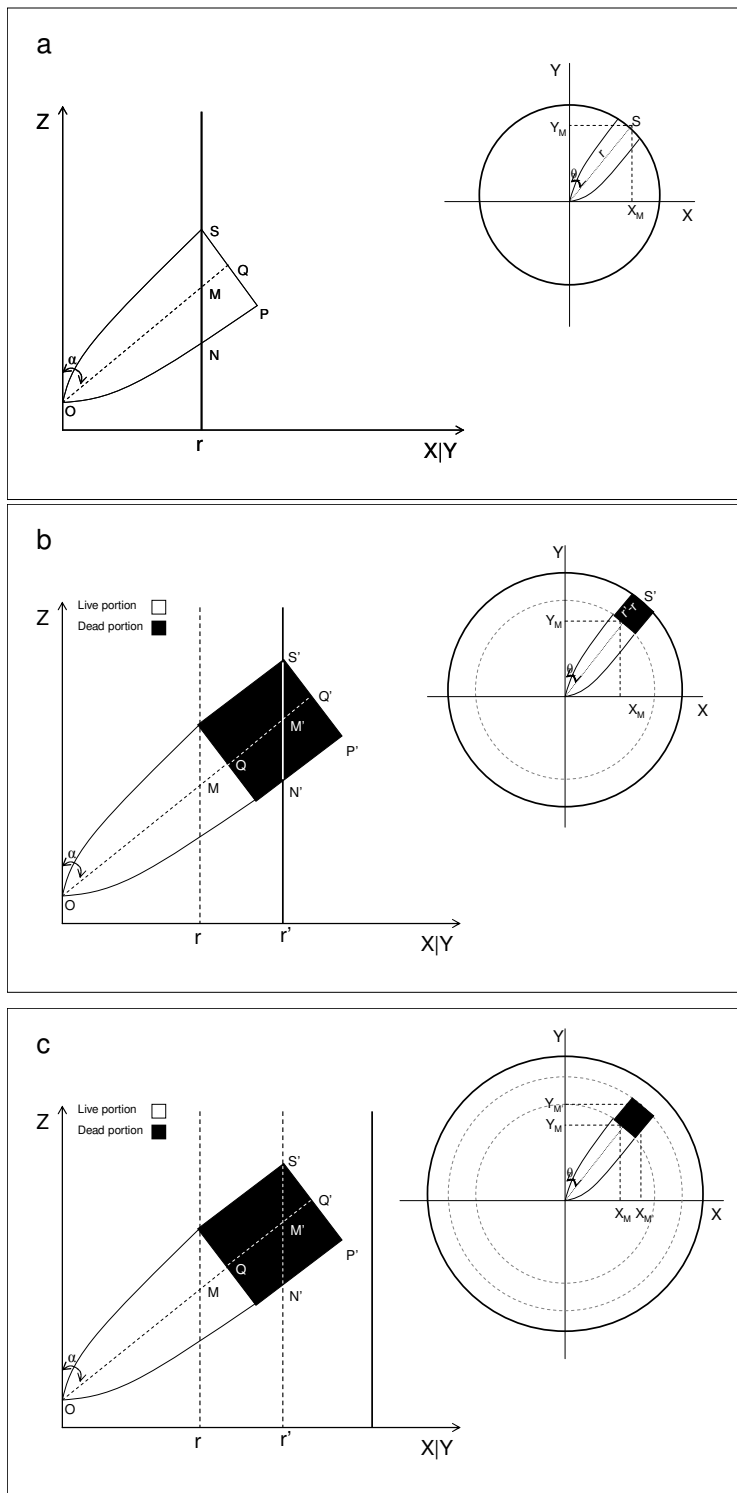


**Figure 3.4.** Type of branch conditions on simulated trees (a) live branch, (b) non-occluded dead branch, and (c) occluded dead branch, where  $r$  and  $r'$  represent the stem radius at the height a branch arises from the stem bole.

$$\begin{aligned}
X_M &= r \sin(\theta), \\
Y_M &= r \cos(\theta), \\
Z_M &= Z_O + r \tan(90-\alpha).
\end{aligned}$$

All calculations required that the coordinates in each of the three axes (X,Y,Z) were measured in the same units (millimeters). Furthermore, in order to facilitate derivation of an approximation formula for the knot volume, the following variables were defined (see Figure 3.4a)

$$\begin{aligned}
|\overrightarrow{OM}| &= [X_M^2 + Y_M^2 + (Z_O - Z_M)^2]^{1/2}, \\
|\overrightarrow{MQ}| &= \frac{|\overrightarrow{SQ}|}{\operatorname{tg}(\alpha)} = \frac{R}{\operatorname{tg}(\alpha)}, \\
L = |\overrightarrow{OQ}| &= |\overrightarrow{OM}| + |\overrightarrow{MQ}|, \\
l = |\overrightarrow{NP}| &\approx \frac{|\overrightarrow{SP}|}{\operatorname{tg}(\alpha)} = \frac{2R}{\operatorname{tg}(\alpha)}.
\end{aligned}$$

The approximate volume of the live branch contained in the internal part of the stem, referred to as the knot volume of the live portion ( $V_{LP}$ ), was computed as

$$V_{LP} = \pi R^2 \int_0^L \left(\frac{l}{L}\right)^\beta dl - V_L \quad (3.5)$$

where an approximation for the volume of the limb ( $V_L$ ) was obtained using the following formula

$$V_L \approx \frac{\pi R^2 L}{2(\beta+1)} \left[1 - \left(\frac{L-l}{L}\right)^{\beta+1}\right]. \quad (3.6)$$

Thus, the volume of the live portion ( $V_{LP}$ ) of the knot was estimated using the following approximate formula

$$V_{LP} \approx \frac{\pi R^2 L}{2(\beta+1)} \left[ 1 + \left( \frac{L-l}{L} \right)^{\beta+1} \right]. \quad (3.7)$$

For subsequent derivations of different branch conditions, the number of location points was expanded, but the definition of variables already used was maintained.

***Knot volume for a non-occluded dead branch***

The geometrical representation of a live branch and the necessary location of points required to calculate its volume were presented in Figure 3.4b. The following additional variables were needed to characterize spatially a non-occluded dead branch:

$$|\overrightarrow{OM'}| = \left[ X_{M'}^2 + Y_{M'}^2 + (Z_O - Z_{M'})^2 \right]^{1/2},$$

$$|\overrightarrow{M'Q'}| = \frac{|\overrightarrow{S'Q'}|}{\text{tg}(\alpha)} = \frac{R}{\text{tg}(\alpha)},$$

$$L' = |\overrightarrow{QQ'}| = |\overrightarrow{OQ'}| - |\overrightarrow{OQ}| = |\overrightarrow{OM'}| + |\overrightarrow{M'Q'}| - |\overrightarrow{OQ}|,$$

$$l' = |\overrightarrow{N'P'}| \approx \frac{|\overrightarrow{S'P'}|}{\text{tg}(\alpha)} = \frac{2R}{\text{tg}(\alpha)}.$$

The volume of the live knot portion of a non-occluded dead branch was obtained using formula (3.4) as

$$V_{LP} = \frac{\pi R^2 L}{(\beta+1)}, \quad (3.8)$$

and the volume for the dead portion of the knot ( $V_{DP}$ ) was approximated with

$$V_{DP} \approx \pi R^2 (L' - (l'/2)). \quad (3.9)$$

Furthermore, an expression for the total volume of the knot ( $V_T$ ) was obtained by adding the volumes of live and dead portions.

$$V_T = \pi R^2 (L/(\beta + 1) + L' - (l'/2)) \quad (3.10)$$

### ***Knot volume for an occluded dead branch***

The volume for the live portion of an occluded branch (Figure 3.4c) was calculated using formula (3.4) and the dead portion by applying the formula for a cylinder

$$V_{DP} = \pi R^2 L' . \quad (3.11)$$

Thus, the total volume of the knot was estimated using the following formula

$$V_T = \pi R^2 (L/(\beta + 1) + L'). \quad (3.12)$$

The proposed knot model allowed recovering efficiently the shape and volume of internal branches without increasing the amount of data generated for each branch during the simulation process. Only a dynamic update of the three-dimensional location of each point according to branch condition is required to make the necessary calculations (Figure 3.4).

### **3.3.5 Model fitting and validation**

Knot profile data represent multiple observations from the same branch (see Figure 3.2c), violating the assumption of independent observations required in regression analysis (Judge et al. 1985, Neter et al. 1998). Under a well-specified model, the parameter estimates are still unbiased. However, the variance can be underestimated affecting confidence intervals and hypothesis testing (West et al. 1984, Schabenberger and Pierce 2001). A more efficient method to obtain parameter estimates involves using nonlinear mixed-effects modeling techniques. The proposed model under this framework is

$$\frac{r_{ij}^2}{R_i^2} = \left( \frac{l_{ij}}{L_i} \right)^{\beta_i} + \varepsilon_{ij} \quad 0 \leq l_{ij} \leq L_i \quad (3.13)$$

where  $r_{ij}$  represents the  $j$ th ( $j=1, \dots, n_i$ ) radius measurement at a length  $l_{ij}$  for the  $i$ th knot ( $i=1, \dots, n$ ). The within-individual errors were assumed homoscedastic, normally distributed and uncorrelated random variables with mean 0 and variance  $\sigma^2$ . In a preliminary analysis, the between-individual variation was accounted for by the use of a mixed-effects parameter

$$\beta_i = \beta + b_i \quad (3.14)$$

where  $\beta$  and  $b_i$  are the fixed- and random-effects parameters, respectively. Subsequently, the estimated random-effect parameters ( $b_i$ ) were related to other knot variables in order to incorporate covariates to explain additional between-individual variation in shape (Pinheiro and Bates 1998). Alternative model formulations were compared using twice the negative log-likelihood ( $-2\ln(L)$ ) and the Akaike's Information Criterion ( $AIC$ ) defined as:

$$AIC = -2 \ln(L) + 2k \quad (3.15)$$

where  $L$  = likelihood function and  $k$  = number of parameters. The model with the smallest values for the goodness-of-fit criteria was considered the best.

The parameter estimates were evaluated by double cross-validation; the 218 branch profiles were randomly and equally split into model building and validation data set. Then, the parameters were re-estimated in the validation data set and their stability was compared with the parameters obtained from the model building data set. Using similar procedures for each data set, measures of precision and bias were computed and compared. The error statistics utilized corresponded to the mean absolute error (precision)

$$|E| = \frac{\sum_{i=1}^n |y_i - \hat{y}_i|}{n} \quad (3.16)$$

and mean error (bias)

$$E = \frac{\sum_{i=1}^n (y_i - \hat{y}_i)}{n} \quad (3.17)$$

where  $y_i$  is the observed value,  $\hat{y}_i$  is the predicted value and  $n$  is the total number of observations. After evaluation of prediction error both data sets were combined and a final set of parameters was estimated using the entire data set, making use of all available information (Myers 1990).

### 3.4 Results and Discussion

#### 3.4.2 Testing for knot curvature

One of the most important assumptions of the proposed model is that the internal branch inclination of knots can be assumed constant. This assumption was evaluated by fitting a separate quadratic equation to the branch pith for each knot profile considering only the live portion (see Figure 3.3b)

$$y_i = \beta_0 + \beta_1 x_i + \beta_2 x_i^2 + \varepsilon_i \quad (3.18)$$

and testing for the significance of the parameter  $\beta_2$  ( $H_0: \beta_2 = 0$  versus  $H_1: \beta_2 \neq 0$ ). The test statistics was

$$t^* = \frac{b_2}{s\sqrt{c_{jj}}} \quad (3.19)$$



where  $b_2$  is the estimated parameter,  $s$  is the estimated error variance and  $c_{jj}$  is the  $j$ th diagonal element of  $(X'X)^{-1}$  for the quadratic model (Myers 1990). The null hypothesis was rejected if  $|t^*| > t_{(1-\alpha/2), (n-3)}$ . The parameters were estimated using the procedure PROC REG available in SAS/STAT (SAS Institute, 2001).

The number of times the null hypothesis was accepted at significance levels of  $\alpha=0.001$  and  $\alpha=0.01$  is presented in Table 3.2. In most cases the parameter  $\beta_2$  was found to be not significant. Even for those cases in which the parameter  $\beta_2$  was significant the curvature of the live portion of the knot was not severe (Figure 3.5). Under this evidence the inclination of knots inside the stem was assumed to be constant and a linear regression was considered appropriate to smooth the knot data.

### 3.4.2 Knot profile model

The fit of the model for both the model building and validation data sets showed that parameter estimates were not different (Table 3.3). However, in both cases, the random-effects parameter was positively related to the maximum branch radius (Figure 3.6). Thus, the original model was modified in order to represent the effect of maximum branch diameter on the shape parameter  $\beta_i$ . The vector of nonlinear mixed-effects parameters was modeled assuming the following form

$$\beta_i = \beta_0 R^{\beta_1 + b_{1i}} \quad (3.20)$$

where  $\beta_0$  and  $\beta_1$  are fixed-effects and  $b_{1i}$  is a random-effects parameter, respectively (Table 3.4). According to the fit statistics this model fitted better only for the validation data set. However, the structure of this model was maintained because the relative knot profiles appear to be clearly related to the maximum branch radius ( $R_i$ ).

**Table 3.2.** Number of times the null hypothesis  $H_0: \beta_2 = 0$  was accepted (n= 218 branch profiles).

| Significance level ( $\alpha$ ) | Acceptance $H_0$ <sup>a</sup> |
|---------------------------------|-------------------------------|
| 0.001                           | 205 (94.0%)                   |
| 0.01                            | 192 (88.0%)                   |

<sup>a</sup> percentage over 218 branch profiles in parenthesis.

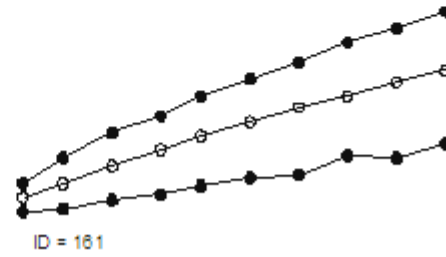
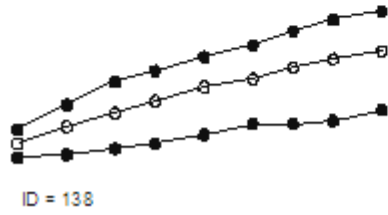
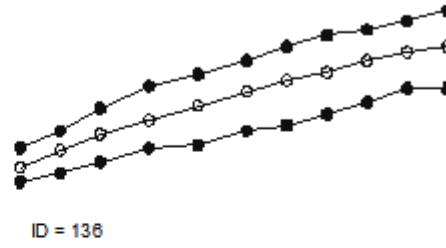
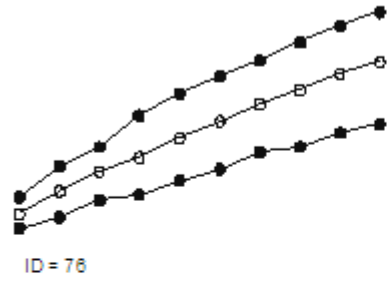


**Figure 3.5.** Randomly selected knot profiles for the live portion, where  $\beta_2$  was found to be significant ( $\alpha=0.001$ ).

**Table 3.3.** Parameter estimates and goodness-of-fit for the fitting and validation data sets.

| Parameter                | Fitting (n=654) |          | Validation (n=615) |          |
|--------------------------|-----------------|----------|--------------------|----------|
|                          | Estimate        | S.E.     | Estimate           | S.E.     |
| $\beta$                  | 0.8329          | 0.04566  | 0.7598             | 0.04227  |
| Variance Components      |                 |          |                    |          |
| $\sigma_\varepsilon^2$   | 0.001594        | 0.000097 | 0.001470           | 0.000093 |
| $\sigma_b^2$             | 0.2229          | 0.03110  | 0.1910             | 0.02668  |
| Goodness-of-fit          |                 |          |                    |          |
| -2LL (smaller is better) | -1887           |          | -1807              |          |
| AIC (smaller is better)  | -1881           |          | -1801              |          |

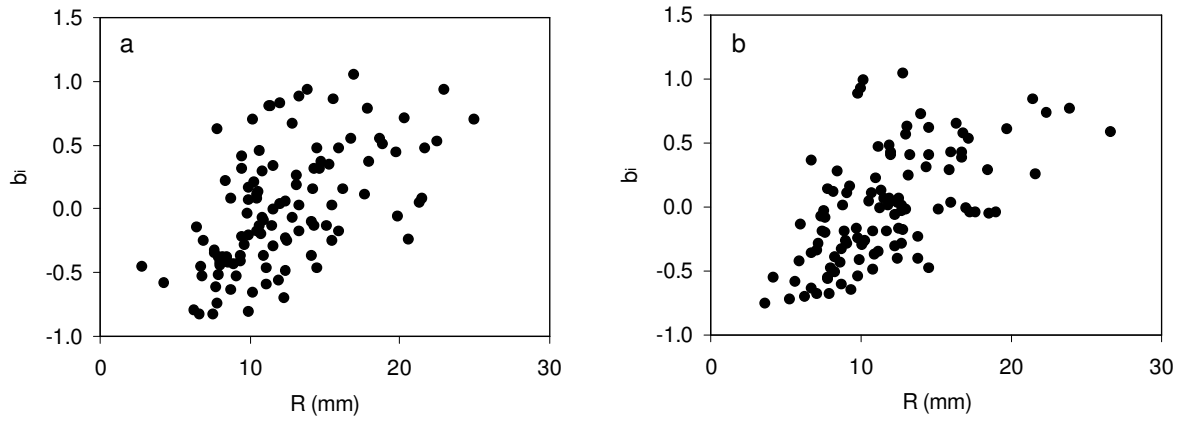


**Figure 3.6.** Relationship between the random effect parameter  $b_i$  and the maximum branch radius  $R_i$  for the (a) fitting and (b) validation datasets.

**Table 3.4.** Parameter estimates and goodness-of-fit for the fitting and validation data sets.

| Parameter                | Fitting (n=654) |         | Validation (n=615) |         |
|--------------------------|-----------------|---------|--------------------|---------|
|                          | Estimate        | S.E.    | Estimate           | S.E.    |
| $\beta_0$                | 0.06351         | 0.02235 | 0.02150            | 0.00769 |
| $\beta_1$                | 0.96480         | 0.14890 | 1.40550            | 0.15330 |
| Variance Components      |                 |         |                    |         |
| $\sigma_\varepsilon^2$   | 0.00164         | 0.00010 | 0.00150            | 0.00009 |
| $\sigma_{b_1}^2$         | 0.07169         | 0.01122 | 0.06189            | 0.00953 |
| Goodness-of-fit          |                 |         |                    |         |
| -2LL (smaller is better) | -1881           |         | -1829              |         |
| AIC (smaller is better)  | -1873           |         | -1821              |         |

The validation of the model showed different behavior for both data sets (Table 3.5). Comparatively a larger bias was observed for the building data set using the parameter estimates obtained using the validation data set. The bias in percentage was close to 1% tending to overestimate observed values. In terms of precision both data sets presented similar values.

A final set of parameters for the proposed model was obtained by combining both data sets (Table 3.6). All parameter estimates were significant and a graphical analysis showed that the model represented adequately the mean trend of observed knot profiles (Figure 3.7). Modeled knot profiles with smaller maximum branch diameters (R) tend to be more cylindrical than those with larger branch diameters which presented a more parabolic or conical shape.

### **3.4.3 Practical implementation**

The presented model permits modeling of different knot shapes while maintaining spatial information on internal location of live and dead portion of knots. As an example of application let's consider that both the spatial location of knots as well as their dimensions within a whorl is required. The branch whorl is located at a stem height of 36 ft (11m) on a simulated tree that has a DBH of 7 inches (18 cm) and a total tree height of 72.2 ft (22 m).

This numerical example considers that the whorl contains three different types of branches, namely a live branch, a non-occluded dead branch and an occluded dead branch (Table 3.7). Both dead branches were assumed to die at the same age, however, one of them is occluded (Branch C).

**Table 3.5.** Validation of the knot profile model where residuals are calculated by the model developed using the other data set.

| Dataset    | Bias (mm) |        | Precision (mm) |       |
|------------|-----------|--------|----------------|-------|
|            | $E$       | %      | $ E $          | %     |
| Building   | -0.107    | -1.068 | 0.613          | 6.131 |
| Validation | 0.025     | 0.239  | 0.759          | 7.287 |



**Table 3.6.** Parameter estimate and goodness-of-fit for the entire data set.

|                        | Estimate | S.E.    | T     | Pr >  T  |
|------------------------|----------|---------|-------|----------|
| Parameter              |          |         |       |          |
| $\beta_0$              | 0.03777  | 0.00951 | 3.97  | < 0.0001 |
| $\beta_1$              | 1.17380  | 0.10730 | 10.94 | < 0.0001 |
| Variance Components    |          |         |       |          |
| $\sigma_\varepsilon^2$ | 0.00158  | 0.00007 | 22.52 | < 0.0001 |
| $\sigma_{b_1}^2$       | 0.06733  | 0.00747 | 9.01  | < 0.0001 |
| Goodness-of-fit        |          |         |       |          |
| -2LL                   | -3702    |         |       |          |
| AIC                    | -3694    |         |       |          |

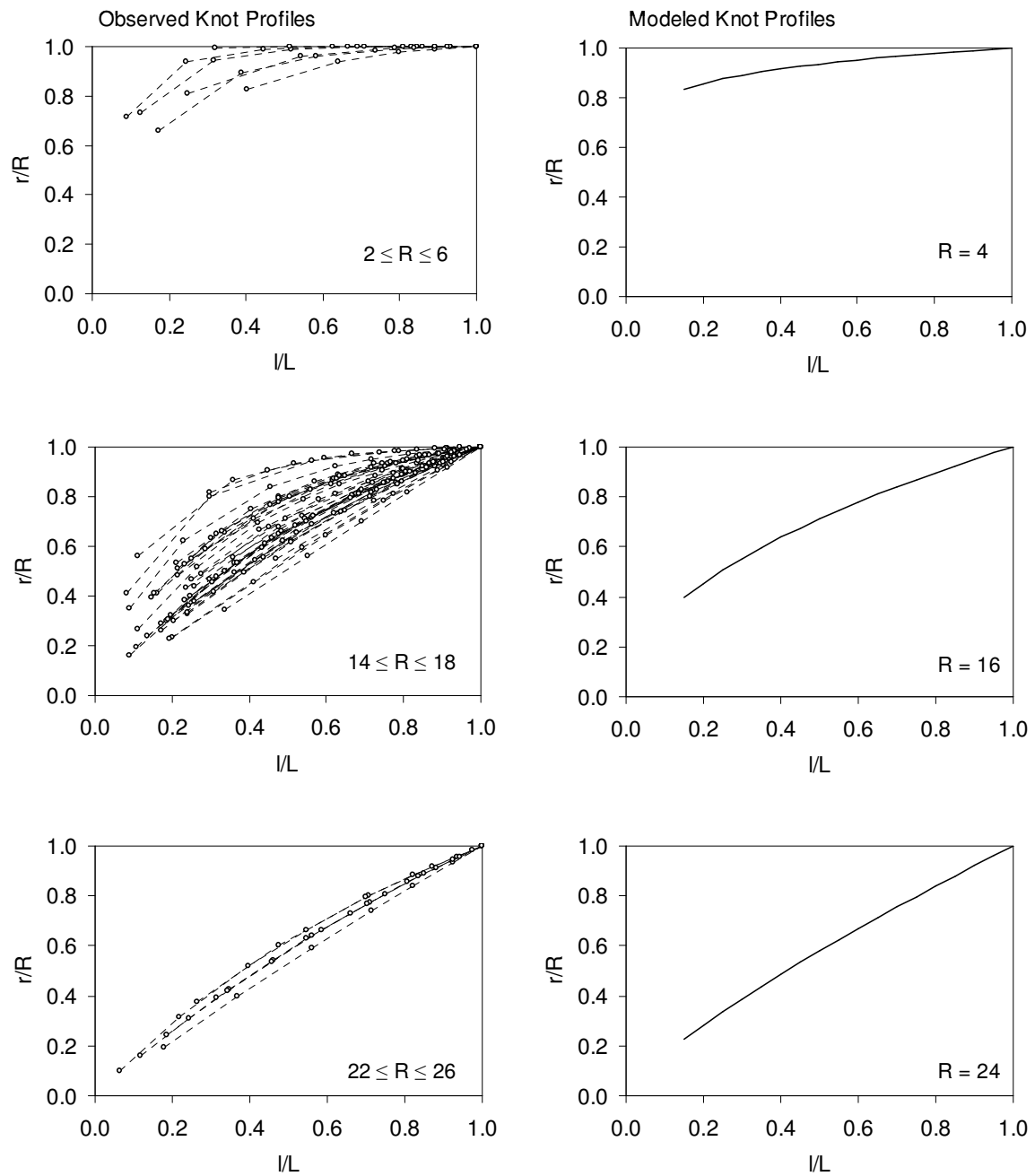


**Figure 3.7.** Observed and modeled relative knot profiles for different values of maximum branch radius ( $R$ ) in mm.

**Table 3.7.** Branch characteristics for a simulated whorl composed of three branches.

| Branch <sup>a</sup> | Type         | Azimuth, $\theta$<br>(degrees) | Inclination, $\alpha$<br>(degrees) | Branch diameter <sup>b</sup><br>(mm) | Stem radius<br>(cm) |     |
|---------------------|--------------|--------------------------------|------------------------------------|--------------------------------------|---------------------|-----|
|                     |              |                                |                                    |                                      | r                   | r'  |
| A                   | live         | 45                             | 45                                 | 35                                   | -                   | -   |
| B                   | non-occluded | 285                            | 60                                 | 20                                   | 2.8                 | -   |
| C                   | occluded     | 190                            | 80                                 | 15                                   | 2.8                 | 4.0 |

<sup>a</sup> see Figure 3.4 for additional details on the definition of each variable.

<sup>b</sup> maximum branch diameter located in the live portion of a knot.

The location of branches in a 3-D space can be recovered using a taper equation (Table 3.8). The upper stem diameters for Branch A were obtained using the Max and Burkhardt (1976) taper equation considering the following parameter values:  $b_1=-3.0257$ ,  $b_2=1.4586$ ,  $b_3=-1.4464$ ,  $b_4=39.1081$ ,  $a_1=0.7431$  and  $a_2=0.1125$ . The estimated stem diameter inside bark at a stem height of 36 ft (11 m) is 4.1 inches (10.39 cm).

Information on spatial location and angle of insertion of each knot is utilized to compute the necessary variables for estimating the volume of each knot (Table 3.9). A detailed explanation and derivation of each variable can be found in section 3.3.4. Afterwards, the value of the shape parameter  $\beta_i$  is computed for each branch using equation (3.20) and parameter estimates given in Table 3.6. Finally, the volume of the live and dead portions can be easily calculated utilizing formulas given above for each branch type (Table 3.10).

### **3.5 Conclusions**

The procedure selected for dissecting branches allowed for recovering information on knot shape in a radial/tangential plane. However, to get consistent information on branch growth (e.g. monotonically increasing branch diameter) a smoothing process was required. The equation utilized to smooth the data corresponded to a modified Weibull function, where an adequate fitting was obtained when at least five observations per knot were available. In total, 15 knot samples failed to converge when fitting the Weibull function. A simple linear regression model was adequate to smooth branch inclination. Most of the dissected branches exhibited little or no pronounced curvature. The procedure utilized to smooth the raw data and reconstruct the branch profiles helped to enhance the pattern and avoid noise due to possible measurement errors. Recovering information on branch growth by using information of past crown recession and measurements of ring width of a disk taken above the whorl was shown to be feasible. However, no evaluation or comparison with other dissection techniques was performed. Further comparative studies on dissection techniques that evaluate accuracy, time and operational implementation may be helpful.

**Table 3.8.** Spatial location of simulated branches.

| Branch | Origin<br>(cm) |                |                | Live portion<br>(cm) |                |                | Dead portion<br>(cm) |                 |                 |
|--------|----------------|----------------|----------------|----------------------|----------------|----------------|----------------------|-----------------|-----------------|
|        | X <sub>O</sub> | Y <sub>O</sub> | Z <sub>O</sub> | X <sub>M</sub>       | Y <sub>M</sub> | Z <sub>M</sub> | X <sub>M'</sub>      | Y <sub>M'</sub> | Z <sub>M'</sub> |
| A      | 0.0            | 0.0            | 1100           | 3.67                 | 3.67           | 1105.20        | -                    | -               | -               |
| B      | 0.0            | 0.0            | 1100           | -2.70                | 0.72           | 1101.62        | -5.02                | 1.35            | 1203.00         |
| C      | 0.0            | 0.0            | 1100           | -0.49                | -2.76          | 1100.49        | -0.69                | -3.94           | 1100.71         |

**Table 3.9.** Variables required for computing knot volume. All values are given in cm.

| Branch <sup>a</sup> | $ \overrightarrow{OM} $ | $ \overrightarrow{MQ} $ | $L$         | $l$         | $ \overrightarrow{OM}' $ | $ \overrightarrow{MQ}' $ | $L'$        | $l'$        |
|---------------------|-------------------------|-------------------------|-------------|-------------|--------------------------|--------------------------|-------------|-------------|
| A                   | 7.35                    | 1.75                    | <b>9.10</b> | <b>3.50</b> | -                        | -                        | -           | -           |
| B                   | 3.23                    | 1.62                    | <b>4.85</b> | 1.44        | 6.00                     | 0.72                     | <b>1.87</b> | <b>1.44</b> |
| C                   | 2.84                    | 0.49                    | <b>3.34</b> | 0.26        | 4.06                     | 0.71                     | <b>1.43</b> | 0.26        |

<sup>a</sup> values to compute volume are in bold.

**Table 3.10.** Computed knot volumes for the live and dead portions for the simulated branches.

| Branch | Type         | $\beta_i$ | Volume (cm <sup>3</sup> ) |                      | Total |
|--------|--------------|-----------|---------------------------|----------------------|-------|
|        |              |           | Live portion<br>(LP)      | Dead portion<br>(DP) |       |
| A      | live         | 1.09      | 28.59                     | -                    | 28.59 |
| B      | non-occluded | 0.73      | 13.74                     | 5.65                 | 19.39 |
| C      | occluded     | 0.40      | 4.21                      | 2.53                 | 6.74  |

The knot model developed can represent a variety of shapes, and it allows users to readily derive analytical formulas for volume calculations. The diameter of the branches was related to their shape. Branches presenting smaller diameters were more cylindrical. Those with larger diameters were more paraboloid or conical.

The use of a taper equation and additional information on angle of insertion (inclination) and horizontal orientation (azimuth) of branches allowed specification of knot spatial locations inside the stem. A numerical example showed the required steps for implementing the proposed knot model in an individual-tree growth simulation system.

### **3.6 Acknowledgements**

Financial support for this research was provided through the Loblolly Pine Growth and Yield Research Cooperative at Virginia Tech. Financial support from the Sustainable Engineered Materials Institute, Virginia Tech, and USDA/CSREES Fund Number 2005-06172 is gratefully acknowledged. Necessary equipment and facilities to analyze wood samples were kindly provided by the Harvesting Research Laboratory. Dr. Phil Radtke, Dr. Carolyn Copenhaver and Dr. Rien Visser provided helpful directions during the development of this study which is deeply appreciated. Also, we thank Mr. Tal Roberts and Mr. Noah Adams for valuable and excellent assistance during the dissection of whorl samples.



### 3.7 Literature Cited

- Amateis, R.L., H.E. Burkhart, and S.M. Zedaker. 1988. Experimental design and early analysis for a set of loblolly pine spacing trials. P. 1058-1065 *in* Forest Growth Modeling and Prediction, Ek, A.R. , S.R. Shifley and T.E. Burk (eds.). USDA For. Serv. Gen. Tech. Rep. NC-120.
- Amateis, R.L., P.J. Radtke, and G.D. Hansen. 2004. The effect of spacing rectangularity on stem quality in loblolly pine plantations. *Can. J. For. Res.* 34:498-501.
- Baldwin, V.C.Jr., K.D. Peterson, A. Clark III, R.B. Ferguson, M.R. Strub, and D.R. Bower. 2000. The effects of spacing and thinning on stand and tree characteristics of 38-year-old loblolly pine. *For. Ecol. Manage.* 137:91-102.
- Barbour, R.J., D.L. Parry, J. Panches, J. Forsman, and R. Ross. 2003. AUTOSAW simulations of lumber recovery for small-diameter Douglas-fir and Ponderosa pine from Southwestern Oregon. USDA For. Serv. Research Note. PNW-RN-333. 11p.
- Briggs, D. 1996. Modeling crown development and wood quality. *J. For.* 94(12): 24-25.
- Burkhart, H.E., R.L. Amateis, J.A. Westfall, and R.F. Daniels. 2004. PTAEDA 3.1: Simulation of individual tree growth, stand development and economic evaluation in loblolly pine plantations. Department of Forestry, Virginia Polytechnic Institute and State University. 23p.
- Clark III, A., and R.H. McAlister. 1998. Visual tree grading systems for estimating lumber yields in young and mature southern pine. *Forest Prod. J.* 48(10):59-67.
- Clark III, A., J.R. Saucier, V.C. Baldwin, and D R. Bower. 1994. Effect of initial spacing and thinning on lumber grade, yield, and strength of loblolly pine. *For. Prod. J.* 44 (11-12):14-20.
- Clark III, A., M. Strub, L. R. Anderson, H.G. Lloyd, R.F. Daniels, and J.H. Scarborough. 2004. Impact of early pruning and thinning on lumber grade yield from Loblolly pine. P. 199-204 *in* Proceedings of the 12<sup>th</sup> biennial southern silvicultural research conference, Connor, K.F. (ed.). USDA For. Serv. Gen. Tech. Rep. SRS-71. 594p.
- García, O. 1987. A visual sawing simulator. Part II: The SEESAW computer program. P. pp. 107-116 *in* Proceedings of the conversion planning conference”, Kininmonth J.A. (ed.). Ministry of Forestry, FRI Bulletin No. 128.

- Gartner, B.L. 2005. Assessing wood characteristics and wood quality in intensively managed plantations. *J. For.* 103(2):75-77.
- Grace, J.C., D. Pont, and C.J. Goulding. 1999. Modelling branch development for forest management. *N. Z. J. For. Sci.* 29:391-408.
- Haygreen, J.G., and J.L. Bowyer. 1996. *Forest products and wood science: an introduction*. Third Edition, Iowa State University Press, Iowa. 484p.
- Husch, B., T.W. Beers, and J.A. Kershaw, Jr. 2003. *Forest mensuration*. Fourth Edition, John Wiley and Sons, Inc., Hoboken, New Jersey.
- Judge, G.G., W.E. Griffiths, R.C. Hill, H. Lütkepohl, and T.C. Lee. 1985. *The theory and practice of econometrics*. Second Edition, Wiley and Sons, New York.
- Leban, J.M., and G. Duchanois. 1990. SIMQUA: un logiciel de simulation de la qualité des bois. *Ann. Sci. For.* 47:483-493.
- Lemieux, H., M. Samson, and A. Usenius. 1997. Shape and distribution of knots in a sample of *Picea abies* logs. *Scand. J. For. Res.* 12:50-56.
- Lemieux, H., M. Beaudoin, and S.Y. Zhang. 2001. Characterization and modeling of knots in black spruce (*Picea Mariana*) logs. *Wood and Fiber Science* 33:465-475.
- Lin, C., and P.M. Morse .1975. A compact design for spacing experiments. *Biometrics* 31:661-671.
- Max, T.A., and H.E. Burkhart. 1976. Segmented polynomial regression applied to taper equations. *For. Sci.* 22:283-289.
- Myers, R.H. 1990. *Classical and modern regression with applications*. Duxbury Press, Boston.
- Neter, J., M.H. Kutner, C.J. Nachtsheim, and W. Wasserman. 1998. *Applied linear statistical models*. Fourth Edition, McGraw-Hill Companies, Inc., Boston.
- Pinheiro, J.C., and D.M. Bates. 1998. *Model building for non-linear mixed-effect models*. Technical Report, Department of Statistics, University of Wisconsin-Madison. 11p.
- Samson, M., I. Bindzi and L.M. Kamoso. 1996. Représentation mathématique des noeuds dans le tronc des arbres. *Can. J. For. Res.* 26:159-165.
- Schabenberger, O., and F.J. Pierce. 2001. *Contemporary statistical models for the plant and soil sciences*. CRC Press LLC, Boca Raton, FL.

- Sharma, M., H.E. Burkhart, and R.L. Amateis. 2002. Spacing rectangularity effect of the growth of loblolly pine plantations. *Can. J. For. Res.* 32: 1451-1459.
- Todoroki, C.L. 1996. Developments of the sawing simulation software AUTOSAW: linking wood properties, sawing, and lumber end-use. P. 241-247 *in* Second Workshop Connection between silviculture and wood quality through modelling approaches and simulation softwares, Nepveu, G. (ed.). Berg-en-Dal, South Africa.
- West, P.W., D.A. Ratkowsky, and A.W. 1984. Problems of hypothesis testing of regressions with multiple measurements from individual sampling units. *For. Ecol. Manage.* 7:207-224.
- Whiteside, I.D., M.D. Wilcox, and J.R. Tustin. 1977. New Zealand Douglas-fir timber quality in relation to silviculture. *N. Z. Journal of Forestry* 22: 24-45.
- Yang, R.C., A. Kozak, and J.H.G. Smith. 1978. The potential of Weibull-type functions as flexible growth curves. *Can. J. For. Res.* 8:424-431.
- Yu, S., J.L. Chambers, Z. Tang, and J.P. Barnett. 2003. Crown characteristics of juvenile loblolly pine 6 years after application of thinning and fertilization. *For. Ecol. Manage.* 180:345-352.

## Chapter 4

### A Stochastic Framework for Modeling Branch Development and Knot Formation in Loblolly pine

---

**ABSTRACT.** A framework for modeling the dynamics of first-order branches (birth, growth, death and self-pruning) and knot formation in loblolly pine (*Pinus taeda* L.) is presented. Data were obtained from a destructive sampling of 34 trees, 22 years old, from a spacing study. For each tree (*i*) the location of each visible whorl along the stem and (*ii*) number of branches was recorded, as well as, (*iii*) 4 to 8 whorls sections per tree were selected for dissection of the largest branch. Annual measurements of crown recession on each tree until age 10 permitted estimation of the number and location of whorls in the past growing seasons. This information, in combination with the dissection of branches, allowed an estimate of branch growth. Throughout the simulation, whorls and branches are located stochastically in each new growing season along and around the stem, respectively. Thereafter, using a taper equation, the spatial location (X,Y,Z) and dimensions of both live and dead portion of branches (knots) is maintained in order to create a 3D representation of the internal stem structure. This integrated modeling system is intended to support silvicultural management decisions that incorporate wood quality variables in predicted stand volumes and also to allow for a linkage with industrial conversion processes (sawing simulation).

---

**Keywords:** individual-tree simulation, branch dynamics, wood quality, loblolly pine.

## 4.1 Introduction

Growth and yield models have been developed to support forest management decisions for loblolly pine (*Pinus taeda* L.) plantations, the most important commercial tree species in the Southern U.S. The effects of intensive management practices at tree- and stand-levels have been incorporated into existing models to increase accuracy in predicting volume production (e.g. Amateis et al. 2000, Westfall et al. 2004). However, the impact of silvicultural practices on wood quality has not yet been incorporated explicitly in most stand simulators (Clark et al. 1994). Modeling of wood quality characteristics is key to more accurately quantifying value of raw material for specific end products. Only recently has research been undertaken to study and model the effect of silvicultural practices on specific gravity, which is an important determinant for pulp yield and mechanical properties of wood, for loblolly pine trees (Tassisa and Burkhart 1998a, Phillips 2002, Clark et al 2002, Daniels et al. 2002, Mora 2003).

For production of solid wood products, quality and value of standing trees, logs and lumber depends on factors such as the number, position and size of branches. Branches included in the wood of the stem originate knots, which decrease the strength and stiffness of wood intended for structural uses and influences the appearance of timber (Whiteside et al. 1977, Briggs 1996, Gartner 2005). A knot is defined as the portion of a branch contained within the tree stem. Their effect on mechanical properties is due to interruption of continuity, and change in the direction of wood fibers (Grace et al. 1999). Furthermore, compression wood is produced at the lower side of a branch (Schultz 1997). Haygreen and Bowyer (1996) state that for sawlog and veneer production, size and frequency of knots are the most important determinants of quality. Sawlogs and peeler bolts often account for most of the value of a stand (Amateis and Burkhart 2005). For southern pines, the size and location of knots in relation to board width are the key factors used to grading dimension lumber (Clark and McAlister 1998). However, despite the importance of knots in the manufacture of solid wood products, there is limited empirical data on the development of first-order branches under different management practices. First-order branches are those arising from the main stem and having a direct impact on the wood produced.

Individual-tree growth and yield models have incorporated crown dimensions as surrogates for photosynthetic potential and as predictors for other growth components (Daniels and Burkhart 1975, Maguire and Hann 1990). In loblolly pine, at crown-level, research has focused on modeling crown recession process (Dyer and Burkhart 1987, Short and Burkhart 1992, Liu et al. 1995), crown profiles (Doruska and Mays 1998), crown shape (Baldwin et al. 1995, Baldwin and Peterson 1997), foliage weight and surface area (Baldwin et al. 1997), and branch biomass (Zhang et al. 2004). At branch-level, Doruska and Burkhart (1994) developed a static system of equations to predict branch location along and around the stem. However, models to predict the distribution of branches along and around the stem and branch diameter over time, while maintaining information on internal branches (knots), have not been reported. Such a dynamic model of branches would extend the utility of existing growth models for loblolly pine to quantify more adequately value of raw material.

This research focuses on the development of first-order branches and its impact on stem quality in terms of size and internal location of knots along and around the stem for loblolly pine. The objectives were to (i) predict the dynamics of first-order branches (birth, growth, death and self-pruning) through out simulation, (ii) recover information on internal stem structure over time in relation to branches contained within the stem (e.g. knots) from simulated trees, and (iii) link the dynamic branch model with the individual-tree growth and yield model PTAEDA3.1 (Burkhart et al. 2004).

## **4.2 Literature Review**

### **4.2.1 Branch dynamics of loblolly pine**

#### **Height growth patterns and location of whorls**

For loblolly pine annual growth of individual trees typically begins during March and ends in September (Boyer 1970, Griffing and Elam 1971, Mudano et al. 1992). The pattern of annual height growth or stem extension for the genus *Pinus* is characterized by a series of growth cycles or flushes during the growing season (Sweet and Bollmann 1976, Bollmann and Sweet 1976). The growth cycles for loblolly pine present an indeterminate pattern, which is controlled by age, environmental factors (e.g. ozone concentrations), site quality, genetics, as well as, their interactions (Boyer 1970, Lanner 1976, Bridgewater et al. 1985, Bridgewater 1990, Mudano et al. 1992).

The height growth process includes apical meristem activity and cell elongation of flushes formed during the growing season (Bridgewater et al. 1985, Mudano et al. 1992). The end of a flush is morphologically represented by the formation of a cluster of branches known as whorls. The formation of stem flushes and their elongation determine the length and number of internodes. Grace and Carson (1993) define the internode length in mature trees as the vertical distance between the top of a whorl and the base of the next adjacent whorl.

The number of flushes formed annually for loblolly pine trees ranges from two and a maximum of six (Boyer 1970, Griffing and Elam 1971, Bridgewater et al 1985, Schultz 1997). It has been noted that the first flush (internode length) of a growing season is the longest and the last the shortest (Griffing and Elam 1971, Mundano et al. 1992, Gilmore and Seymour 1997, Walker and Oswald 2000). But there is no recognized pattern, in terms of internode length, among flushes located in the middle of the growing season. There is some indication that the number of flushes and their length are positively correlated with height growth (Griffing and Elam 1971, Grace and Carson 1993).

## Branch formation and dynamics

Branch tissues begin to develop before stem tissues at the beginning of the growing season (Shigo 1985, Shigo 1990). Branches originate at the stem pith and the number of branches formed per whorl in loblolly pine ranged from two to five (Paul 1957, Wendel et al. 1967). Morphologically the lower side of a branch contains a higher proportion of compression wood and has a wider growth increment than the upper side at all points along the branch (Schultz 1997). According to Haygreen and Bowyer (1996) compression wood is produced to support the angle of the branch.

There is little existing information about the angle of branch insertion and horizontal distribution (azimuth) of branches around the stem for this tree species at juvenile ages. Doruska and Burkhart (1994) analyzed the horizontal distribution (azimuth) of living branches from unthinned loblolly pine trees ranging from 9 to 30 years old. They determined that on a whole-tree basis branch azimuths were not concentrated around a given horizontal angle. Therefore, branches within a whorl might be appropriately distributed around the stem using a uniform distribution (Batschelet 1981, Jammalamadaka and SenGupta 2001).

The rate of branch growth depends on light conditions, the amount of nutrients and water allocated to the branches, and on the tree genotype (Rapraeger 1939, Larson 1969). For radiata pine (*Pinus radiata* D. Don), Brown (1962) observed that there was an initial phase of rapid diameter growth, followed by a second phase, lasting about twice as long, during which the branch diameter remained almost static although the branch was still alive. When insufficient solar radiation reaches the foliage of lower limbs, production of new needles ceases, mature needles drop, and branches die shortly thereafter (Schutz 1997). After death, branches persist on the bole for a period of time. From a wood quality perspective the retention of dead branches with acute angles is especially deleterious because the resulting knots are not only relatively large but pass through a large volume of stem wood.



For loblolly pine trees, dead limbs persist for an average of 8 years and persistence appeared to depend neither upon the diameter nor the age of the branch (Reynolds 1967). Reynolds (1967) also reported that the average branch took 7 years to disintegrate back or self-prune to a maximum length of 3 inches from the bole. The minimum persistence time for any one branch was 4 years and the maximum 11 years. After self-pruning, the time required for the branch stub to become occluded and to form clear wood depended on the length and diameter of the stub and on the rate of growth of the tree. Reynolds (1967) estimated that the time required for a band of clear wood to grow over the spot formerly occupied by the limb varied from 9 to 13 years, averaging 10.2 years.

#### **4.2.2 Previous work on modeling branch characteristics**

Most of the research on crown structure in relation to first-order branches has been done in other tree species. Colin and Houllier (1991) modeled the vertical trend of maximum branch diameter along the stem for Norway spruce (*Picea abies* (L.) Karst.) in France. Soon thereafter, they expanded their work to include the vertical trend for additional external branch characteristics (known as ‘crown profile models’) such as insertion angle, number and position of branches along the stem (Colin and Houllier 1992).

Based on these ideas, empirical modeling techniques have been developed and evaluated for other important commercial tree species. Roeh and Maguire (1997) developed a system of equations to estimate mean branch diameter, maximum branch diameter, branch angle and branch length inside the crown of Douglas-fir (*Pseudotsuga menziesii* (Mirb.) Franco) in the U.S. Because of the relationship among response variables, the system of equations was fit simultaneously using a nonlinear three-stage least squares (N3SLS) procedure. Maguire et al. (1999) constrained a variable-exponent equation to predict maximum branch diameter at a given relative height within the live crown for the same tree species. To reduce the effect of autocorrelation from observations taken from the same individual they used a nonlinear mixed effects model. In Germany, Wobst (1995) for Douglas-fir and Schmidt (2001) for different tree species modeled the vertical trend of branch diameter. A mixed-effects modeling approach was used by

Meredieu et al. (1998) to estimate branch characteristics within the live crown for Corsica pine (*Pinus nigra* Arnold ssp. *Laricio* (Poiret) Maire) in France. Mäkinen and Colin (1998, 1999) recognized a hierarchical structure in their data and predicted a vertical trend in branch diameter and branch angle along the stem for Scots pine (*Pinus sylvestris* L.) in southern and central Finland using a variance component model. A series of equations to model branch characteristics along the stem were developed by Catchpoole et al. (2002) for Caribbean pine (*Pinus caribea* var. *hondurensis*) in Australia. Three different methods were proposed by Mäkinen and Mäkelä (2003) to model branch diameter along the stem for Scots pine in Finland. Mäkinen et al. (2003a, 2003b) developed models of external branch characteristics along the stem on the basis of routine stand and tree measurements for Norway spruce and planted Silver birch (*Betula pendula* Roth.) in Finland. Recently, Garber and Maguire (2005) utilized as baseline the model proposed by Maguire et al. (1999) to study the influence of spacing and species composition on the vertical trend in maximum branch diameter in four commercial tree species in Oregon, U.S.

Despite the utility of predicting external branch characteristics, there are certain limitations. The first limitation is that the application of this type of equations over time may lead to an inconsistent prediction of branch diameter for certain combinations of predictor variables (Maguire et al. 1999). The second limitation, may be the most important, is that a more detailed description of the distribution of individual branches along and around the stem is required for a complete assessment of wood quality (e.g. Grace et al 1999, Catchpoole et al. 2002). Doruska and Burkhart (1994) modeled explicitly diameter and location of first-order branches, both along and around the bole for unthinned loblolly pine (*Pinus taeda* L.) plantations in U.S, for a more detailed description of crown structure. However, some of the limitations of this model are that it permits the modeling of branches only at one point in time; therefore inconsistent predictions may be obtained if used in a dynamic simulation system. Also, the prediction of external branch characteristics, location and diameter of branches, is limited to the crown. Thus, from a wood quality perspective this model does not provide detailed information on branches and resulting knots over time around and along the stem.

Although models of external branch characteristics in a static context have been developed, few studies have tried to model the process of whorl formation and branch characteristics (external/internal) over time. This approach might permit a more consistent prediction of branch characteristics over time, but currently an important limitation is the lack of longitudinal data from permanent plots. However, some studies have demonstrated that information on branch growth and dynamics can be recovered with destructive sampling of branches (Maguire and Hann 1987, Fujimori 1993). Mäkinen (1999) studied the dynamics of branch growth, suppression, death, natural pruning and knot formation for Scots pine using dissected branches. Using the same data, Mäkinen and Colin (1999) developed equations to model the number of new branches, probability of a branch being alive and the proportion of dead branches for the whorls below the crown base. Grace et al. (1998, 1999) used data from dissected branches to model branch development over time for radiata pine plantations in New Zealand. They presented a series of equations to model the occurrence of branch clusters (whorls) within an annual growing season (annual shoot) and diameter growth of branches at the point of attachment to the tree stem.

Because growth and yield models incorporate the effects of silvicultural treatments on stem growth, a logical approach to predict branch growth while accounting indirectly for silvicultural effects is to study the relationship between branch and stem diameter growth. The relationship between radial increment of the largest branches and stem growth at the same tree height was studied by Briggs et al. (2002) for Douglas-fir. Based on their findings, they proposed a preliminary model to predict branch diameter growth. Initial conditions to start the simulation are the diameter of the stem where the branch is located and the branch diameter at the end of the first growing season must be known.

In general, several static approaches have been proposed to predict external branch characteristics, but limited research has been done to model the dynamics of first-order branches. In all few reported cases, longitudinal data on branch growth to develop empirical models has been obtained from destructive analysis of sample branches.

## **4.3 Data**

### **4.3.1 Loblolly pine spacing trial**

In 1983, spacing trials were established at four locations by the 'Loblolly Pine Growth and Yield Research Cooperative' on site prepared-areas in Virginia and North Carolina. Two of these trials were situated in the Coastal Plain and two in the Piedmont region. The experimental design selected for this spacing study was the nonsystematic design presented by Lin and Morse (1975). The study consists of three replications at each location. In each replication spacing levels of 4 ft (1.2 m), 6 ft (1.8 m), 8 ft (2.4 m) and 12 ft (3.6 m) were assigned randomly both in rows and columns. Each row and column was composed for seven measurement trees. Thus, the intersection of rows and columns defined a plot with 49 measurement trees. The result was a factorial arrangement of 16 treatments with an equal number of trees per plot, but different plot sizes and shapes (see Sharma et al. 2002). In addition, each plot was surrounded by three rows of guard trees. More details on the experimental design used in this long-term study can be found in Amateis et al. (1988).

Growing stock planted at each location was genetically improved 1-0 loblolly pine seedlings from a single nursery. During the first three years after planting, both herbaceous and woody competing vegetation was controlled. From establishment to age 5 the diameter at groundline was measured annually. Beginning at age 5 the diameter at breast height (dbh) was measured annually. Through age 10, total tree height, height to live crown, and crown width were measured annually for all trees. Measures of crown width were carried out until age 12. Categorical tree condition of each individual tree was also recorded. After age 10, total tree height and height to live crown were measured bi-annually, while dbh and tree condition were measured annually.

### 4.3.2 Collection of branch data

Data for this research were obtained from the loblolly pine spacing study located near Appomattox, Virginia (Piedmont region). During the dormant season of 2004-2005, at stand age 22 years old, 34 trees were selected for comprehensive measurements of whorl characteristics and sampling of whorl sections (Table 4.1). Trees with a single stem and no record of visible broken top were selected. The main goal was to collect data to model the morphology of knots and the dynamics of first-order branches. Among the branch characteristics of interest were number of branches per whorl, branch orientation around the stem (azimuth), angle of insertion with respect to the stem pith (inclination) and diameter growth. Additional information on whorl number and location within growing seasons was available from field measurements and past measurements on crown recession. Trees were selected from ten different initial spacings (Table 4.1).

Before each tree was felled, dbh outside bark at 4.5 ft (1.37 m) was measured using a caliper and a vertical line on the within row side of the stem was marked to an approximate height of 6.5 ft (2 m). Once the tree was on the ground, this line was extended along the length of the stem. This line served as a reference (azimuth zero degree) for determining the same orientation of the sampled whorl sections. For each sample tree the stump height (cm) and distance from stump height to tree tip (m) were measured. For each visible whorl the following variables were measured: (i) height above ground (m), (ii) diameter outside bark (cm), (iii) status, and (iv) number of visible branches or branch stubs in each whorl. The status of each whorl was visually categorized as: live, sound, decayed or knot. After that, a variable number of whorl sections was chosen from each sample tree for subsequent laboratory dissection. Each whorl section was labeled for identification and marked on its bottom surface with the position of the reference line. A total of 217 whorl sections was collected in the field from the sample trees.

**Table 4.1.** Number of sampled trees per initial spacing and sampled whorl sections per tree.

| Spacing<br>(feet x feet) | N | DBH (inches) |            | H (feet) |             | Sampled whorls<br>per tree |     |
|--------------------------|---|--------------|------------|----------|-------------|----------------------------|-----|
|                          |   | mean         | range      | mean     | range       | min                        | max |
| 4 x 4                    | 4 | 5.5          | 4.2 – 7.5  | 53.7     | 46.9 – 61.7 | 5                          | 8   |
| 4 x 6                    | 3 | 6.0          | 4.9 – 7.5  | 59.9     | 56.4 – 61.7 | 7                          | 8   |
| 4 x 8                    | 2 | 7.1          | 6.3 – 7.8  | 61.4     | 59.1 – 63.6 | 6                          | 7   |
| 4 x 12                   | 3 | 7.3          | 4.8 – 10.0 | 57.8     | 47.9 – 63.6 | 6                          | 8   |
| 6 x 8                    | 2 | 8.0          | 6.3 – 9.7  | 60.9     | 60.1 – 61.7 | 4                          | 4   |
| 8 x 4                    | 3 | 6.8          | 6.2 – 7.9  | 65.2     | 62.3 – 67.6 | 7                          | 8   |
| 8 x 6                    | 3 | 6.5          | 4.5 – 8.8  | 60.4     | 51.5 – 66.3 | 6                          | 7   |
| 8 x 8                    | 3 | 8.0          | 7.0 – 10.1 | 63.2     | 60.4 – 68.6 | 6                          | 8   |
| 8 x 12                   | 3 | 7.7          | 5.5 – 10.4 | 56.6     | 50.5 – 66.6 | 6                          | 8   |
| 12 x 6                   | 3 | 10.0         | 9.8 – 10.4 | 64.1     | 61.0 – 66.8 | 6                          | 7   |
| 12 x 8                   | 2 | 8.6          | 7.1 – 10.0 | 64.0     | 59.8 – 68.2 | 4                          | 5   |
| 12 x 12                  | 3 | 10.5         | 8.1 – 11.8 | 63.9     | 57.4 – 67.6 | 4                          | 5   |

## 4.4 Methods

### 4.4.1 Reconstruction of whorl location and frequency per growing season

The reconstruction of whorl location and frequency per growing season was performed by linking the information on whorl location along the stem measured in the field and information on past crown recession measured annually on each individual tree until stand age 10 years. During the reconstruction it was assumed that (i) in each growing season no damage has occurred in the apical part of the sampled trees, (ii) measurement errors of crown recession were insignificant, and (iii) each growing season ended with a new whorl.

The number of whorls formed in each growing season for a sample tree is presented in Figure 4.1. The segmented line represents measured total tree height at a given age, the circles represent the location of whorls, the dots represent the location of the last whorl formed in the previous growing season, and  $\Delta h$  the estimated height increment for each growing season. The reconstruction of location of whorls was based on the empirical observation that during a growing season the first flush is the largest (Griffing and Elam 1971, Mundano et al. 1992, Walker and Oswald 2000). This procedure allowed for getting an estimate of the number of whorls and their absolute and relative location per growing season. For instance, during growing season seven a total of four whorls was produced. These estimates were then used for modeling the number of whorls and their relative location within a growing season.

The number of whorls and their relative position within a growing season was computed for each sample tree between two and eight years old. The age range was restricted because measurement of whorl location along the lower stem was difficult to perform accurately on the field; therefore only whorls contained since the second year were considered for analysis. Also, growing seasons that presented apparent missing whorls (not measured in the field) were eliminated for this analysis.

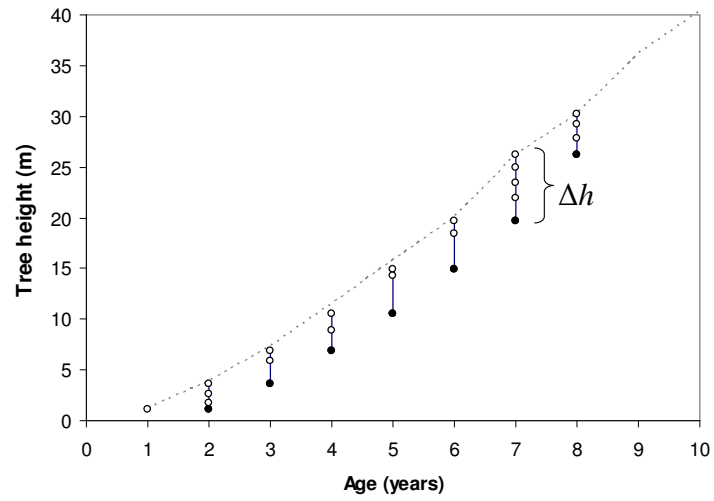


**Figure 4.1.** Reconstruction of whorl location within each growing season until tree age 8 years old.



Field measurements along the stem were done below the live crown, which for most of the trees was equivalent to a total tree height reached at an age between eight and ten years old.

In addition, this reconstruction allowed for an estimate of the tree age when the whorl was generated and the number of years it was alive. A whorl and its branches were assumed to die when they were located under the live crown based on past height measurements done on each sample tree. The estimated number of years when a branch was alive was linked with the ring measurements from the disk taken above the whorl, permitting recovery of information on branch attributes for the living part of the knot.

#### **4.4.2 Dissection of branches and reconstruction of branch attributes**

A dissection technique similar to that reported by Lemieux et al. (2001) was used in this study to collect information on knot shape. Before dissection each whorl was dried, debarked and when necessary trimmed to fit on the band saw. After that, the sample whorl preparation procedure included: (i) identifying and labeling each visible branch proceeding clockwise from the reference line, (ii) marking the largest branch and possibly a second branch on the opposite side of the stem, and (iii) marking the top of the whorl section with the horizontal direction (azimuth) from the pith to bark of each branch identified in (i). From the 217 whorl sections only 198 whorl sections were suitable for dissection. Only one branch was selected from 42 whorl sections and two branches from 156 whorl sections, for a total of 354 dissected knots. In addition, a disk was cut from the top and used to determine branch azimuth with a protractor; and ring width was measured to the nearest 0.002 mm in the direction of branches selected for dissection. Ring width was measured using an unslide measurement system (Velmex). Only 341 knots proved suitable for measurement of ring width, providing the final sample size for this study.

The distance between faces of consecutive slices from bark to pith was approximately 5 mm with 3mm thicknesses and 2 mm of kerf. In each slice the distance from the bottom of the whorl section to the top, pith and bottom of the knot was measured (vertical direction). The dissected knots on the radial/tangential (R/T) plane were used to recover information on knot profiles and branch development using a procedure previously described (Chapter 3).

#### **4.4.3 Dynamic modeling of branches along and around the stem**

An initial step was to identify all relevant entities of the system and define their components and logical relationships (e.g. Daniels and Burkhart 1975). Similar to Grace et al. (1998, 1999) for radiata pine plantations in New Zealand, the entities identified for this system were whorl, branch and knots. A simplified flow chart with the relationships existing between the entities and their components is presented in Figure 4.2.

Complete development and parameterization of empirical equations was not possible when developing the model. Because of scarcity of knowledge and empirical data about branch dynamics for loblolly pine trees, all components of the system could not be estimated. In cases, where adequate empirical data were lacking, information from other studies was used to quantify the dynamics of those branch attributes over time.

#### **Whorl Components**

##### ***Number of whorls per growing season***

The number of whorls produced during a growing season is a nominal response variable with  $J$  possible categories showing; hence a multinomial distribution results. This type of data can be analyzed and the response probabilities  $\{\pi_1, \dots, \pi_J\}$  predicted by using a multicategory (or polychotomous) logistic regression, which is an extension of logistic regression models for binary responses (Hosmer and Lemeshow 1989). The multicategory logistic model pairs each response category with a base line category, often the last one (Agresti 2002).

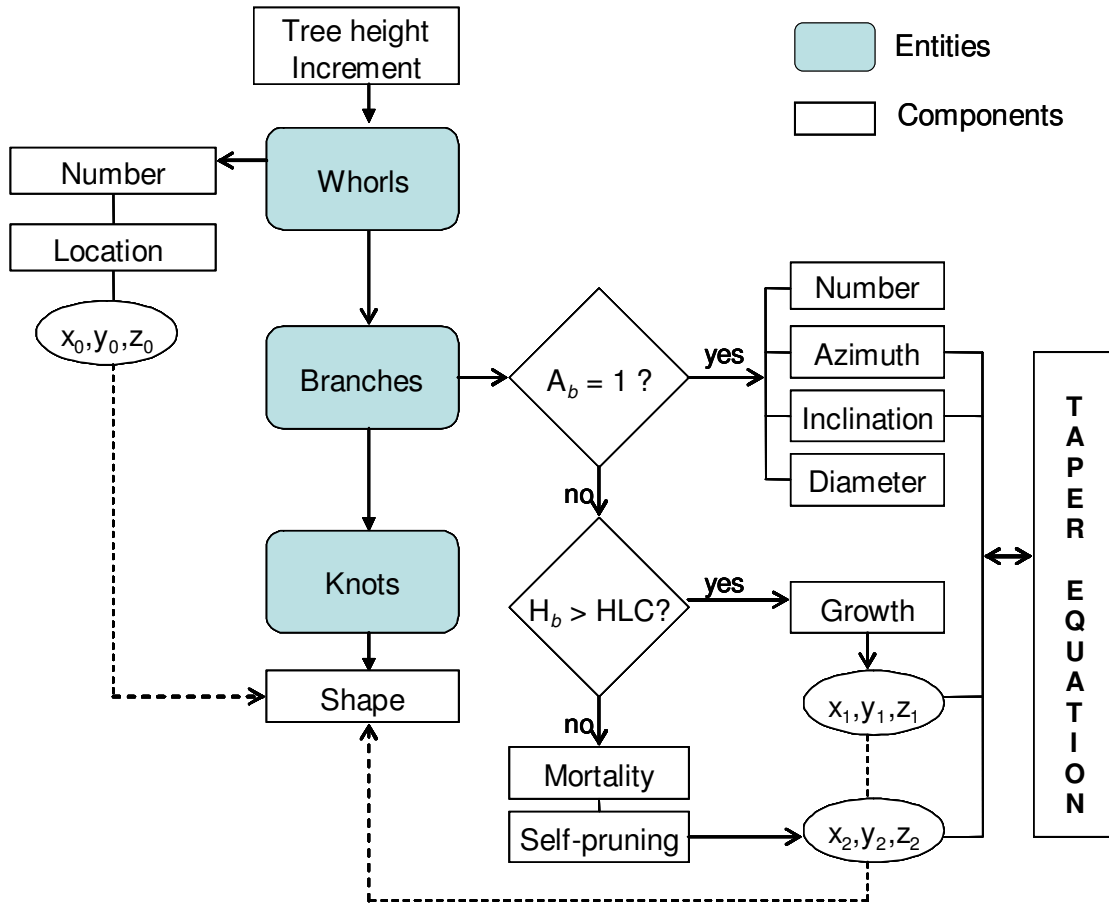


**Figure 4.2.** Relationship between the different entities and components for the proposed branch growth model, where  $A_b$ = branch age,  $H_b$  = height of the branch above the ground and HLC = height to live crown.

The logistic model can be defined as

$$\log \frac{\pi_j}{\pi_J} = \alpha_j + \beta_j' \mathbf{x} \quad j = 1, \dots, J-1, \quad (4.1)$$

where  $\mathbf{x}$  is the vector of predictor variables,  $j$  represents a given category (e.g. number of whorls per growing season) and  $J$  the base line category. Therefore,  $J-1$  equations need to be simultaneously estimated using a maximum likelihood estimator (Hosmer and Lemeshow 1989).

Under this methodology, the response probabilities for each of the  $J-1$  categories or the probability of producing a given number of whorls in a given growing season can be obtained by

$$\pi_j = \frac{\exp(\alpha_j + \beta_j' \mathbf{x})}{1 + \sum_{h=1}^{J-1} \exp(\alpha_h + \beta_h' \mathbf{x})}, \quad (4.2)$$

and because  $\sum_{j=1}^J \pi_j = 1$  the probability for the last category can be easily computed as

$$\pi_J = 1 - \sum_{j=1}^{J-1} \pi_j.$$

### ***Location of whorls within a growing season.***

The location of whorls was first investigated by determining the relative mean location of whorls within each growing season. This analysis was performed separately according to the number of whorls produced for each growing season. The information was utilized to develop a predictive equation or utilized to construct a look up table using the observed relative mean location of whorls within a growing season.

## **Branch Components**

### ***Number of branches per whorl***

The data collected in the field were used to determine if there were differences in the number of branches per whorl produced within a growing season. This analysis was performed by applying an ANOVA, where a square root transformation was applied to the count data (number of branches per whorl) with the purpose of stabilizing variances (Kuehl 1994 p. 121).

The main purpose was to detect possible relationships that can be used to develop a predictive equation for the number of branches within each growing season. In case that any relationship was found, a stochastic procedure was implemented to simulate data using a distribution function for a discrete variable.

### ***Branch orientation (Azimuth)***

Doruska and Burkhart (1994) investigated the branching patterns of 68 loblolly pine trees. They tested for statistical evidence of directedness of branches on a whole tree basis using a Raleigh Test for circular data (Batschelet 1981). They concluded that the orientation of branches around the stem for most of the trees followed a uniform or isotropic distribution (Jammalamadaka and SenGupta 2001). In this study a more limited data set was available for each individual tree; therefore the algorithm proposed by Doruska and Burkhart was implemented.

### ***Branch inclination***

The inclination of branches was modeled by sampling from a probability distribution function for a continuous variable. The inclination was assigned stochastically to each individual branch during the first growing season according to the distribution observed in the entire data set. This procedure assumed that the inclination of branches contained inside the stem is constant throughout the simulation process.

### ***Initial branch diameter***

The simulation process requires that at the end of the first growing season an initial diameter must be assigned for each individual branch. The only information available for simulating this variable comes from the reconstruction of branch profiles. Therefore, no information of initial branch diameter within a whorl and between whorls generated during the same growing season was available. However, these limited data were used to investigate the effect of initial stand density on the initial branch diameter for the biggest branches sampled. A distribution approach was utilized for modeling stochastically this component until more data becomes available.

### ***Diameter growth of first-order branches***

A predictive equation for branch diameter growth was derived from the following monomolecular growth function

$$BD = \alpha (1 - \beta \exp(-\gamma BA)) \quad (4.3)$$

where  $BD$  is the branch diameter (mm) and  $BA$  is the branch age. The first derivative of the growth function (4.3) with respect to the branch age ( $BA$ ) gives an expression for the current annual increment

$$\Delta BD = k \exp(q BA) \quad k > 0 \text{ and } q < 0 \quad (4.4)$$

where  $\Delta BD$  is the branch diameter increment (mm),  $k = \alpha \beta \gamma$  and  $q = -\gamma$ . The parameter  $k$  represents the rate of constant increase and  $\exp(q BA)$  represents the rate of exponential decrease. According to Zeide (1993) this general expression corresponds to an exponential decline (ED) type of growth equation. The strategy used to develop an equation for predicting branch diameter increment was to identify explanatory variables that affect the increasing and decreasing rate of growth for individual branches. Then,

these variables were included into equation (4.4) and the significance of the parameters and the reduction in mean square error ( $MSE$ ) evaluated. The mean square error reduction ( $MSER$ ) was computed using the following expression

$$MSER = \left(1 - \frac{MSE_2}{MSE_1}\right) 100 \quad (4.5)$$

where  $MSE_1$  is the mean square error of the baseline equation (4.4) and  $MSE_2$  is the mean square error of a model including additional predictor variables.

### ***Mortality of branches***

The process of branch mortality was modeled considering their location along the stem in relation to the height to live crown. A branch was assumed to die when it was located below the height to live crown (Figure 4.2). Even though it is expected that there is mortality of branches located inside the crown, it was not possible to model because lack of knowledge and data on this process.

### ***Self-pruning process***

There is scarce quantitative information about the process of natural pruning (self-pruning) in loblolly pine trees. After branch death, limbs persist for a period of time attached to the stem. Reynolds (1967) reported one of the few observational studies on this topic. He observed that the persistence of branches was independent of the branch diameter and its age. Also, the range of time required for disintegrating back to a length of 3 inches or less was between 4 and 11 years. Based on this information, a general procedure was devised to model the process of self-pruning based on a cumulative density function (c.d.f.).

## **Knot shape**

The knot model utilized considered that the live portion of a knot can be modeled using a predictive equation and the dead portion assuming the shape of a cylinder. The equation utilized to model the live portion has been previously developed by applying mixed-effects modeling techniques and has the following form

$$\frac{r^2}{R^2} = \left( \frac{l}{L} \right)^{\beta_0 R^{\beta_1}} \quad 0 \leq l \leq L \quad (4.6)$$

where  $r$  is the radius of the live portion of a knot at a length  $l$ ,  $R$  is the maximum radius,  $L$  is the total length. The parameters estimated from the dissected branches and standard error (in parenthesis) were  $\beta_0 = 0.03777$  (0.000508) and  $\beta_1 = 1.1738$  (0.1073). Major details on the development of the knot model can be found in Chapter 3.

### **4.4.4 Incorporation of branch model into PTAEDA 3.1**

The proposed components to model branch development and knot shape were linked to the individual-tree growth model PTAEDA 3.1 (Burkhardt et al. 2004). The linkage consisted in using PTAEDA 3.1 to simulate the development of trees until a given stand age. During the simulation process the surviving trees at each stand age and their dimensions (*i*) breast height diameter, (*ii*) total height, and (*iii*) crown ratio were exported to an external file. A computational routine selects only those trees that survive until the end of the simulation and sorts them by age. Subsequently, the program uses the information of individual tree growth and simulates the development and distribution of first-order branches along and around the stem.

During the simulation process information on the internal structure of the stem in relation to knots is maintained in a 3D-space. The external location of those points where first-order branches arise from the stem and internal location of knots are assigned using a taper equation. In this study, the stem profile was modeled using the segmented taper equation proposed by Max and Burkhardt (1976).



## 4.5 Results and Discussion

### 4.5.1 Modeling whorl components

The analysis of sampled trees indicated that during each growing season between two and five flushes (whorls) were produced, where the modal value was three whorls (Table 4.2). The number of whorls (flushes) estimated using this methodology and their relative locations agreed closely with observations reported in past studies for the same tree species (Boyer 1970, Griffing and Elam 1971, Bridgewater et al. 1985, Schultz 1997).

A graphical examination between the number of whorls produced and the height increment ( $\Delta h$ ) during each growing season does not show any apparent trend (Figure 4.3a). However, a positive relationship can be observed after generating intervals each 1.0 feet and computing the mean value for the number whorls within each class (Figure 4.3b).

Contrary to height increment, tree age did not show any relationship and was not significant when included as predictor variable in the multcategory logistic regression. Therefore, the final logistic model to predict the number of whorls considered as predictor variable only the height increment ( $\Delta h$ ). The set of equations generated taking as base line the category presenting five whorls were

$$\log \frac{\pi_2}{\pi_5} = 8.1075 - 1.5515 \Delta h,$$

$$\log \frac{\pi_3}{\pi_5} = 5.2983 - 0.6300 \Delta h,$$

$$\log \frac{\pi_4}{\pi_5} = 2.0261 - 0.0471 \Delta h.$$

**Table 4.2.** Number of whorls produced and mean relative location (%) within a growing season.

| Number of Whorls | Observations |       | Whorl number |      |      |      |      |
|------------------|--------------|-------|--------------|------|------|------|------|
|                  | N            | %     | 1            | 2    | 3    | 4    | 5    |
| 2                | 58           | 26.0  | 54.0         | 46.0 |      |      |      |
| 3                | 108          | 48.4  | 40.5         | 34.6 | 24.9 |      |      |
| 4                | 49           | 22.0  | 31.1         | 26.4 | 23.8 | 18.7 |      |
| 5                | 8            | 3.6   | 21.4         | 21.2 | 22.5 | 18.3 | 16.6 |
| Total            | 223          | 100.0 |              |      |      |      |      |

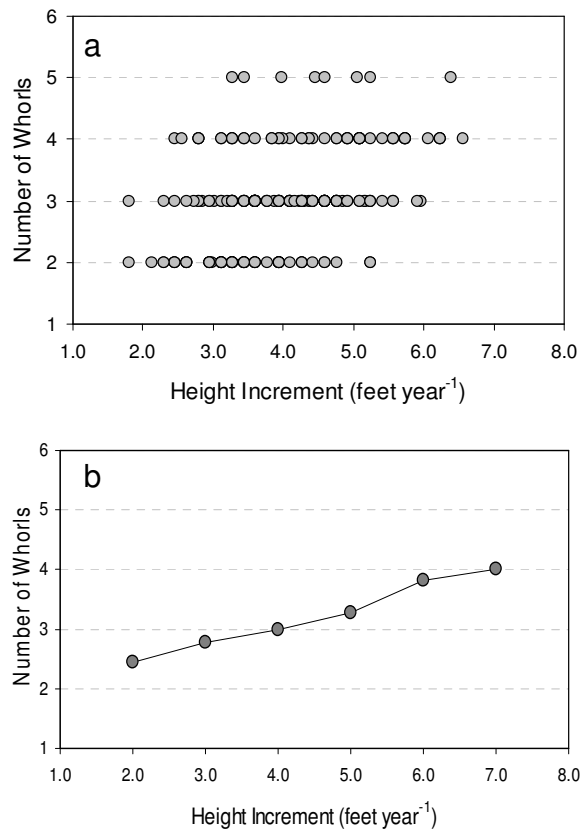


**Figure 4.3.** Relationships between (a) observed number of whorls versus height increment and (b) mean number of whorls vs height increment classes.

Note that the sub index used for each category represents the number of whorls produced. The likelihood-ratio test performed to test the hypothesis that the number of whorls is independent of the height increment e.g.  $H_0: \beta = 0$  for  $j=2, \dots, 5$  was rejected (p-value  $< .0001$ ). Therefore, there was evidence that the number of whorls produced is related to height increment as reported previously by other authors (Griffing and Elam 1971). Assuming that the height increment ( $\Delta h$ ) for a growing season is 4 feet the response probability of producing two whorls can be computed using formula (4.2) as:

$$\pi_2 = \frac{\exp(5.2983 - 0.6300 \cdot 4)}{1 + \exp(8.1075 - 1.5515 \cdot 4) + \exp(5.2983 - 0.6300 \cdot 4) + \exp(2.0261 - 0.0471 \cdot 4)} = 0.223.$$

Thus, the response probabilities for three, four and five whorls can be computed as  $\pi_3 = 0.535$ ,  $\pi_4 = 0.209$  and  $\pi_5 = 1 - (\pi_2 + \pi_3 + \pi_4) = 0.033$ . Predicted response probabilities for different values of height increments ( $\Delta h$ ), following the same procedure, are presented in Figure 4.4.

For the most common range of observed height increments (3.0 and 5.0 feet) the response probabilities behave as expected where the maximum probability is to produce three flushes, which was identified as the modal value in the sample data (Table 4.2). The response probability for producing five flushes, even though small, increases with increasing height increments.

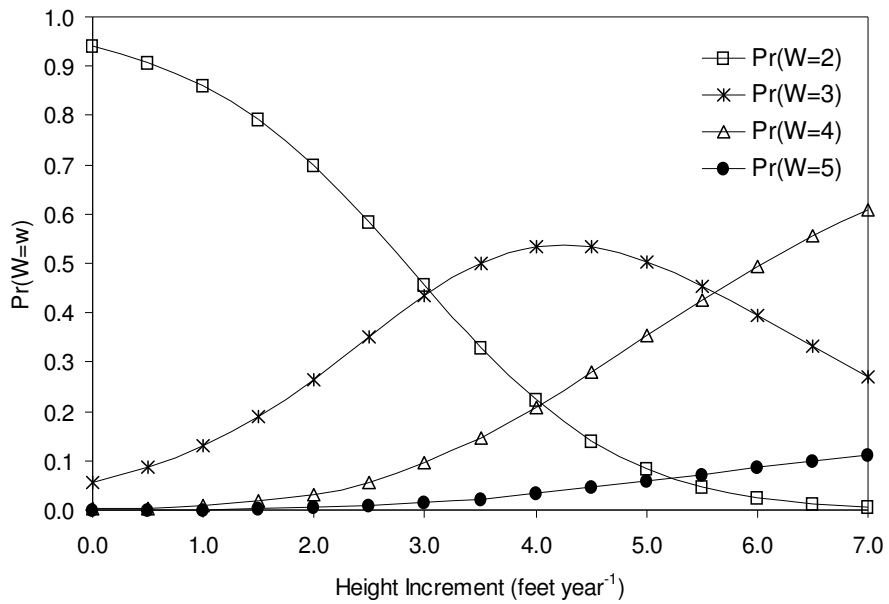


**Figure 4.4.** Predicted response probabilities for the number of whorls produced within a growing season.

The algorithm implemented to assign the *number of whorls per growing season* throughout the simulation includes the following steps:

(i) Predict the response probabilities of each category ( $\pi_j, j=1, \dots, J$ ) for a given value of the predictor variable ( $\Delta h$ , height increment),

(ii) generate  $J$  intervals defined as

$$[0, \pi_1], [\pi_1, \sum_{j=1}^2 \pi_j), [\sum_{j=1}^2 \pi_j, \sum_{j=1}^3 \pi_j), \dots, [\sum_{j=1}^{J-1} \pi_j, 1], \quad (4.7)$$

(iii) generate a random number  $z$  from a continuous uniform distribution  $U(0,1)$  (Casella and Berger 2002)

$$f(z|0,1) = \begin{cases} 1 & \text{if } z \in [0,1] \\ 0 & \text{otherwise,} \end{cases} \quad (4.8)$$

and

(iv) determine the interval that contains the random number; this defines the category (or number of whorls) that will be assigned as a stochastic process during the simulation.

On the other hand, the *location of whorls* along the stem within each growing season was determined using the observed relative mean location (Table 4.2). For instance, if for a given growing season it is predicted that two whorls (flushes) were produced, then the first whorl has to be located at a relative height of 0.54 of the predicted height increment ( $0.54 * \Delta h$ ) and the second at the end. During the simulation it was assumed that each growing season ended with a new whorl.

## 4.5.2 Modeling branch components

### Number of branches per whorl

Doruska and Burkhart (1994) estimated that the average number of living branches per whorl for loblolly pine was 2.6. Here, with a more limited data set, the average number of branches per whorl was 3.2 (Table 4.3). This larger average number of branches can be explained because in this study not only living branches were counted per whorl along the stem. However, the measurements done over bark along the stem will ultimately underestimate the real number of branches produced per whorl.

Differences were detected in the number of branches per whorl within growing seasons with an equal number of whorls ( $P < .05$ ). The apparent trend is that the number of branches for each consecutive whorl within a growing season increases (Table 4.3). However, the number of branches produced in each whorl was not significantly different in years when five whorls were produced. This conclusion was based on a small sample size ( $n = 8$  observations).

To account for the effect of increasing probability of having a larger number of branches per whorl through out the growing season, a stochastic procedure was implemented to assign the number of branches per whorl. The stochastic procedure consisted of sampling from a double truncated Poisson distribution (Johnson et al. 2005)

$$P(X = x | \theta) = \frac{\theta^x}{x!} \left( \sum_{j=1}^7 \frac{\theta^j}{j!} \right) \quad 1 \leq x \leq 7, \quad (4.9)$$

where one and seven are the minimum and maximum number of branches per whorl observed in the data set (Figure 4.5). The truncated Poisson distribution for the number of branches was fit to each combination of number of whorls and whorl number per annual shoot (Table 4.3). Then, the relationship between the parameter  $\theta$  and the whorl number within an annual shoot was analyzed (Figure 4.6). The general trend was an increasing value of the parameter  $\theta$  with increasing whorl number until whorl number three after

which the value of the parameter remains constant. A high value of  $\theta$  shifts the discrete distribution to the right giving more probability to higher values of  $x$  (number of branches). Even though the observed relationship was weak it was used to develop an equation to predict the parameter of the truncated Poisson distribution:

$$\hat{\theta} = 3.46799 - \frac{0.65751}{x} \quad 1 \leq x \leq 7 \quad (4.10)$$

The root mean square error of the equation (*RMSE*) was 0.299 and the coefficient of determination ( $R^2$ ) was 0.3365 ( $F = 6.09$ ,  $P = 0.0297$ ). The use of this procedure requires determining the number of whorls formed in a given growing season, which is accomplished using the multcategory logistic model. Once the number of whorls is predicted, equation (4.10) can be used to predict the parameter of the double truncated Poisson distribution. Assuming that three whorls were produced, the values of the parameter  $\hat{\theta}$  and probabilities for the number of branches in each whorl are given in Table 4.4. Clearly, the probability of obtaining a larger number of branches  $P(X=x)$  increases slightly with the whorl number within an annual shoot. The procedure requires generation, for each whorl, of a random number  $z$  from a continuous uniform distribution  $U(0,1)$  and comparison of it with its cumulative probability distribution  $P(X \leq x)$ . If the number  $z \geq P(X \leq x)$ , then  $x$  branches are assigned to the whorl. Assuming that for each whorl the following random numbers were generated  $Z = \{0.52, 0.85, 0.42\}$ , then the first whorl will have 3 branches, the second whorl 5 branches and the third whorl 3 branches (indicated in bold on Table 4.4).



**Table 4.3.** Number of branches per whorl disaggregated by the number of whorls produced per annual shoot.

| Whorls per<br>annual shoot | n          | Whorl<br>number | Branches per Whorl |          |          | F-value | P-value |
|----------------------------|------------|-----------------|--------------------|----------|----------|---------|---------|
|                            |            |                 | Mean               | Min      | Max      |         |         |
| 2                          | 58         | 1               | 2.97               | 1        | 6        | 4.81    | 0.0303  |
|                            |            | 2               | 3.45               | 1        | 6        |         |         |
| 3                          | 108        | 1               | 3.01               | 1        | 5        | 9.04    | 0.0002  |
|                            |            | 2               | 3.18               | 1        | 6        |         |         |
|                            |            | 3               | 3.64               | 1        | 7        |         |         |
| 4                          | 49         | 1               | 2.63               | 1        | 5        | 7.23    | 0.0001  |
|                            |            | 2               | 2.98               | 1        | 5        |         |         |
|                            |            | 3               | 3.43               | 1        | 5        |         |         |
|                            |            | 4               | 3.35               | 1        | 5        |         |         |
| 5                          | 8          | 1               | 3.00               | 1        | 4        | 0.17    | 0.9508  |
|                            |            | 2               | 3.36               | 2        | 5        |         |         |
|                            |            | 3               | 3.36               | 1        | 6        |         |         |
|                            |            | 4               | 3.00               | 1        | 4        |         |         |
|                            |            | 5               | 3.00               | 2        | 5        |         |         |
| <b>Total</b>               | <b>676</b> |                 | <b>3.21</b>        | <b>1</b> | <b>7</b> |         |         |

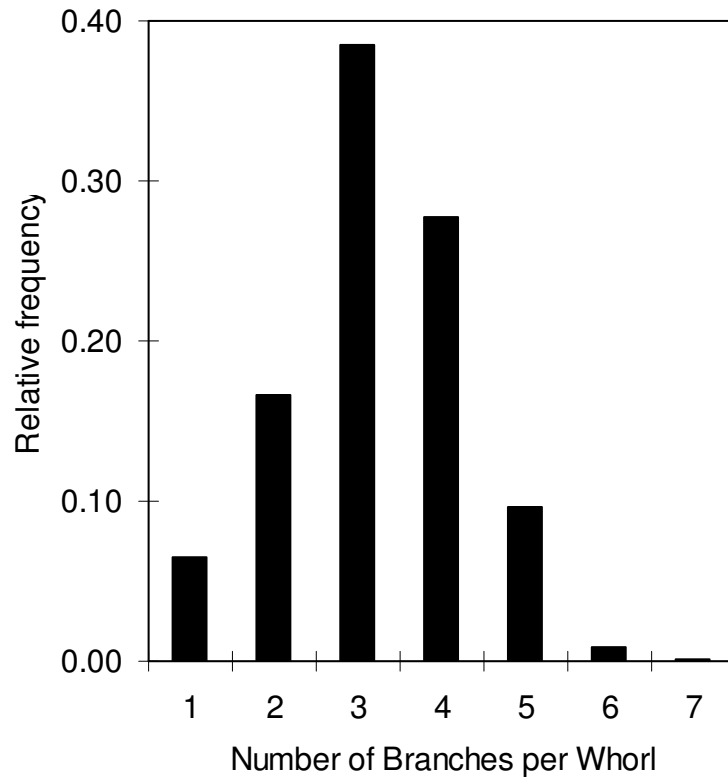


**Figure 4.5.** Empirical distribution of the number of branches per whorl for the destructive data set.

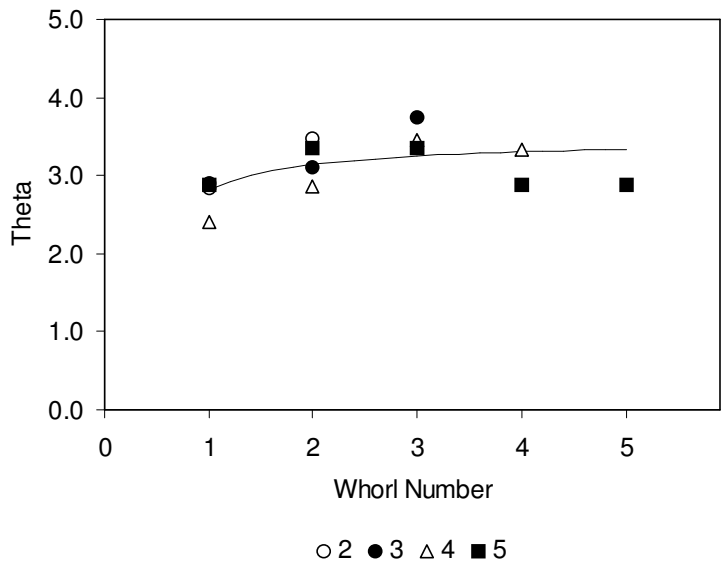


**Figure 4.6.** Relationship between parameter  $\theta$  and whorl number. The line represents the fit of equation (4.7).

**Table 4.4.** Probability and cumulative probability for the number of branches ( $x$ ) in each whorl, assuming that three whorls were formed in a growing season.

| Whorl<br>Number | $\hat{\theta}$ | Number of branches per whorl ( $x$ ) |      |      |             |      |             |      |      |
|-----------------|----------------|--------------------------------------|------|------|-------------|------|-------------|------|------|
|                 |                | 1                                    | 2    | 3    | 4           | 5    | 6           | 7    |      |
| 1               | 2.8            | P( $X=x$ )                           | 0.18 | 0.26 | 0.24        | 0.17 | 0.09        | 0.04 | 0.02 |
|                 |                | P( $X \leq x$ )                      | 0.18 | 0.44 | <b>0.68</b> | 0.85 | 0.94        | 0.98 | 1.00 |
| 2               | 3.1            | P( $X=x$ )                           | 0.15 | 0.23 | 0.24        | 0.18 | 0.11        | 0.06 | 0.03 |
|                 |                | P( $X \leq x$ )                      | 0.15 | 0.38 | 0.62        | 0.80 | <b>0.91</b> | 0.97 | 1.00 |
| 3               | 3.3            | P( $X=x$ )                           | 0.13 | 0.21 | 0.23        | 0.19 | 0.13        | 0.07 | 0.03 |
|                 |                | P( $X \leq x$ )                      | 0.13 | 0.34 | <b>0.58</b> | 0.77 | 0.90        | 0.97 | 1.00 |

### Branch orientation (Azimuth)

Doruska and Burkhart (1994) reported on branch orientation around the stem in loblolly pine trees and concluded that (i) on a whole-tree basis the azimuth of branches followed a uniform distribution and (ii) consecutive whorls with similar number of branches were positively correlated. Because of lack of data to perform a similar analysis, the algorithm suggested by Doruska and Burkhart (1994) was implemented. The azimuth was assigned for each new branch sampling from an a uniform distribution (Jammalamadaka and SenGupta 2001)

$$f(\phi) = \frac{1}{2\pi} \quad 0 \leq \phi \leq 2\pi \quad (4.11)$$

where  $\phi$  is measured in radians. If the number of branches ( $n$ ) assigned per whorl was one or two, then the orientation of each branch ( $m$ ) was randomly assigned by generating a random number from a continuous uniform distribution  $U(0,1)$  and substituting in the following expression

$$\phi(m) = 2\pi U(0,1) \quad m=1, \dots, n \text{ and } n=1, 2 \quad (4.12)$$

Contrarily, for those cases in which the number of branches assigned per whorl was equal or larger than three, the azimuth for the first branch was randomly selected using expression (4.12) and the azimuth for the others was obtained using the concept of equidistant distribution

$$\phi(m) = \frac{2\pi}{n}(m-1) + \phi(1) \quad m=2, \dots, n \text{ and } n=3, \dots, 7 \quad (4.13)$$

According to Doruska and Burkhart (1994) consecutive whorls with the same number of branches (e.g.  $n=n'$ ) were positively correlated; therefore, the azimuths of the upper whorl within the same growing season were assigned using the following expression

$$\phi(m') = \phi(m) + \zeta(n) \quad m=1, \dots, n \text{ and } n=3, \dots, 7 \quad (4.14)$$

where  $\zeta(n)$  is the difference in angles between consecutive whorls (Table 4.5). During the simulation consecutive whorls with same number of branches, but located in different growing seasons, were considered as independent realizations. In cases where two consecutive whorls contained seven branches, the difference angle for six branches was utilized.

### **Branch inclination**

The assignment of branch inclination was performed using a sampling distribution approach (Figure 4.7). The function selected was a three-parameter Weibull distribution defined by the probability density function (p.d.f.)

$$f(x | \alpha, \beta, \gamma) = \left(\frac{\gamma}{\beta}\right) \left(\frac{x - \alpha}{\beta}\right)^{\gamma-1} \exp\left(-\left(\frac{x - \alpha}{\beta}\right)^\gamma\right) \quad \alpha \leq x < \infty \quad (4.15)$$

where  $\alpha$  is referred as the location parameter (lower limit of the distribution),  $\beta$  is the scale parameter and  $\gamma$  is the shape parameter. This distribution function was introduced by Bailey and Dell (1973) in the forestry literature and since then it has been used in numerous forestry applications. Some important characteristics of this p.d.f. are its flexibility to represent diverse unimodal distributions and the existence of an analytic expression for its cumulative distribution function (c.d.f.). The parameter estimates are presented in Table 4.6 and were obtained using a modified non-linear maximization algorithm implemented in SAS 9.1 (SAS Institute, 2001).

**Table 4.5.** Difference angle (in degrees) for consecutive whorls having the same number of branches (NB) obtained by Doruska and Burkhart (1994).

| Difference angle | NB for consecutive whorls (n) |    |    |     |
|------------------|-------------------------------|----|----|-----|
|                  | 3                             | 4  | 5  | 6   |
| $\zeta(n)$       | 12                            | -5 | -3 | -53 |

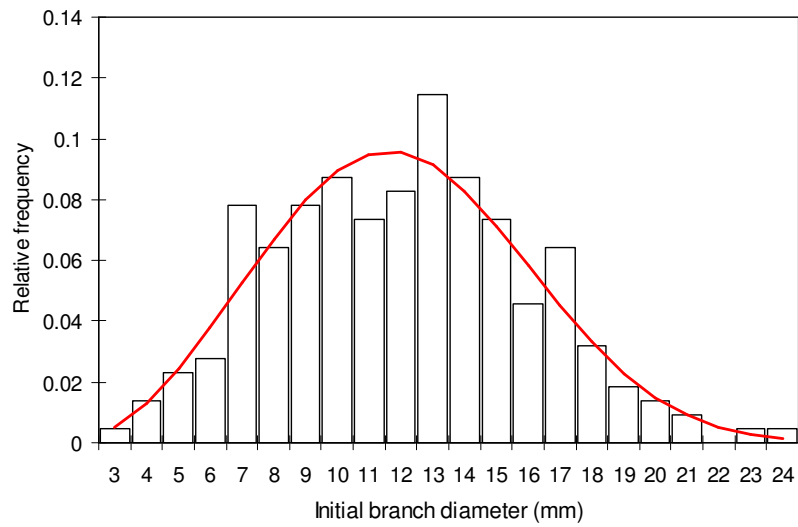
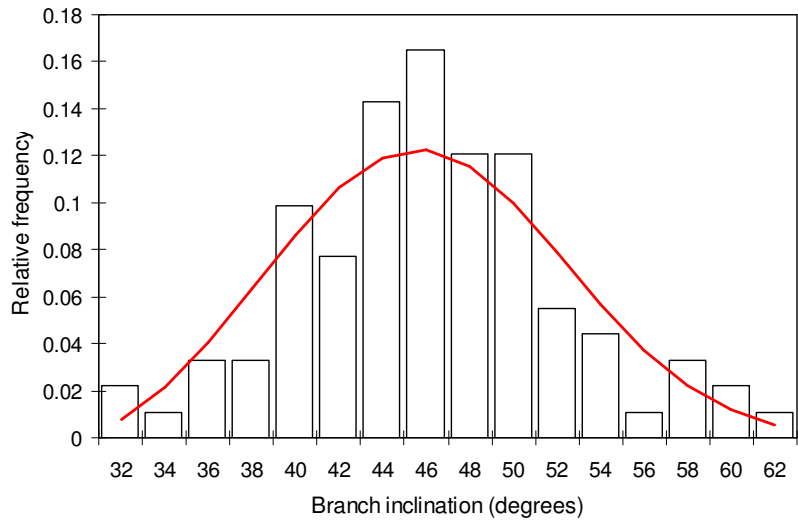


**Figure 4.7.** Empirical distribution and fit of the Weibull probability distribution function for (a) branch inclination (*BI*) and (b) the initial branch diameter (*IBD*).



**Table 4.6.** Parameter estimates and goodness of fit test for the Weibull probability density function (p.d.f.).

| Variables <sup>a</sup> | Parameters |         |          | KS test         |
|------------------------|------------|---------|----------|-----------------|
|                        | $\alpha$   | $\beta$ | $\gamma$ | <i>P</i> -value |
| BI                     | 29.1483    | 18.9318 | 2.9727   | > 0.25          |
| IBD                    | 1.6556     | 11.6227 | 2.8261   | > 0.50          |

<sup>a</sup> BI = branch inclination (degrees) and IBD = initial branch diameter (mm).

In order to constraint the upper limit of  $f(x)$  to the observed maximum inclination value ( $BI_{\max} = 62.86$  degrees), but maintaining the total probability area equal to one, a truncated Weibull distribution can be defined as (see Murphy and Farrar 1988)

$$g(x | \alpha, \beta, \gamma) = \frac{f(x | \alpha, \beta, \gamma)}{\int_{\alpha}^{BI_{\max}} f(x | \alpha, \beta, \gamma) dx} \quad \alpha \leq x \leq BI_{\max} \quad (4.16)$$

An analytical expression for the cumulative density function (c.d.f.) for  $g(x)$  is obtained integrating over the constrained domain of the random variable  $x$  ( $\alpha \leq x \leq BI_{\max}$ )

$$G(x | \alpha, \beta, \gamma) = \frac{1 - \exp[-((x - \alpha) / \beta)^{\gamma}]}{1 - \exp[-((BI_{\max} - \alpha) / \beta)^{\gamma}]} \quad \alpha \leq x \leq BI_{\max} \quad (4.17)$$

Finally, the initial branch diameter is randomly generated by sampling from  $G(x)$  where no sample will be larger than the upper bound defined as the maximum observed inclination value ( $BI_{\max} = 62.86$  degrees) from the data set. This process is accomplished by solving for  $x$  in formula (4.17) and replacing  $G(x)$  by a random variable from a continuous uniform distribution  $U(0,1)$

$$x = \alpha + \beta [\ln(1 - U(0,1) Z)]^{1/\gamma} \quad (4.18)$$

where  $Z = 1 - \exp[-((BI_{\max} - \alpha) / \beta)^{\gamma}]$ . This direct method for generating a random sample from a Weibull probability distribution function has been widely used in forestry for simulation (Daniels and Burkhart 1975, Westfall et al. 2004).

### **Initial branch diameter**

The approach implemented to determine the initial branch diameter for a new branch was similar to that used for simulating branch inclination. A three-parameter Weibull probability density function, constrained on its upper limit to the observed maximum inclination value ( $IBD_{\max} = 23.69$  mm) but maintaining the total probability area equal to one (Equation 4.17), was fitted to the empirical data (Figure 4.7 and Table 4.6).

### **Diameter growth of first-order branches**

The relationship between branch diameter increment ( $\Delta BD$ ) with other potential predictor variables was analyzed through graphical analysis (Figure 4.6). Branch diameter increment was negatively related with branch age ( $BA$ ), decreasing exponentially with increasing branch age. An increasing trend was observed between branch diameter increment and the increment in length of a live branch within the stem ( $\Delta BL$ ). The internal increment in length of a live branch was determined by the increment in stem growth and its angle of inclination. During the simulation process this variable can be estimated using information on branch inclination and stem growth from a taper equation.

A similar pattern as with branch age was observed between branch diameter increment and the relative position of a branch within the live crown (Figure 4.6). The relative position of a branch within the live crown is defined as:

$$Z = \frac{TH - BH}{CL} \quad 0 \leq Z \leq 1 \quad (4.19)$$

where  $TH$  is the total tree height (feet),  $BH$  is the height of the branch (feet) above the ground and  $CL$  is the crown length (feet). Branches located close to the tree tip ( $Z \rightarrow 0$ ) had higher rates of increment than those located close to the base of the live crown ( $Z \rightarrow 1$ ).

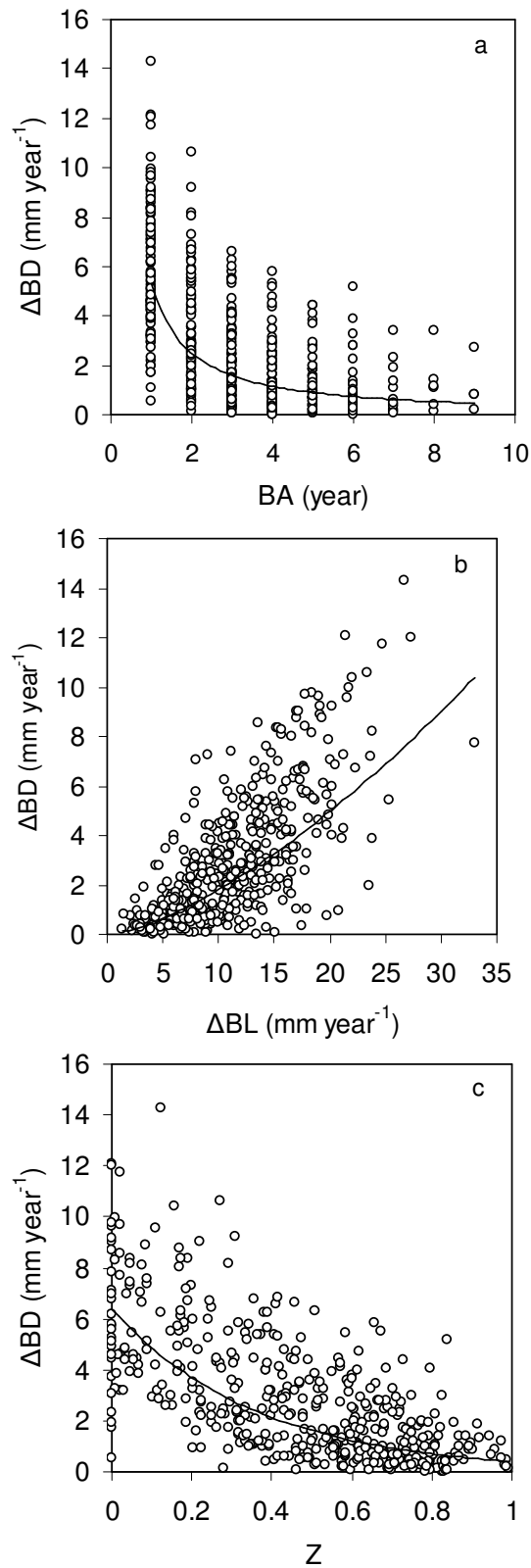


**Figure 4.8.** Relationships between branch diameter increment ( $\Delta BD$ ) with (a) branch age ( $BA$ ), (b) increment in branch length ( $\Delta BL$ ), and (c) relative position of the branch within the live crown ( $Z$ ).

The different equations evaluated to predict annual branch diameter increment (mm/year) were

$$\Delta BD = \beta_0 \exp(-\beta_1 BA) \quad (4.20)$$

$$\Delta BD = \beta_0 \Delta BL^{\beta_1} \exp(-\beta_2 BA) \quad (4.21)$$

$$\Delta BD = \beta_0 \Delta BL^{\beta_1} \exp(-(\beta_2 BA + \beta_3 Z)) \quad (4.22)$$

The inclusion of  $\Delta BL$  as an additional predictor variable decreases the MSE by 22.37% and the inclusion of both  $\Delta BL$  and  $Z$  decreases the MSE by 30.4% (Table 4.7). However, branch age ( $BA$ ) was found to be not significant under the presence of  $Z$ . It can be explained because of the high correlation between the branch age ( $BA$ ) and the relative position ( $Z$ ) of a branch within the live crown ( $r = 0.86, P < .0001$ ). Thus, an equation containing the increment in branch length and relative position of the branch within the live crown was selected for modeling annual branch diameter increment ( $\Delta BD$ )

$$\Delta BD = 0.7796 \Delta BL^{0.8272} \exp(-1.5344 Z) \quad (4.23)$$

where all parameter were significant at  $\alpha = .05$ , the fit index (FI) was 0.83, and the mean square error was 2.56. The studentized residuals were homogeneous for the predicted values (Figure 4.8).

**Table 4.7.** Parameter estimates and mean square error for the candidate equations to predict branch diameter increment ( $\Delta$ BD).

| Equation | Parameter | Estimate | SE     | Fit Index<br>(FI) | MSE  | MSER(%) <sup>a</sup> |
|----------|-----------|----------|--------|-------------------|------|----------------------|
| 4.20     | $\beta_0$ | 8.8467   | 0.4801 | 0.75              | 3.71 | -                    |
|          | $\beta_1$ | 0.4287   | 0.0288 |                   |      |                      |
| 4.21     | $\beta_0$ | 0.9237   | 0.1972 | 0.81              | 2.88 | 22.37                |
|          | $\beta_1$ | 0.8327   | 0.0746 |                   |      |                      |
|          | $\beta_2$ | 0.3060   | 0.0262 |                   |      |                      |
| 4.22     | $\beta_0$ | 0.7697   | 0.1520 | 0.83              | 2.56 | 30.4                 |
|          | $\beta_1$ | 0.8295   | 0.0687 |                   |      |                      |
|          | $\beta_2$ | -0.0074  | 0.0408 |                   |      |                      |
|          | $\beta_3$ | 1.5656   | 0.2080 |                   |      |                      |

<sup>a</sup> Mean square error reduction.

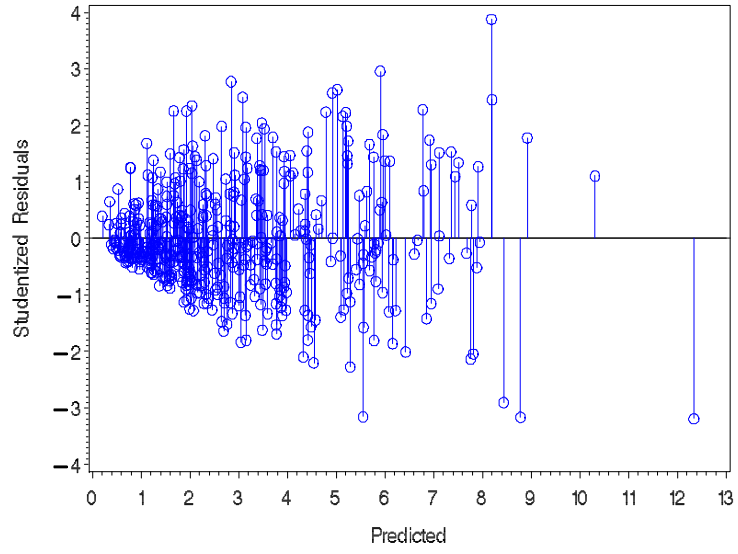


**Figure 4.9.** Studentized residuals for equation (4.23) plotted versus predicted values.

### Self-pruning process

The time after branch death when a limb breaks off was modeled stochastically based on the following cumulative distribution function (c.d.f.) for a continuous random variable ( $\Delta t$ )

$$F(\Delta t | \underline{\theta}) = \begin{cases} 0 & 0 \leq \Delta t \leq \theta_0 \\ \frac{1}{(\theta_1 - \theta_0)}(\Delta t - \theta_0) & \theta_0 \leq \Delta t \leq \theta_1 \end{cases} \quad (4.24)$$

The parameter  $\theta_0$  represents the minimum time after branch death that a branch takes to drop off and the parameter  $\theta_1$  represents the maximum time required to self-prune. Based on the study of Reynolds (1967) the values for the parameters were set to  $\theta_0 = 4$  and  $\theta_1 = 11$  years. Under this model the probability to drop off during the first four years after branch death is zero (Figure 4.10). After that, the probability of a branch to self-prune increases linearly between  $\theta_0 = 4$  and  $\theta_1 = 11$  years old.

During the simulation process, when  $\Delta t \geq 4$  years a number  $z$  is randomly selected from a continuous uniform distribution  $U(0,1)$  and compared to the value of the proposed c.d.f. If the value of this random number is smaller than the value of the c.d.f., then the year of self-pruning ( $\Delta t$ ) after branch death is assigned to a given branch. Subsequently, and estimate the size of the limb (LS in mm) left on the stem is required. The size of the limb was assigned stochastically using values generated from a continuous uniform distribution  $(0, \theta_3)$ . Values are assigned by inverting the c.d.f. and generating a random number from a continuous uniform distribution  $(0,1)$

$$LS = \theta_3 U(0,1) \quad (4.25)$$

Based on the observational study from Reynolds (1967) the parameter value given to  $\theta_3$  was 76 mm (3 inches). The proposed self-pruning model, even though simple in nature, can be easily parameterized.



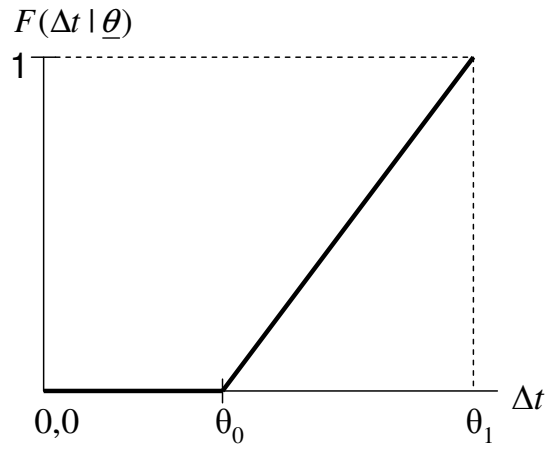


**Figure 4.10.** Probability of a branch to self-prune after branch death, where  $\theta_0 = 4$  years and  $\theta_1 = 11$  years.

### **4.5.3 Prediction of branch diameter growth and internal stem structure**

The usefulness of the prediction system is illustrated using information of growth from a simulated tree. The simulation was performed in PTAEDA3.1 for the Coastal Plain Physiographic region considering an initial spacing of 8 ft x 8 ft, site index of 65 ft (base age 25 years), and a rotation age of 30 years. All the information required for simulating the process of branch dynamics and knot formation is presented in Table 4.8. Because the proposed branch model does not require information on tree location (distance-independent), the model can be linked with any individual-tree growth simulator that may provide with similar information.

At the end of the simulation period the tree has a diameter at breast height of 10.7 inches (27.3cm), total height of 72.7 ft (22.2m) and height to base of live crown of 48.7 ft (14.8m).

#### **Number of whorls and branches per growing season**

The number of whorls per growing season is assigned stochastically and the probability of producing more whorls increases with increasing increment in total tree height. The stochastic assignment of whorls for the simulated tree illustrates this behavior, where the minimum of whorls produced was 2 and the maximum 4 (Figure 4.11a). In this case, the maximum number of whorls was assigned between tree ages 4 and 7 years. The location of each predicted whorl along the stem within each growing season and the number of branches assigned is presented in Figure 4.11b. As expected when sampling from the double truncated Poisson distribution, the number of branches per whorl ranged between 1 and 7. The number of branches simulated per whorl showed an indeterminate pattern between the range of observed values. The same type of relationship between number of branches in a whorl and whorl height was reported by Doruska and Burkhart (1994) for loblolly pine.

**Table 4.8.** Simulated growth for a dominant tree using PTAEDA3.1.

| Age<br>(years) | DBH<br>(inches) | TH<br>(feet) | HLC<br>(feet) |
|----------------|-----------------|--------------|---------------|
| 1              | 0.19            | 1.61         | 0.23          |
| 2              | 0.49            | 4.07         | 0.46          |
| 3              | 0.74            | 6.96         | 0.69          |
| 4              | 1.54            | 10.17        | 1.12          |
| 5              | 2.35            | 13.71        | 1.64          |
| 6              | 3.17            | 17.49        | 2.36          |
| 7              | 4.00            | 21.52        | 3.35          |
| 8              | 4.84            | 25.75        | 6.33          |
| 9              | 5.37            | 27.76        | 9.42          |
| 10             | 5.79            | 29.66        | 10.83         |
| 11             | 6.26            | 32.35        | 12.70         |
| 12             | 6.72            | 35.20        | 14.73         |
| 13             | 7.10            | 37.80        | 16.77         |
| 14             | 7.43            | 40.12        | 18.70         |
| 15             | 7.78            | 43.01        | 21.10         |
| 16             | 7.97            | 44.72        | 22.77         |
| 17             | 8.03            | 45.41        | 23.79         |
| 18             | 8.19            | 46.98        | 25.39         |
| 19             | 8.38            | 48.92        | 27.23         |
| 20             | 8.65            | 51.51        | 29.46         |
| 21             | 8.86            | 53.61        | 31.40         |
| 22             | 8.98            | 55.05        | 32.87         |
| 23             | 9.19            | 57.12        | 34.78         |
| 24             | 9.34            | 58.83        | 36.42         |
| 25             | 9.72            | 62.37        | 39.30         |
| 26             | 9.82            | 63.52        | 40.58         |
| 27             | 9.91            | 64.67        | 41.80         |
| 28             | 10.22           | 67.65        | 44.32         |
| 29             | 10.68           | 71.88        | 47.74         |
| 30             | 10.74           | 72.70        | 48.69         |

<sup>a</sup> DBH is the diameter at groundline when total height less than 4.5'.

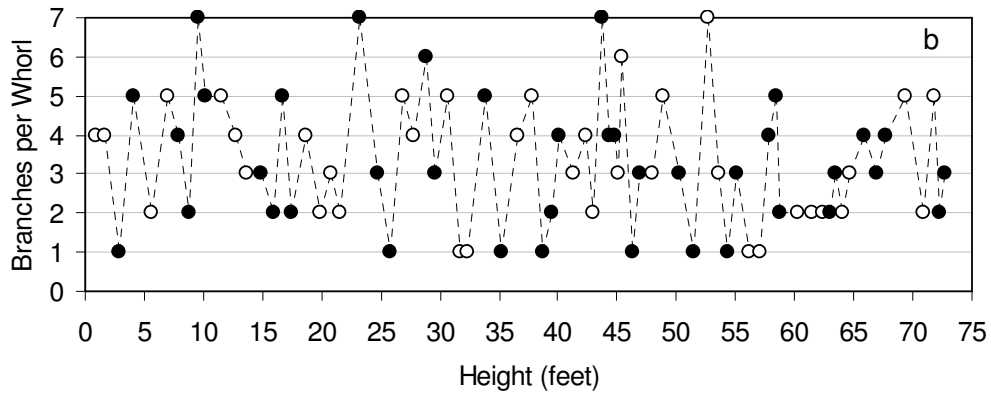
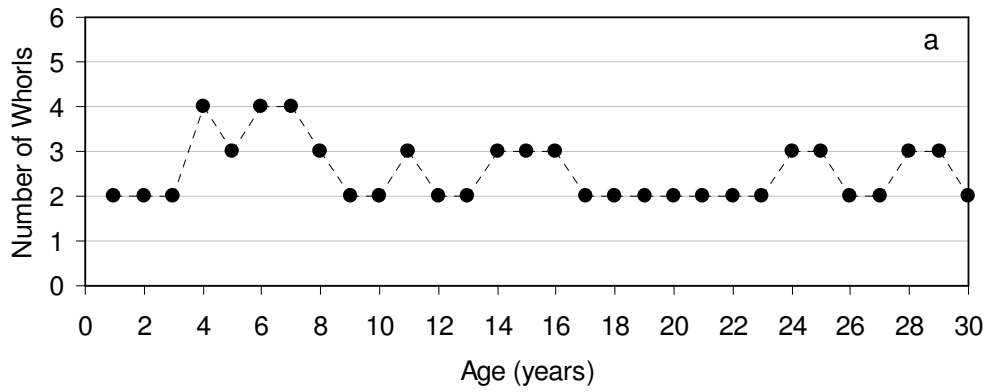


**Figure 4.11.** Simulated (a) number of whorls per growing season and (b) number of branches per whorl, where consecutive points with similar symbol belong to the same growing season.

### **Vertical trend of branch diameters**

For each branch, information on spatial location, size and type (live or dead) is dynamically updated and maintained in the output-file. Therefore, at the end of the simulation period, is possible to obtain information on the vertical trend of branch diameter along the stem (Figure 4.11). From the bottom, the diameter of the branches increases rapidly until a stem height of about 10 ft, then, until the height to crown base, they maintain a similar range of diameters. From the crown base to the tip, the branch diameters decrease, as expected, because of differences in branch age within the live crown. The smaller branch diameters at the bottom of the tree result from the accelerated crown recession process at early ages; after that, branches are retained comparatively for a longer period of time within the live crown. Therefore, it is expected that the first butt log should contain smaller branch diameters in comparison to the second butt log. This behavior has been reported in yield recovery studies performed in loblolly pine (Clark et al. 2004).

Information generated for each tree can be summarized by computing the mean, maximum and minimum branch diameter for each whorl. In addition to branch dimensions valuable information is generated in terms of type of branches found along the stem. For the simulated tree, occluded branches can be found below the stem height of 10 feet (Figure 4.11). In conjunction, both quantitative and qualitative information can be used to estimate the expected value of each tree and logs obtained along the stem.

The internal location of knots and the prediction of the live and dead portions permitted the simulation of the internal stem structure. This information can be useful to determine the zones inside the stem that contain defects in terms of branches, as well as zones where it is possible to obtain clear wood (Figure 4.13). Note that the zone with live branches is consistent with the crown recession (left-side) predicted by PTAEDA3.1 and utilized to simulate branch mortality. As a result of branch dynamics and knot formation, the simulated tree shows a small amount of clear wood can be obtained at the bottom where occluded branches can be found (Figure 4.12).

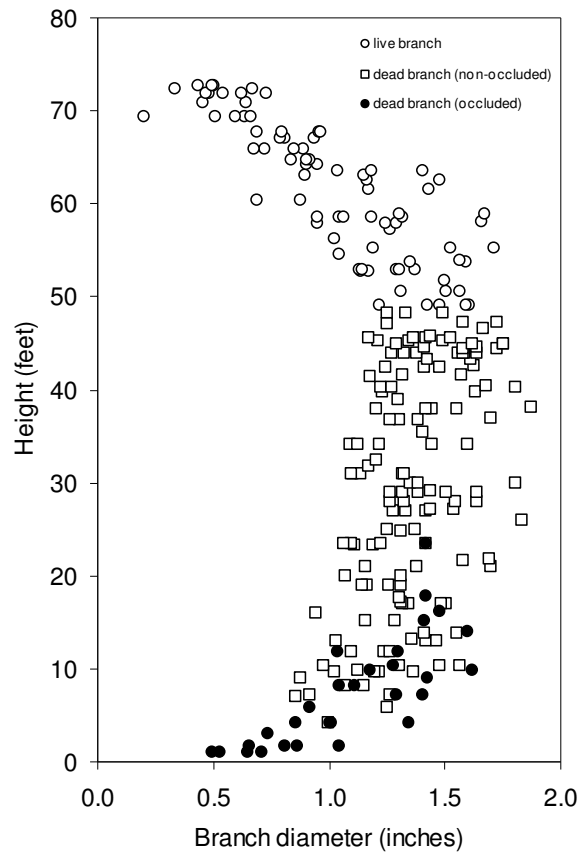


**Figure 4.12.** Vertical trend of simulated branch diameters.

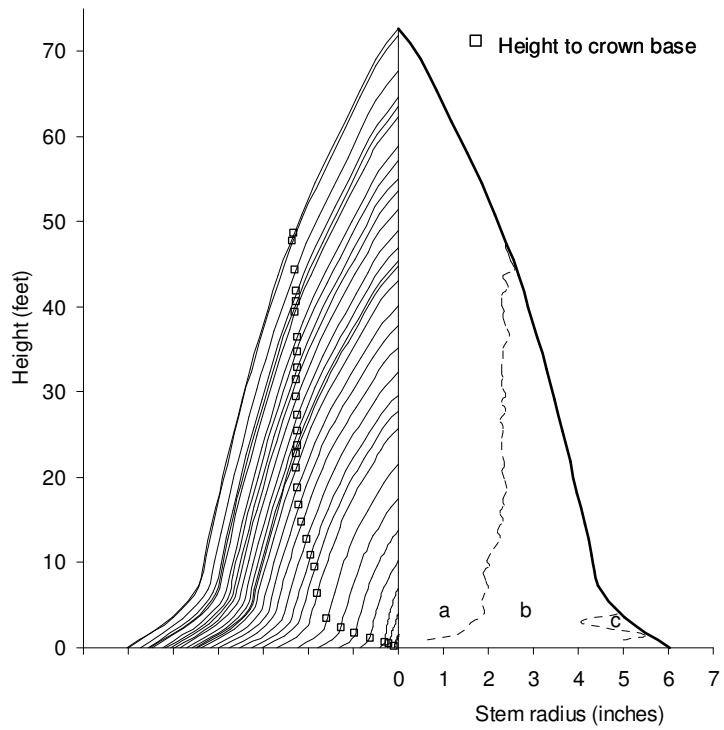


**Figure 4.13.** Internal stem structure in terms of ring-width (left-side) and branch defects (right-side) derived for the simulated tree (DBH = 10.7 inches, TH = 72.7 feet and HLC = 48.7 feet), where a: zone with live branches, b: zone with dead branches and c: clear-wood zone.

Under this framework, additional information on internal stem structure such as ring width for a given stem height (Figure 4.13, left-side) or specific gravity (Tasissa and Burkhart 1998, Daniels et al. 2002) can be easily added. Also, under the assumption that juvenile wood is produced in the live crown, its volume can be easily derived.

### **Vertical trend of knot volume and cumulative distribution**

Even though, the volume of knots does not occupy a large part of the stem, it could be of interest to investigate via simulation their vertical trend and cumulative distribution in terms of volume type (live or dead) along the stem. For the simulated tree the total amount of knot volume was 0.317 cu ft (0.009 m<sup>3</sup>), which corresponds to 1.988 percent of the total stem volume 15.985 cu ft (0.452 m<sup>3</sup>) obtained by integrating the taper equation ( $b_1=-3.0257$ ,  $b_2=1.4586$ ,  $b_3=-1.4464$ ,  $b_4=39.1081$ ,  $a_1=0.7431$  and  $a_2=0.1125$ ). Considering the process of crown and branch dynamics is expected that larger amount of total volume of individual knots should be found near the stem bottom. According to the simulation, the total volume of individual knots increases from the bottom to a point close to the 10 ft and decreases to the tip (Figure 4.14a). A separate analysis considering only the volume contained in the live portion of the knots showed similar vertical trend as that of branch diameter (Figure 4.14b). From the bottom, knot volume of the live portion increases until a point where it remains constant along the stem and after that decreases to the tip. Comparatively, in the bottom part of the stem, the volume contained in the dead portion is larger than the amount of volume contained in the live portion of knots (Figure 4.14c). It clearly illustrates the effect of dead branches (limbs) that persist for a long period of time on the surface in the most valuable portion of the stem. Even though the branch diameters at the bottom are smaller, the high proportion of dead knots can reduce the value of logs located in this portion of the stem.



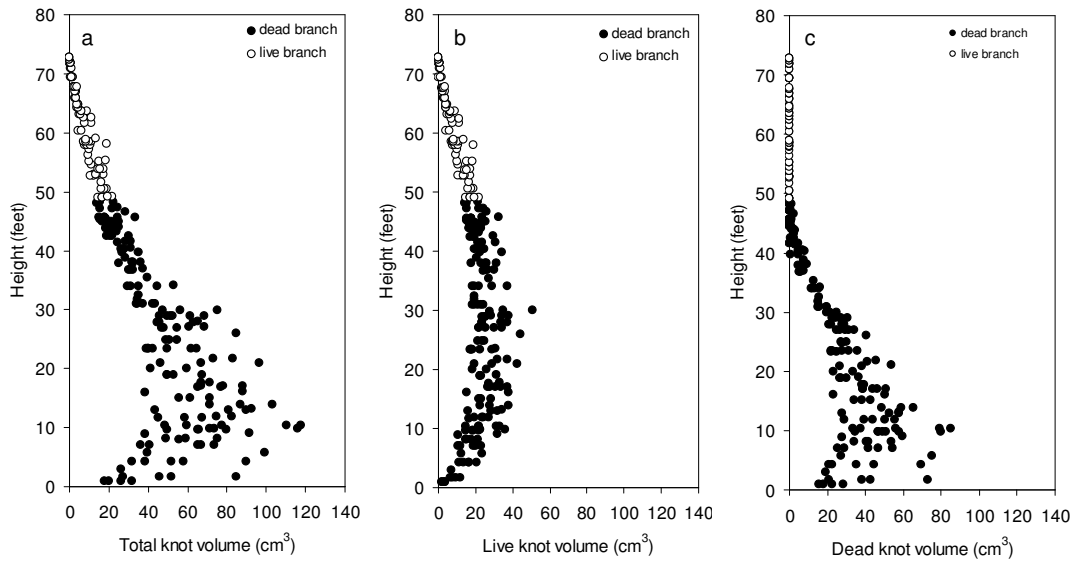


**Figure 4.14.** Volume of individual knots along the stem (a) total knot volume, (b) live knot volume and (c) dead knot volume.

Even though, a significant amount of dead branches is attached internally in the bottom portion of the stem, at upper stem level there is a larger amount of knot volume contained in live branches (Figure 4.15). This conclusion, however, is only valid for the simulated tree. The simulation framework and output-file can be useful to investigate these types of relationships for trees growing under different management conditions.

### **Three-dimensional representation of internal branch structure**

Determination of spatial location of branches over time along and around the stem required information on tree shape at each age. The procedure implemented assumed that when a tree has a predicted total height less than or equal to 4.5 ft (1.37m) the shape of the tree is a cone; otherwise the stem shape is recovered using the Max and Burkhardt (1976) taper equation. The first assumption was facilitated because before a tree reaches 4.5ft in total tree height, PTAEDA3.1 predict the diameter at groundline (Westfall et al. 2004). However, during this transition phase the simulated stem profiles may cross-over inconsistently below a stem height of 4.5 ft e.g. the predicted stem diameter may be smaller at older ages when using a taper equation at the same stem height. The main problem is that predicted stem diameter increments at some points along the stem may be negative. Furthermore, prediction of branch diameter growth requires determining stem diameter growth at the point a branch arises from the stem surface.

To overcome this inconsistency the groundline diameter was estimated using the following formula

$$GLD_i = TH_i (GLD / TH) \quad (4.25)$$

where  $GLD_i$  is the corrected groundline diameter at age  $i$ ,  $TH_i$  is the total tree height at age  $i$ ,  $GLD$  is the groundline diameter estimated with the taper equation at the age when  $TH > 4.5$  ft.



**Figure 4.15.** Cumulative knot volume along the stem for the total, live and dead portions.

This procedure was applied to the simulated tree presented in Table 4.7. For instance, the total tree height is larger than 4.5 feet at the age 3 years and the groundline diameter estimated at that age was 0.83 inches. Thus,  $GLD/TH = 0.11925$ ; multiplying this value times the total tree height predicted at ages 1 and 2, gives the predicted groundline diameters included in Table 4.7.

In conjunction with the quantification of branch diameters and knot dimensions, the simulation framework maintains the necessary spatial information to allow for a graphical visualization of the internal location of knots (Figure 4.16). Accordingly, sections of the stem can be extracted for comprehensive 3D visual analysis ('glass log'), which might be enhanced if the developed knot model (see Chapter 3) is graphically incorporated in the visualization.

#### **4.5.4 Application, limitations and future work**

The developed modeling framework can provide detailed information over time on branch diameter along and around the stem. The information generated can be used to evaluate the effect of silvicultural management regimes on branch diameter growth and the formation of internal defects (knots). The framework can be used to incorporate a model to predict the effect of pruning on production of clear wood (e.g. O'Hara and Buckland 1996), juvenile-mature wood demarcation (Tassisa and Burkhart 1998b) and prediction of specific gravity model at any stem height (Tassisa and Burkhart 1998a, Daniels et al. 2002). A 3D representation and visualization of internal defects in conjunction with prediction of additional wood properties can describe the internal stem structure making it possible to establish a linkage with virtual sawing processes (e.g. sawing simulator). Currently, costly data for sawing simulation is obtained by scanning sample logs, peeling and performing posterior reconstruction of internal defects (Pinto et al. 2003, Pinto et al. 2005). These studies can be performed by utilizing simulated trees. Additionally, simulated trees can meet data needs while reducing the time and cost involved in collecting data by destructive sampling methods as lumber grade recovery studies (Clark and McAlister 1998, Hilpp and Pelkki 2003, Clark et al. 2004).

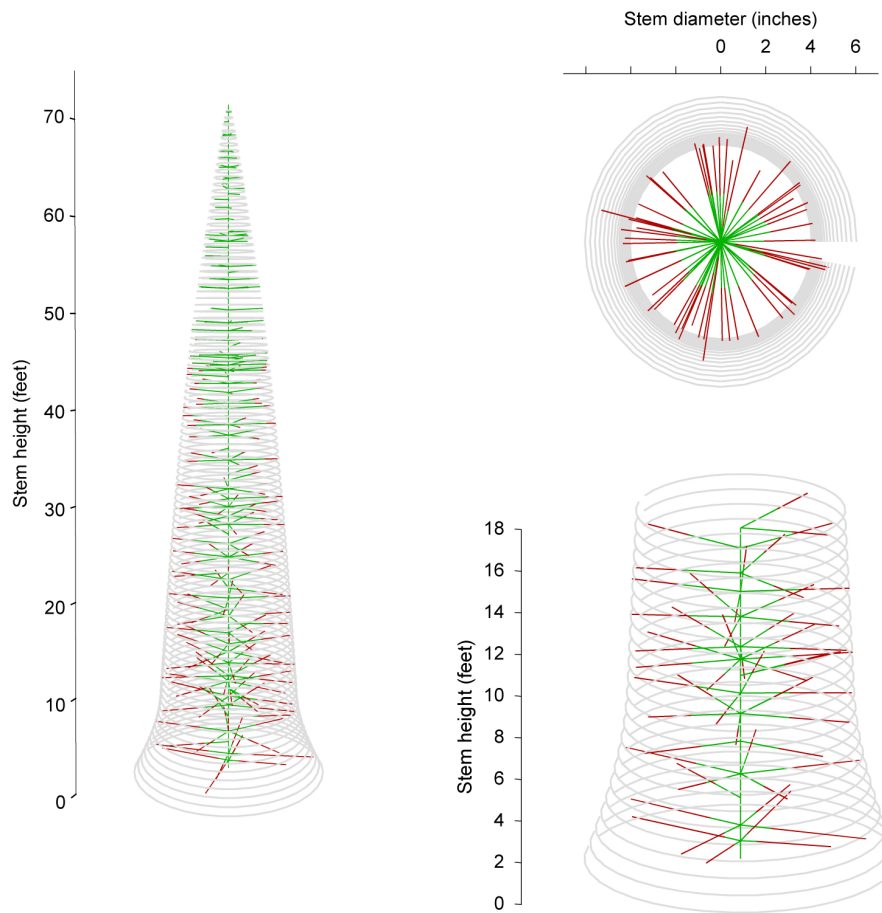


**Figure 4.16.** Three-dimensional representation of internal branches (knots) indicating live and dead portions.

Briefly, the proposed modeling framework allows enhancing the utility of individual-tree growth models and the integration of forest growth and industrial process simulation. Consideration of the complete production chain (forest and industry) provides a better evaluation of the effects of alternative silvicultural regimes with the aim of producing specific end products.

However, an evident shortcoming of this branch model is that it is limited to the genetic stock, site quality and environmental conditions where data were taken. All of these factors greatly influence branch development (Bridgwater et al. 1985, Bridgwater 1990, Mudano et al. 1992). Crown structure and branch development in loblolly pine is not only affected by initial planting density and spacing (e.g. Clark et al. 1994, Sharma 2002), but also by other silvicultural practices including thinning (e.g. Baldwin et al. 2000), pruning (e.g. Clark et al. 2004) and fertilization (e.g. Yu et al. 2003). The model assumes that the effect of silvicultural practices on branch growth is accounted for indirectly through their effects on stem growth. However, this logical relationship has not been fully studied for loblolly pine. Regardless, this idea is partially supported from findings in other tree species (e.g. Briggs et al. 2002). Mäkinen (1999) found in Scots pine that radial growth of the stem and the thickest branches were interconnected, and factors that influence growth of the stem have a similar influence on the growth of branches. Several studies have indicated consistently that external branch characteristics can be successfully modeled utilizing tree dimensions, which explains most of the variability. The use of site index has demonstrated inconsistent results, where in most cases it has been found to be not significant. Because measures of competition have explained only a small amount of variability when modeling external branch characteristics, their incorporation in a predictive model is considered to be not necessary.

Even though, spatial location of branches along and around the stem is known during the simulation, the model has not incorporated the effect of spacing between neighbor trees on branch dimensions and self-pruning processes. Amateis et al. (2004) found significant differences in mean maximum branch diameter between two spacing treatments, with the 1:3 spacing having larger maximum branch diameter in the butt log than the 3:4 spacing. In absolute terms the reported differences can be considered minor.

The demonstrated utility of a dynamic branch model should motivate the collection of longitudinal data, in the form of direct measurements or applying analysis of data gathered by destructive sampling techniques. For instance, mortality of branches within the live crown was not incorporated in the model structure due to lack of information from experimental and/or observational studies. Knowledge of the self-pruning process is incomplete, although most of the internal defects (knots) of the butt logs can be attributed to dead branches.

#### **4.6 Conclusions**

A general stochastic framework for predicting the growth of first-order branch diameter and internal location of knots was developed. The prediction system assumes that branch diameter growth is driven by crown dynamics and tree stem growth. Thus, only information on diameter, total height and height to live crown growth is required for incorporating the proposed model. Simulated trees show logical behavior in terms of vertical trend in branch diameters along the stem, which was consistent with observations in other tree species.

The developed system allows including additional wood properties in the simulation (e.g. ring width at any stem height, juvenile-mature wood stem volumes and specific gravity). Because during the simulation information on spatial location and dimension of knots is maintained, the dynamic branch model should be adequate to link with existing bucking and sawing simulators. The main utility could be to generate an integrated modeling system that considers the complete chain of wood production.

Some processes of branch dynamics (e.g. branch mortality within the crown) were not included in the branch model and others (e.g. self-pruning) were included although available knowledge and data is limited. An adequate understanding of branch dynamics in loblolly pine requires information from diverse silvicultural practices, especially from those aimed at producing solid wood products.

The demonstrated potential of the branch model should promote further research to obtain necessary longitudinal data on crown and branch dynamics, which is required to validate the overall performance of the proposed branch model and eventually to improve its components.

#### **4.7 Acknowledgements**

Financial support for this research was provided through the Loblolly Pine Growth and Yield Research Cooperative at Virginia Tech. Financial support from the Sustainable Engineered Materials Institute, Virginia Tech, and USDA/CSREES Fund Number 2005-06172 is also gratefully acknowledged. Necessary equipment and facilities to analyze wood samples were kindly provided by the Forest Harvesting and Dendrocronological Laboratories. Dr. Phil Radtke, Dr. Carolyn Copenhaver and Dr. Rien Visser provided helpful directions during the development of this study which is deeply appreciated. Also, we thank Mr. Tal Roberts and Mr. Noah Adams for valuable and excellent assistance during the dissection of whorl samples.

#### **4.8 Literature Cited**

- Agresti, A. 2002. Categorical data analysis. Second Edition, John Wiley and Sons, Inc. 710p.
- Amateis, R.L., H.E. Burkhart, and S.M. Zedaker. 1988. Experimental design and early analysis for a set of loblolly pine spacing trials. P. 1058-1065 *in* Forest Growth Modeling and Prediction, Ek, A.R. , S.R. Shifley and T.E. Burk (eds.). USDA For. Serv. Gen. Tech. Rep. NC-120.



- Amateis, R.L., and H.E. Burkhart. 2005. The influence of thinning on the proportion of peeler, sawtimber, and pulpwood trees in loblolly pine plantations. *South. J. Appl. For.* 29:158-162.
- Amateis, R.L., J. Liu, M.J. Ducey, and H.L. Allen. 2000. Modeling response to midrotation nitrogen and phosphorus fertilization in loblolly pine plantations. *South. J. Appl. For.* 24:207-212.
- Amateis, R.L., P.J. Radtke, and G.D. Hansen. 2004. The effect of spacing rectangularity on stem quality in loblolly pine plantations. *Can. J. For. Res.* 34:498-501.
- Baldwin, V.C., Jr., K.D. Peterson, and D.R. Simmons. 1995. A program to describe the crown shape of loblolly pine trees. *Compiler* 13:17-19.
- Baldwin, V.C., Jr., and K.D. Peterson. 1997. Predicting the crown shape of loblolly pine trees. *Can. J. For. Res.* 27:102-107.
- Baldwin, V.C. Jr., K.D. Peterson, A. Clark III, R.B. Ferguson, M.R. Strub, and D.R. Bower. 2000. The effects of spacing and thinning on stand and tree characteristics of 38-year-old loblolly pine. *For. Ecol. Manage.* 137:91-102.
- Batschelet, E. 1981. *Circular statistics in biology*. Academic Press, London.
- Bailey, R.L., and T.R. Dell. 1973. Quantifying diameter distributions with the Weibull function. *For. Sci.* 19(2):97-104.
- Bollman, M.P. and G.B. Sweet. 1976. Bud morphogenesis of *Pinus radiata* in New Zealand: The initiation and extension of the leading shoot of one clone at two sites. *N. Z. J. For. Sci.* 6:376-392.
- Boyer, W.D. 1970. Shoot growth patterns of young loblolly pine. *For. Sci.* 16:472-482.
- Bridgwater, F.E. 1990. Shoot elongation patterns of loblolly pine families selected for contrasting growth potential. *For. Sci.* 36:641-656.
- Bridgwater, F.E., C.G. Williams, and R.G. Campbell. 1985. Patterns of leader elongation in loblolly pine families. *For. Sci.* 31:93-944.
- Briggs, D. 1996. Modeling crown development and wood quality. *J. For.* 94(12): 24-25.
- Briggs, D., E. Turnblom, O. Høibø, and S. Irmen. 2002. Relationship between branch diameter growth and stem growth in young coastal US Douglas-fir. P. 282-289 *in* Fourth Workshop Connection between silviculture and wood quality through

- modelling approaches and simulation softwares, Nepveu, G. (ed.). Harrison Hot Spring, B.C., Canada.
- Brown, G.S. 1962. Stages in branch development and their relation to pruning. *The New Zealand Journal of Forestry*. 8:608-622.
- Burkhart, H.E., R.L. Amateis, J.A. Westfall, and R.F. Daniels. 2004. PTAEDA 3.1: Simulation of individual tree growth, stand development and economic evaluation in loblolly pine plantations. Department of Forestry, Virginia Polytechnic Institute and State University. 23p.
- Casella, G., R.L. Berger. 2002. *Statistical inference*. Second edition, Duxbury. 660p.
- Catchpole, K., I. Andrew, M.R. Nester, K. Harding and B. Hogg. 2002. Development of branch models for use in a silvicultural decision support system. P. 406-414 *in* Fourth Workshop Connection between silviculture and wood quality through modelling approaches and simulation softwares, Nepveu, G. (ed.). Harrison Hot Spring, B.C., Canada.
- Clark III, A., and R.F. Daniels. 2002. Modeling the effect of physiographic region on wood properties of planted loblolly pine in Southeastern United States. p. 54-60 *in* Fourth Workshop Connection between silviculture and wood quality through modelling approaches and simulation softwares, Nepveu, G. (ed.). Harrison Hot Spring, B.C., Canada.
- Clark III, A., and R.H. McAlister. 1998. Visual tree grading systems for estimating lumber yields in young and mature southern pine. *Forest Prod. J.* 48(10):59-67.
- Clark III, A., J.R. Saucier, V.C. Baldwin, and D R. Bower. 1994. Effect of initial spacing and thinning on lumber grade, yield, and strength of loblolly pine. *For. Prod. J.* 44 (11-12):14-20.
- Clark III, A., M. Strub, L. R. Anderson, H.G. Lloyd, R.F. Daniels, and J.H. Scarborough. 2004. Impact of early pruning and thinning on lumber grade yield from Loblolly pine. P. 199-204 *in* Proceedings of the 12<sup>th</sup> biennial southern silvicultural research conference, Connor, K.F. (ed.). USDA For. Serv. Gen. Tech. Rep. SRS-71.
- Colin, F. and F. Houllier. 1991. Branchiness of Norway spruce in north-eastern France: modeling vertical trends in maximum nodal branch size. *Ann. Sci. For.* 48:679-693.

- Colin, F. and F. Houllier. 1992. Branchiness of Norway spruce in north-eastern France: predicting the main crown characteristics from usual tree measurements. *Ann. Sci. For.* 49:511-538.
- Daniels, R.F., and H.E. Burkhart. 1975. Simulation of individual tree growth and stand development in managed loblolly pine plantations. Virginia Polytechnic Institute and State University, Pub. FWS-5-75.69p.
- Daniels, R.F., R. He, A. Clark III, and R.A. Souter .2002. Modeling wood properties of planted loblolly pine from pith to bark and stump to pith. P. 238-245 *in* Fourth Workshop Connection between silviculture and wood quality through modelling approaches and simulation softwares, Nepveu, G. (ed.). Harrison Hot Spring, B.C., Canada.
- Doruska, P.F., and H.E. Burkhart. 1994. Modeling the diameter and locational distribution of branches within the crowns of loblolly pine trees in unthinned plantations. *Can. J. For. Res.* 24:2362-2376.
- Doruska, P.F., and J.E. Mays. 1998. Crown profile modeling of loblolly pine by nonparametric regression. *For. Sci.* 44:445-453.
- Dyer, M.E., and H.E. Burkhart. 1987. Compatible crown ratio and crown height models. *Can. J. For. Res.* 17:572-574.
- Fujimori, T. 1993. Dynamics of crown structure and stem growth based on knot analysis of a hinoki cypress. *For. Ecol. Manage.* 56:57-68.
- Garber, S.M., and D.A. Maguire. 2005. Vertical trends in maximum branch diameter in two mixed-species spacing trials in the central Oregon Cascades. *Can. J. For. Res.* 35:295-307.
- Gartner, B.L. 2005. Assessing wood characteristics and wood quality in intensively managed plantations. *J. For.* 103(2):75-77.
- Gilmore, D.W., and R.S. Seymour. 1997. Crown architecture of *Abies balsamea* from four canopy positions. *Tree Physiology* 17:71-80.
- Grace, J.C., and M.J. Carson. 1993. Prediction of internode length in *Pinus radiata* stands. *N. Z. J. For.* 23:10-26.
- Grace, J.C., W. Blundell, and D. Pont. 1998. Branch development in pinus radiata – model outline and data collection. *N. Z. J. For. Sci.* 28:182-194.

- Grace, J.C., D. Pont, and C.J. Goulding. 1999. Modelling branch development for forest management. *N. Z. J. For. Sci.* 29:391-408.
- Griffing, C.G., and W.W. Elam. 1971. Height growth of loblolly pine saplings. *For. Sci.* 17:52-54.
- Haygreen, J.G., and J.L. Bowyer. 1996. *Forest products and wood science: an introduction*. Third Edition, Iowa State University Press, Iowa. 484p.
- Hilpp, G.K., and M.H. Pelkki. 2003. Log grade prediction for standing yellow-poplar trees in eastern Kentucky. *South. J. Appl. For.* 27:61-65.
- Hosmer, D.W., and S. Lemeshow. 1989. *Applied logistic regression*. John Wiley and Sons, Inc. 307p.
- Johnson, N.L., A.W. Kemp, S. Kotz. 2005. *Univariate discrete distributions*. Third Edition, John Wiley and Sons, Inc., Hoboken, New Jersey.
- Kuehl, R.O. 1994. *Statistical principles of research design and analysis*. Second Edition, Duxbury Press. 699p.
- Lanner, R.M. 1976. Patterns of shoot development in *Pinus* and their relationship to growth potential. P. 223-243 *in* *Physiology and yield improvement*, Cannell, M.G.R and Last, F.T. Academic Press, London.
- Larson, P.R. 1969. Wood formation and the concept of wood quality. *Yale Univ. School of Forestry, Bull.* 74. 54p.
- Lemieux, H., M. Beaudoin, and S.Y. Zhang. 2001. Characterization and modeling of knots in black spruce (*Picea Mariana*) logs. *Wood and Fiber Science* 33:465-475.
- Lin, C., and P.M. Morse .1975. A compact design for spacing experiments. *Biometrics* 31:661-671.
- Liu, J., H.E. Burkhart, and R.L. Amateis. 1995. Projecting crown measures for loblolly pine trees using a generalized thinning response function. *For. Sci.* 41:43-53.
- Jammalamadaka, S.R., A. SenGupta. 2001. *Topics in circular statistics*. World Scientific Publishing Co. Pte. Ltd. 319p.
- Maguire, D.A. and D.W. Hann. 1987. A stem dissection technique for dating branch mortality and reconstruction past crown recession. *For. Sci.* 33:858-871.
- Maguire, D.A., D.W. Hann. 1990. A sampling strategy for estimating past crown recession on temporary growth plots. *For. Sci.* 36:549-563.

- Maguire, D.A., S.R. Johnston and J. Cahill. 1999. Predicting branch diameters on second-growth Douglas-fir from tree-level descriptors. *Can. J. For. Res.* 29:1829-1840.
- Max, T.A., and H.E. Burkhart. 1976. Segmented polynomial regression applied to taper equations. *For. Sci.* 22:283-289.
- Mäkinen, H. 1999. Growth, suppression, death, and self-pruning of branches of scots pine in southern and central Finland. *Can. J. For. Res.* 29:585-594.
- Mäkinen, H. and F. Colin. 1998. Predicting branch angle and branch diameter of scots pine from usual tree measurements and stand structural information. *Can. J. For. Res.* 28:1686-1696.
- Mäkinen, H. and F. Colin. 1999. Predicting the number, death, and self-pruning of branches in scots pine. *Can. J. For. Res.* 29:1225-1236.
- Mäkinen, H. and A. Mäkelä. 2003. Predicting basal area of scots pine branches. *For. Ecol. Manage.* 179:351-362.
- Mäkinen, H., R. Ojansuu, P. Sairanen and H. Yli-Kojola. 2003a. Predicting branch characteristics of Norway spruce (*Picea abies* (L.) Karst.) from simple stand and tree measurements. *Forestry* 76:525-546.
- Mäkinen, H., R. Ojansuu and P. Niemistö. 2003b. Predicting external branch characteristics of planted silver birch (*Betula pendula* Roth.) on the basis of routine stand and tree measurements. *For. Sci.* 49:301-317.
- Meredieu, C., F. Colin, and J-C. Hervé. 1998. Modeling branchiness of Corsica pine with mixed-effect models (*Pinus nigra* Arnold ssp. *Laricio* (Poiret) Maire). *Ann. Sci. For.* 55:359-374.
- Mora. 2003. Effects of early intensive silviculture on wood properties of loblolly pine. M.Sc. Thesis, North Carolina State University, Raleigh, NC.70p.
- Mudano, J.E., H.L. Allen, and L.W. Kress. 1992. Stem and foliage elongation of young loblolly pine as affected by ozone. *For. Sci.* 38:324-335.
- Murphy, P.A., and R.M. Farrar, Jr. 1988. A framework for stand structure projection of uneven-aged loblolly-shortleaf pine stands. *For. Sci.* 34:312-332.
- O'Hara, K.L., and P.A. Buckland. 1996. Prediction of pruning wound occlusion and defects core size in ponderosa pine. *W. J. of Appl. For.* 11:40-43.

- Paul, B.H. 1957. Juvenile wood in conifers. FPL Rep. 2094, Madison, WI: U.S. Department of Agriculture, Forest Service, Forest Products Laboratory. 6p.
- Phillips, K.M. 2002. Modeling within-tree changes in wood specific gravity and moisture content for loblolly pine in Georgia. M.Sc. Thesis, University of Georgia, Athens, GA. 95p.
- Pinto, I., Pereira A., A. Usenius. 2003. Analysis of log shape and internal knots in twenty Maritime pine (*Pinus pinaster* Ait.) stems based on visual scanning and computer aided reconstruction. *Ann. For. Sci.* 60:137-144.
- Pinto, I., A. Usenius, T. Song, H. Pereira. 2005. Sawing simulation of maritime pine (*Pinus pinaster* Ait.) stems for production of heartwood-containing components. *Forest Prod. J.* 55(4):88-96.
- Rapraeger, E.F. 1939. Development of branches and knots in western white pine. *J. For.* 37: 239-245.
- Reynolds, R.R. 1967. Natural pruning of loblolly pine. *Forest Farmer* 26(6): 8-9.
- Roeh, R.L., and D.A. Maguire. 1997. Crown profile models based on branch attributes in Coastal Douglas-fir. *For. Ecol. Manage.* 96:77-100.
- SAS Institute, Inc. 2004. SAS/STAT 9.1 User's Guide. SAS Publishing. 5136p.
- Schmidt, M. 2001. Prognosemodelle für ausgewählte Holzqualitätsmerkmale wichtiger Baumarten. Dissertation, University of Göttingen, Germany. 302p.
- Schultz, R.I. 1997. The ecology and culture of Loblolly pine (*Pinus taeda* L.). U.S. Department of Agriculture, Forest Service, Southern Forest Experiment Station, New Orleans, Louisiana, Agricultural Handbook 713.
- Sharma, M., H.E. Burkhart, and R.L. Amateis. 2002. Spacing rectangularity effect of the growth of loblolly pine plantations. *Can. J. For. Res.* 32:1451-1459.
- Shigo, A.L. 1985. How the branches are attached to trunks. *Can. J. Bot.* 63:1391-1401.
- Shigo, A.L. 1990. Tree branch attachment to trunks and branch pruning. *HortScience* 25:54-59.
- Short, E.A., and H.E. Burkhart. 1992. Predicting crown-height increment for thinned and unthinned loblolly pine plantations. *For. Sci.* 38:594-610.
- Sweet, G.B., and M.P. Bollman. 1976. The terminology of pine shoot growth. *N. Z. J. For. Sci.* 6:393-396.

- Tasissa, G., and H.E. Burkhart. 1998a. Modeling thinning effects on ring specific gravity of loblolly pine (*Pinus taeda* L.). *For. Sci.* 44:212-223.
- Tasissa, G., and H.E. Burkhart. 1998b. Juvenile-mature wood demarcation in loblolly pine trees. *Wood and Fiber Science* 30:119-127.
- Walker, L.C., B.P. Oswald. 2000. *The southern forest: geography, ecology and silviculture*. CRC Press. 332p.
- Wendel, K.W.v., B.J Zobel, and C.J.A. Shelbourne. 1967. Knot wood in loblolly pine. *Sch. For. Tech. Rep.* Raleigh, NC: North Carolina State College. 45p.
- Westfall, J.A., H.E. Burkhart, and H.L. Allen. 2004. Young stand growth modeling for intensively-managed loblolly pine plantations in southeastern U.S. *For. Sci.* 50:823-835.
- Whiteside, I.D., M.D. Wilcox, and J.R. Tustin. 1977. New Zealand Douglas-fir timber quality in relation to silviculture. *N. Z. Journal of Forestry* 22: 24-45.
- Wobst, J. 1995. Auswirkungen von Standortsgüte und Durchforstungsstrategien auf wertungsrelevante Holzeigenschaften von Douglasie. Dissertation, University of Göttingen, Germany. 210p.
- Yu, S., J.L. Chambers, Z. Tang, and J.P. Barnett. 2003. Crown characteristics of juvenile loblolly pine 6 years after application of thinning and fertilization. *For. Ecol. Manage.* 180:345-352.
- Zeide, B. 1993. Analysis of growth equations. *For. Sci.* 39:594-616.
- Zhang, Y., B.E. Borders, R.E. Will, and H. De Los Santos Posadas. 2004. A model for foliage and branch biomass prediction for intensively managed fast growing loblolly pine. *For. Sci.* 50:65-80.

## Chapter 5

### Simulating the Impact of Initial Spacing and Thinning Intensity on Sawlog Quality in Loblolly pine

---

**ABSTRACT.** A dynamic branch model was linked to the stand simulator PTAEDA3.1 to study the effects of initial spacing (6 ft x 6 ft, 8 ft x 8 ft and 12 ft x 12 ft) and thinning intensity at age 12 years old (SI = 65 ft) on sawlog quality. The analysis performed considered the quality of the first and second 16-ft sawlog of sawtimber trees for a rotation age of 30 years. The arithmetic mean diameter of the largest four branches, one from each radial quadrant of the log (i.e. Branch Index, BI) and the number of whorls per log were considered as indicators of log quality. Smaller BI and reduced number of whorls are considered desirable sawlog characteristics. In all simulations the second 16-ft sawlog presented larger maximum branch diameters than the first sawlog. Branch index increased with increasing initial spacing and with increasing tree size (DBH) for the bottom sawlogs. Sawtimber trees with the same DBH but growing at wider spacing had larger BI for the first 16-ft sawlog, and similar BI for the second sawlog. Inference on the number of whorls produced under different initial growing space was inconclusive due to anomalies detected in the pattern of height increment in the juvenile phase for simulated trees. In terms of thinning intensity (no thinning and 20%, 40% and 60% of the BA removed), the major impact on branch diameter growth were detected on the second 16-ft sawlog, when applying a heavy thinning (60% BA removed). Sawtimber trees produced under different thinning intensities resulted in similar BI for the bottom sawlog. It can be concluded that a thinning intervention at 12 years old has a lower impact on sawlog quality (e.g. branch diameter growth) in comparison to initial spacing.

---

**Keywords:** log quality, thinning, initial spacing, individual-tree growth mode1, loblolly pine.



## 5.1 Introduction

One of the most important silvicultural decisions to influence growth and yield in forest plantations is regulation of the growing space (Assman 1970 p.101, Sharma et al. 2002). Growing space can be controlled at stand establishment by initial spacing or later on by reducing the number of trees through thinning. Both silvicultural decisions affect crown dynamics and therefore have a direct impact on the size of branches produced. In plantations managed for production of solid wood products, quality and value of standing trees, logs and lumber depends on factors such as the number, position and size of branches. For loblolly pine, tree and lumber grading rules consider among others, attributes related to number and size of branches and knots (Clark and McAlister 1998). Accordingly, silvicultural practices that promote production of large diameter branches will reduce considerably lumber grade yield (Clark et al. 1994). Branches included in the wood of the stem originate knots, which decrease the strength and stiffness of wood intended for structural uses and influences the appearance of timber (Whiteside et al. 1977, Briggs 1996, Gartner 2005). Their effect on mechanical properties is due to interruption of continuity and change in the direction of wood fibers (Grace et al. 1999).

Existing growth and yield projection systems for loblolly pine plantations intended to support management decisions do not account for wood quality in term of branch dimensions and other wood properties. The optimal management regime is the regime that maximizes wood volume production under the assumption that the raw material is uniform in terms of quality. During the last decades, research on wood quality in fast-grown loblolly pine plantations has indicated clearly that some important wood properties are affected by intensive management practices. Trees planted at wider initial spacing and utilization of intensive management practices have increased forest productivity and reduced the rotation age. However, wood produced on short rotations has a higher proportion of juvenile wood and larger branches along the stem bole which impact the quality of the raw material for some end-products. Under this scenario, efforts are needed to model and incorporate wood properties and stem characteristics that influence wood quality into existing growth and yield models. An integrated modeling system that includes tree and log quality attributes can permit a better evaluation on the effect of

silvicultural regimes on the value of the raw material being produced. Furthermore, it may allow for a more accurate economical evaluation of different management regimes.

The effect of branches on wood quality has not been incorporated in simulation systems because modeling approaches to represent branch dynamics and structure in loblolly pine have not been developed. Doruska and Burkhart (1994) proposed a system of equations to predict branch diameter and location along and around the stem. However, some of the limitations of this model are that it permits the modeling of branches only at one point in time and prediction of external branch characteristics is limited to the crown. Motivated by these limitations, another effort was made to model the diameter growth of first-order branches and knot formation. The modeling system was developed to be incorporated into an individual-tree growth and yield model and to provide detailed information on internal stem structure (e.g. knots).

This research reports the linkage of the dynamic branch model into an existing individual-tree growth system. Because of their influence on crown and branch development, the interest was on simulating the effect of initial spacing (e.g. planting density) and thinning intensity on branch development in sawtimber trees. Thus, the objectives established for this study were to *(i)* to link the dynamic branch simulation model with PTAEDA3.1, a distance-dependent individual-tree growth and yield simulator (Burkhart et al. 2004), *(ii)* simulate the effect of initial spacing and thinning intensity on sawlog quality, and *(iii)* verify that simulated responses were consistent with current knowledge of branch dynamics and empirical observations from reported spacing studies. At this stage, a more complete validation of the developed model is not possible because of the scarcity of empirical data on branch dynamics in loblolly pine.

## **5.2 Material and Methods**

### **5.2.1 Simulation of first-order branch dynamics**

The branch model uses a hierarchical structure for modeling the process of first-order branch dynamics and knot formation. First-order branches are those arising from the main stem and having a direct impact on the wood produced. Three different components were considered as modeling units: *whorl*, *branches* and *knot* formation. In each growing season the number and location of whorls are predicted and branches are allocated in each whorl. The last whorl formed in a growing season is located at the tree tip. In subsequent growing seasons, additional whorls and branches are included along and around the stem and the dynamics of old branches (growth, death and self-pruning) predicted. The model assumes that the effect of silvicultural practices on branch growth is accounted for indirectly through their effects on stem growth and crown dynamics (e.g. crown recession). Thus, trees with higher rates of growth and larger crowns will produce larger branches. A similar modeling approach was utilized by Grace et al. (1998, 1999) to predict the development of branches for radiata pine (*Pinus radiata* D. Don) trees in New Zealand.

The branch model developed was linked with PTAEDA3.1, a distance-dependent individual-tree growth and yield model (Burkhart et al. 2004). The linkage with PTAEDA3.1 was possible through the annual height growth, diameter growth and crown recession components. Spatial information on the internal location of branches (e.g. knots) was maintained through out the simulation using the Max and Burkhart (1976) taper equation.

### **5.2.2 Effect of initial spacing and thinning intensity on sawlog production**

For this study, simulations were performed considering a rotation age of 30 years and site index of 65 ft (base age 25 years) for a stand located in the Coastal Plain region. At the end of the simulation period only sawtimber trees were selected for the analysis. Sawtimber trees were defined as those trees that had a breast height diameter (DBH) outside bark greater than or equal to 9 inches (22.9 cm) (Clark and McAlister 1994). For

each tree only the volume and quality of the first- and second 16-ft (4.9m) butt logs were analyzed. To classify as sawlog the log must have a minimum top diameter (inside bark) equal or greater than 6 inches. Accordingly, the volume of the first butt log was computed from a stem height of 0.7 ft to 17.0 ft (0.2m to 5.2m) and the second log from a stem height of 17.0 ft to 33.3 ft (5.2m to 10.1m) using the Max and Burkhardt (1976) taper equation ( $b_1=-3.0257$ ,  $b_2=1.4586$ ,  $b_3=-1.4464$ ,  $b_4=39.1081$ ,  $a_1=0.7431$  and  $a_2=0.1125$ ).

In the simulations, initial spacing and thinning intensity were evaluated separately from their effects on production of sawtimber trees and sawlog quality. The effect of initial spacing was evaluated considering three different initial spacings corresponding to: 6 ft x 6ft (1210 trees per acre), 8ft x 8ft (680 trees per acre) and 12ft x 12ft (302 trees per acre). Based on our knowledge of whorl and branch dynamics a series of hypotheses were defined to examine the effect of initial spacing on sawlog quality: (1a)  $H_0$ : branch diameters increase with initial spacings, (2a)  $H_0$ : the second 16-ft sawlog contains larger branch diameters than the first 16-ft sawlog, (3a)  $H_0$ : trees with larger DBH present branches with larger diameters, (4a)  $H_0$ : trees with the same DBH, but growing at a wider spacing develop larger branch diameters, and (5a)  $H_0$ : the number of whorls formed for the first 16-ft sawlog is similar regardless of the initial spacing.

In addition, to evaluate the effect of thinning intensity on sawlog quality four different treatments were compared considering an initial spacing of 8ft x 8ft (680 trees per acre) and thinning at 12 years old. The thinning intensities involved no-thinning (control), and reductions in basal area of 20, 40 and 60% of the beginning value. All simulated thinnings were from below, which involved the extraction of the smaller trees until reaching the target residual basal area. The hypotheses tested were that (1b)  $H_0$  : thinning intensity does not affect branch diameter of the first sawlog, (2b)  $H_0$  : increased thinning intensity promotes the growth of branches in the second 16-ft sawlog, (3b)  $H_0$ : trees with the same DBH, but produced under different thinning intensities, present similar branch diameters, and (4b)  $H_0$  : the number of whorls of the first and second sawlogs decreases with increasing thinning intensity.

### **5.2.3 Assessment of sawlog quality**

The assessment of the sawlog quality was based on (a) the branch index (BI) and (b) the number of whorls per log. The branch index was defined as the arithmetic mean diameter of the largest four branches, one from each radial quadrant of the log. This index has been widely used to evaluate the effects of branch size on log grading in different tree species (Whiteside et al. 1977, Bier 1986, Maguire et al. 1991, DeBell and Gartner 1997). Both log characteristics are hypothesized to be directly influenced by the crown and branch dynamics and therefore by the silvicultural regime adopted.

The statistical analysis considered the application of a two-factor analysis of variance (ANOVA) procedure, where the response variables were the branch index (BI) and the number of whorls (NW) per log. The main two-factors considered were initial spacing or thinning intensity and sawlog location.

## **5.3 Results and Discussion**

### **5.3.1 Effect of initial spacing**

A wider initial spacing produced a higher number of sawtimber trees and therefore more sawlog volume (Table 5.1). As expected, the volume of the first two 16-ft sawlogs increases with increasing spacing and the first sawlog has a larger volume than the second sawlog. A graphical analysis of the mean response profiles for the branch index (BI) shows that BI increases with initial spacing and sawlog position (Figure 5.2). The differences between the first and second 16-ft sawlogs can be explained because branches located in the lower part of the bole are retained a shorter time within the live crown in comparison to branches formed in the upper part. On the other hand, the crown recession process in trees growing at wider spacing is slower in comparison with trees growing at narrower spacing; thus branches are bigger because they stay a longer time growing in the live crown.

**Table 5.1.** Production of sawtimber trees, sawlog volume and log volume at age 30 years under different initial spacing (Coastal Plain, SI=65 ft).

| Spacing<br>(ft x ft) | Sawtimber trees<br>per acre<br>(percentage) | Sawlog volume<br>ft <sup>3</sup> i.b. per acre<br>(percentage) | Log volume (ft <sup>3</sup> i.b.) |          |                  |          |
|----------------------|---|--|-----------------------------------|----------|------------------|----------|
|                      |   |  | First 16-ft log                   |          | Second 16-ft log |          |
|                      |   |  | mean                              | range    | mean             | Range    |
| 6 x 6                | 36.4 ( 6.2)                                 | 1480.9 (15.8)  | 7.4                               | 6.3-9.1  | 4.9              | 4.2-6.0  |
| 8 x 8                | 91.5 (20.5)                                 | 3817.1 (37.3)  | 7.7                               | 6.3-12.3 | 4.9              | 4.2-8.4  |
| 12 x 12              | 163.6 (73.5)                                | 8391.9 (84.0)  | 9.2                               | 6.3-15.9 | 6.0              | 4.2-10.5 |

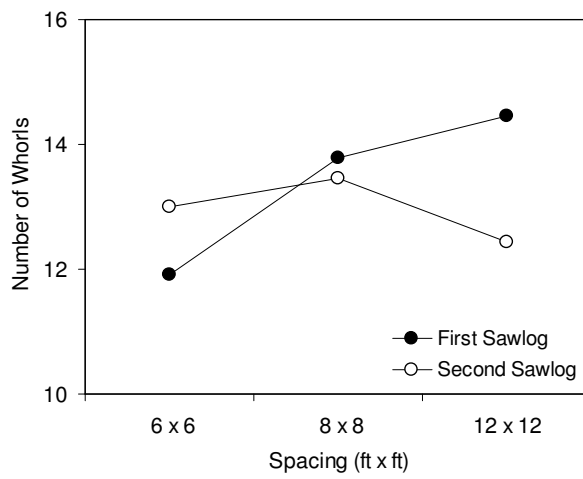
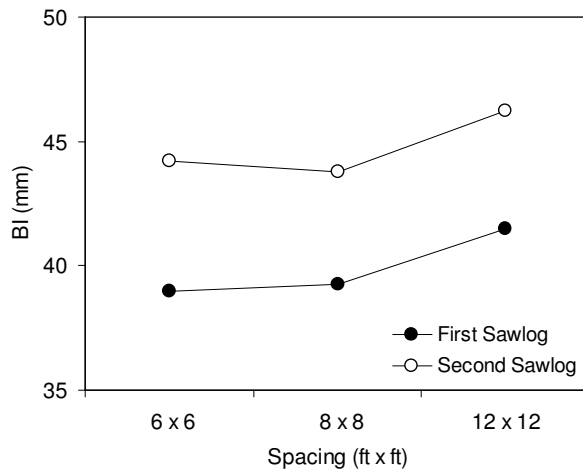


**Figure 5.1.** Mean response profiles for the (a) branch index (BI) and (b) number of whorls for the first (●) and second (○) 16-ft butt sawlog under different initial spacing.

The ANOVA indicated that the main effects initial spacing ( $P < 0.0001$ ) and sawlog location ( $P < 0.0001$ ) were highly significant and there was no interaction between both factors (Figure 5.1). A significant difference in BI between the initial spacing 6ft x 6ft and 12ft x 12ft, and between 8ft x 8ft and 12ft x 12ft was detected when applying a Tukey's pairwise comparison tests on the mean responses at  $\alpha = 0.05$ . These results supported the stated hypotheses (1a) and (2a). The simulation agrees with the belief that the most valuable portion of the stem is contained in the first 16-ft sawlog, because of more volume and smaller branch diameters (e.g. BI) in comparison to upper logs.

For all spacing there was a positive relationship between BI and the diameter at breast height (Figure 5.2). This observation confirmed hypothesis (3a). Only some of the sawtimber trees ( $DBH > 12$  inches) produced at a spacing of 12 ft x 12 ft contained a second sawlog with a BI larger than 50 mm. To investigate hypothesis (4a) the data were disaggregated by DBH-classes and spacing (Table 5.2). The analysis was performed separately for the first and second 16-ft sawlog using ANOVA. For the first sawlog both spacing ( $P = .0102$ ) and DBH ( $P = 0.0016$ ) were significant. Therefore, trees with larger DBH have larger branches. On the other hand, trees with the same DBH but growing in a wider spacing also contain branches with larger diameters. Contrarily, for the second 16-ft sawlog DBH was significant ( $P < 0.0001$ ) and spacing was found to be not significant ( $P = 0.3742$ ). Thus, for the second 16-ft sawlog one expects similar BI for trees with similar DBH but growing in different initial spacings. It means that the difference in growing space might affect only the first 16-ft butt log in terms of BI for sawtimber trees. The stated hypothesis (3a) was supported for the first and second 16-ft sawlog, where bigger trees have bigger branches. Contrarily, hypothesis (4a) was valid only for the first 16-ft sawlog.



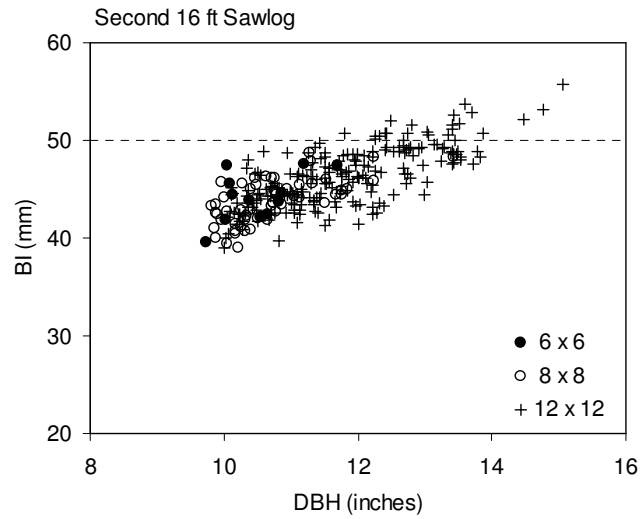
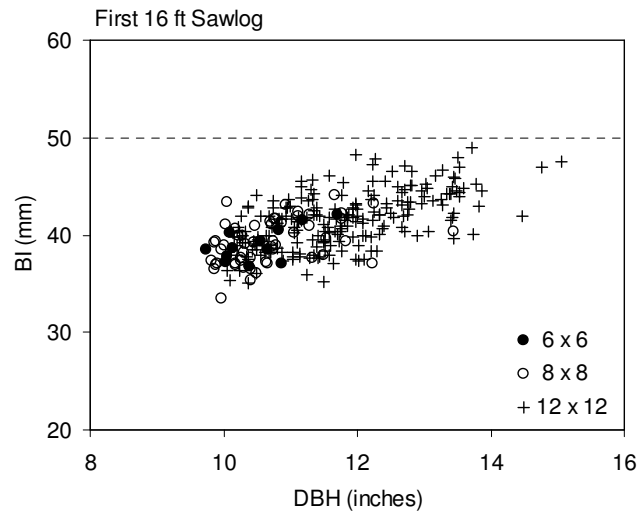


**Figure 5.2.** Relationships between branch index (BI) and the diameter at breast height for three different initial spacing for the first and second 16-ft butt sawlogs.

**Table 5.2.** Average branch index for the first and second 16-ft butt sawlog disaggregated by DBH-classes and initial spacing.

| DBH<br>(inches) | First Sawlog |       |         | Second Sawlog |       |         |
|-----------------|--------------|-------|---------|---------------|-------|---------|
|                 | 6 x 6        | 8 x 8 | 12 x 12 | 6 x 6         | 8 x 8 | 12 x 12 |
| 10              | 39.0         | 39.2  | 40.4    | 44.2          | 43.5  | 44.9    |
| 12              | -            | 40.2  | 43.2    | -             | 47.5  | 48.2    |
| 14              | -            | -     | 45.5    | -             | -     | 53.7    |
| All             | 39.0         | 39.3  | 41.5    | 42.2          | 43.8  | 46.2    |

Results for hypothesis (5a) were inconclusive due to anomalies in the stand simulator used. PTAEDA3.1 contains a juvenile growth routine (which is required for these analysis); however, the transition from the juvenile height growth predictions to the more mature stand portion is not entirely smooth. Furthermore, the juvenile phase shows decreased height growth at wider spacings whereas height increment is impeded by closer spacing in the mature stand phases. This lack of consistency in height development makes interpretation of simulation results for number of whorls by sawlog position especially difficult.

### **5.3.2 Effect of thinning intensity**

At age of thinning the simulated stand had a basal area of 99.5 ft<sup>2</sup>/acre (22.8 m<sup>2</sup>/ha) a mean total tree height of 33.5ft (10.2 m) and a mean crown ratio (%) of 52.6. The residual basal areas corresponding to a thinning intensity of removal of 20%, 40% and 60% of the basal area were 79.6 ft<sup>2</sup>/acre (18.3 m<sup>2</sup>/ha), 59.7 ft<sup>2</sup>/acre (13.7 m<sup>2</sup>/ha) and 39.8 ft<sup>2</sup>/acre (9.1 m<sup>2</sup>/ha), respectively. At 12 years old on average the crown base has receded to 16-ft (4.9 m), thus the major effect of thinning in terms of branch diameter can be expected to occur on the second 16-ft sawlog. An increase in thinning intensity results in a stop to crown recession and an increase in length of time within the live crown.

An increase in thinning intensity until removing 40% of the basal area increased the number of sawtimber trees and volume of sawlogs (Table 5.3). Contrarily, a reduction of 60% of basal area reduced the number of sawtimber trees and sawlog volume. An increase in thinning intensity promoted the production of sawlogs of larger dimensions.

A graphical analysis of the mean response profiles for the branch index (BI) shows that BI increases with sawlog position for all thinning intensities (Figure 5.3a). As expected, the BI for the first 16-ft butt sawlog seems to be similar for all thinning intensities, which support hypothesis (1b). It can be explained because at the time of thinning the average crown base has already receded to 16-ft (4.9 m); therefore, branches below the crown base have reached their maximum size before the thinning.

The BI for the second 16-ft sawlog increased more profoundly when 60% of the basal area was extracted. However, the ANOVA performed indicated that both thinning intensity ( $P < 0.0001$ ) and sawlog location ( $P < 0.0001$ ) were highly significant. A Tukey's pairwise comparison test on the mean responses ( $\alpha = 0.05$ ) showed that the thinning intensity of 60% was different than the other intensities, due to the peak observed in the BI for the second 16-ft sawlog at this thinning level. These results confirmed that hypothesis (2b) is only valid when applying heavy thinning intensities (such as 60% of basal area removed). Thus, less intensive thinning might not have any effect on the diameter of branches located in the second 16-ft sawlog.

Under different thinning intensities a positive relationship was observed between BI and breast height diameter for the first and second 16-ft butt sawlog (Figure 5.4). The application of thinning (20%, 40% and 60%) resulted in some of the second sawlog formed branches with diameters larger than 50 mm. For the first 16-ft butt sawlog the relationships between BI and breast height diameter is stronger than for the second sawlog. Again, this relationships seem logical because at the time of thinning branches located at the first sawlog have reached their maximum diameters, thus major effects of thinning are expected to occur on the second sawlog.

To investigate hypothesis (3b) the data were disaggregated by DBH-classes and thinning levels (Table 5.4). As before, this analysis was performed separately for the first and second 16-ft butt sawlog using ANOVA. For the first 16-ft sawlog DBH was the only significant variable ( $P = 0.0009$ ). Similar result was obtained for the second 16-ft butt sawlog ( $P < 0.0001$ ). It indicates that thinning intensity does not affect the maximum branch diameter of trees with similar DBH, which supports hypothesis (3b). Some effect of thinning intensity on BI was expected for the second 16-ft sawlog on trees with similar DBH, but this was only apparent for the DBH-class of 10 inches.

**Table 5.3.** Production of sawtimber trees, sawlog volume and log volume at 30 years old under different thinning intensities for an initial spacing of 8 ft x 8 ft.

| Thinning intensity | Sawtimber trees per acre (percentage) | Sawlog volume ft <sup>3</sup> i.b. per acre (percentage) | Log volume (ft <sup>3</sup> i.b.) |          |                  |          |
|--------------------|---------------------------------------|--|-----------------------------------|----------|------------------|----------|
|                    |                                       |  | First 16-ft log                   |          | Second 16-ft log |          |
|                    |                                       |  | mean                              | range    | mean             | Range    |
| Unthinned          | 91.5 (20.5)                           | 3817.1 (37.3)  | 7.7                               | 6.3-12.3 | 4.9              | 4.2-8.4  |
| 20%                | 125.4 (39.6)                          | 5494.4 (54.4)  | 7.7                               | 6.3-12.7 | 5.3              | 4.2-8.8  |
| 40%                | 184.7 (78.9)                          | 8573.4 (86.4)  | 8.5                               | 6.3-13.1 | 5.6              | 4.2-8.8  |
| 60%                | 137.3 (97.6)                          | 7793.1 (98.7)  | 10.2                              | 6.7-15.2 | 6.7              | 4.2-10.2 |

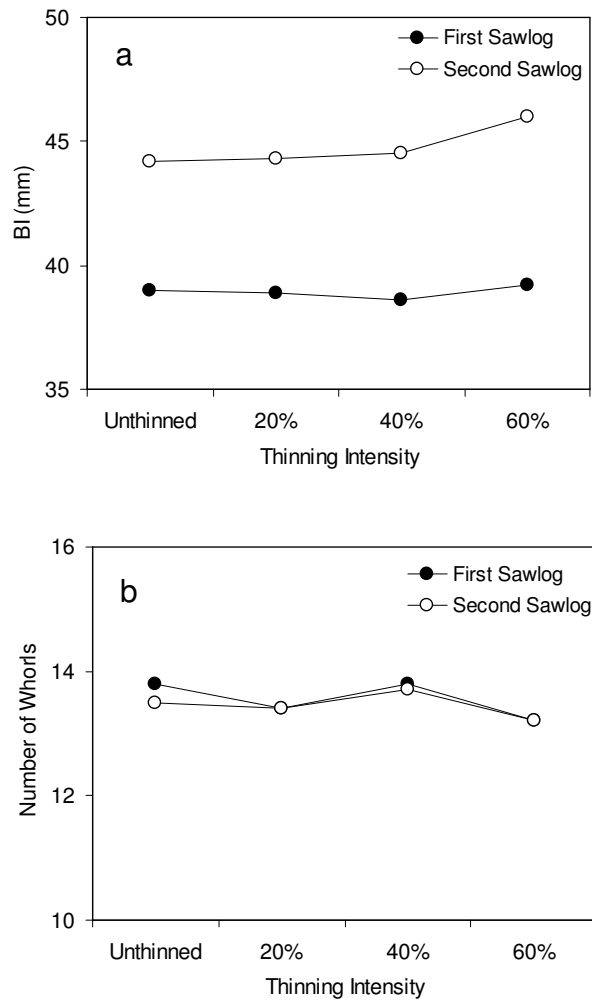


**Figure 5.3.** Mean response profiles for the (a) branch index (BI) and (b) number of whorls for the first (●) and second (○) 16-ft butt sawlog under different thinning intensities.

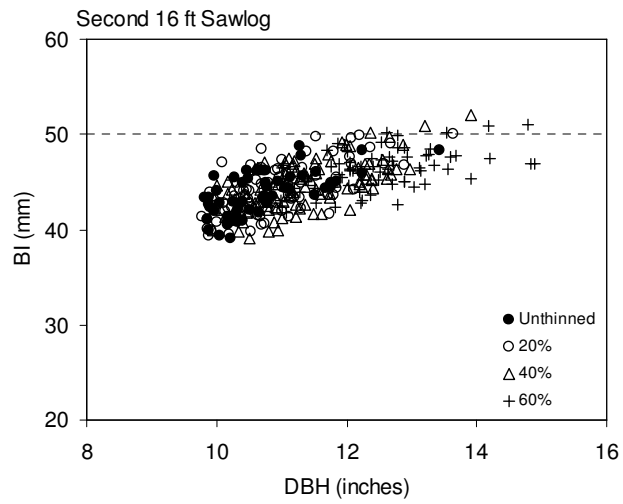
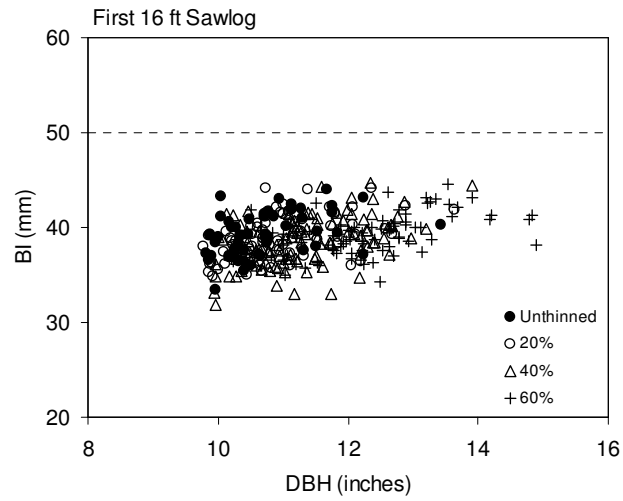


**Figure 5.4.** Relationships between branch index (BI) and the diameter at breast height for different thinning intensities for the first and second 16-ft butt sawlogs.

**Table 5.4.** Average branch index for the first and second 16-ft butt sawlog disaggregated by DBH-classes and thinning intensities.

| DBH<br>(inches) | First Sawlog |      |      |      | Second Sawlog |      |      |      |
|-----------------|--------------|------|------|------|---------------|------|------|------|
|                 | unthin       | 20%  | 40%  | 60%  | unthin        | 20%  | 40%  | 60%  |
| 10              | 39.2         | 38.7 | 38.1 | 38.1 | 43.5          | 43.7 | 43.9 | 44.9 |
| 12              | 40.2         | 40.2 | 40.1 | 39.7 | 47.5          | 47.9 | 46.6 | 46.5 |
| 14              | -            | -    | -    | 40.5 | -             | -    | -    | 48.6 |
| All             | 39.3         | 38.9 | 38.6 | 39.2 | 43.8          | 44.3 | 44.5 | 46.0 |



The number of whorls in the first and second 16-ft butt sawlog was not significantly different  $P = 0.4246$  (Figure 5.3b). The ANOVA applied indicated that thinning intensity was the only factor affecting the number of whorls ( $P = 0.0090$ ). The number of whorls produced in stands thinned with less than 40% was not significantly different applying a Tukey's pairwise comparison test on the mean responses ( $\alpha = 0.05$ ). Contrarily, sawtimber trees left after reducing the basal area by 60% had less whorls in both the first and second 16-ft butt sawlog in comparison to the other thinning intensities ( $\alpha = .05$ ). This result comes from selecting as residual trees the most vigorous ones. These trees have the higher rates of height growth and because the algorithm assigns an average of three whorls per growing, a smaller number of whorls is expected in the bottom sawlogs. The ANOVA indicated that hypothesis (4b) holds as true; however, there was not an important decrease in the number of whorls by thinning intensity as could be expected.

#### **5.4 Conclusions**

A dynamic branch model was linked to PTAEDA3.1, a distance-dependent individual-tree growth and yield simulator, to study the effects of initial spacing and thinning intensity on branch development. The main interest was to evaluate the effects of diverse management regimes on the quality of the first and second sawlog produced by sawtimber trees. Sawlog quality was evaluated and compared for sawlogs located in different positions along the stem using a measure of maximum branch size (branch index, BI) and the number of whorls per log. For both initial spacing and thinning intensity, a series of hypotheses were advanced and tested according to the outcome of the simulations.

The branch diameter in sawlogs increased significantly with initial spacing. Wider initial spacing produced sawlogs with larger branch diameters; especially for the second 16-ft sawlog. The first sawlog had bigger dimensions and smaller branch diameters in comparison to the second sawlog. Maximum branch diameter increased also with increasing tree size (DBH) for both the first and second 16-ft sawlog. However, sawtimber trees with the same DBH but growing at wider spacing presented also larger branch diameters for the first 16-ft sawlog. According to the simulation, comparable

maximum branch diameters are expected in the second 16-ft sawlog for trees with similar DBH, but growing under different spacing. These results indicate that initial spacing is primarily affecting the quality of the bottom sawlog.

Some of the sawtimber trees (DBH > 12 inches) produced at a spacing of 12 ft x 12 ft contained a second sawlog with BI larger than 50 mm. Thus, it is expected that sawtimber trees produced at spacings of 6 ft x 6 ft and 8 ft x 8 ft will contain only sawlogs with BI < 50 mm.

The responses of the simulation in terms of number of whorls per sawlog for different initial spacing were inconclusive. The expected responses were confounded by anomalies found in the stand simulator. These anomalies were a different rate of height increment between the juvenile and mature growth phases and lower height increment at wider spacing during the juvenile phase. The second anomaly resulted in a larger number of whorls being allocated in sawlogs formed at wider spacing, affecting particularly the first 16-ft sawlog.

For all thinning intensities the second 16-ft sawlog had larger branch diameters in comparison to the bottom sawlog. The maximum branch diameter for the first 16-ft sawlog was not affected by thinning intensity, mainly because at time of thinning branches located in the bottom log had reached their maximum size. The main effect of thinning was expected to occur in the second 16-ft sawlog; however, it was only pronounced at the highest thinning intensity applied (60% of the basal area removed). Some sawtimber trees produced at different thinning intensities had a second sawlog with BI > 50 mm. In comparison to the effect of initial spacing, thinning interventions produced a smaller number of second sawlogs with BI > 50 mm. Even though thinning stopped the process of crown recession, at time of thinning branches located within the live crown are smaller than branches developed in trees growing at wider initial spacing. This results indicate that a thinning intervention at 12 years old has a small impact on sawlog quality in comparison to initial spacing.

The linkage of the dynamic branch model and PTAEDA3.1 permitted analysis of the quantity and quality of sawlog produced under different management regimes. The majority of the responses were according to the expected behavior, especially the development of branches along the stem. Therefore, the model can be a useful tool to forest managers to evaluate the effect of silvicultural decisions on the quality of sawlogs produced. The predictive capability of the model in terms of number of whorls produced by sawlogs is imperfect and for this specific application it will require reviewing the equations of height increment for the juvenile phase included in PTAEDA3.1.

## **5.5 Acknowledgements**

Financial support for this research was provided through the Loblolly Pine Growth and Yield Research Cooperative at Virginia Tech. Financial support from the Sustainable Engineered Materials Institute, Virginia Tech, and USDA/CSREES Fund Number 2005-06172 is also gratefully acknowledged. Necessary equipment and facilities to analyze wood samples were kindly provided by the Forest Harvesting and Dendrocronological Laboratories. Dr. Phil Radtke, Dr. Carolyn Copenhaver and Dr. Rien Visser provided helpful directions during the development of this study which is deeply appreciated. Also, we thank Mr. Tal Roberts and Mr. Noah Adams for valuable and excellent assistance during the dissection of whorl samples.

## **5.6 Literature Cited**

- Assmann, E. 1970. The principles of forest yield study. Pergamon Press, New York. 506p.
- Bier, H. 1986. Log quality and the strength and stiffness of structural timber. *N. Z. J. For. Sci.* 16:176-186.
- Briggs, D. 1996. Modeling crown development and wood quality. *J. For.* 94(12): 24-25.
- Burkhart, H.E., R.L. Amateis, J.A. Westfall, and R.F. Daniels. 2004. PTAEDA 3.1: Simulation of individual tree growth, stand development and economic evaluation in loblolly pine plantations. Department of Forestry, Virginia Polytechnic Institute and State University. 23p.

- Clark III, A., and R.H. McAlister. 1998. Visual tree grading systems for estimating lumber yields in young and mature southern pine. *Forest Prod. J.* 48(10):59-67.
- Clark III, A., J.R. Saucier, V.C. Baldwin, and D R. Bower. 1994. Effect of initial spacing and thinning on lumber grade, yield, and strength of loblolly pine. *For. Prod. J.* 44 (11-12):14-20.
- DeBell, J.D. and B.L. Gartner. 1997. Stem characteristics on the lower log of 35-year-old western redcedar grown at several spacings. *Western J. Appl. For.* 12:9-15.
- Doruska, P.F., and H.E. Burkhart. 1994. Modeling the diameter and locational distribution of branches within the crowns of loblolly pine trees in unthinned plantations. *Can. J. For. Res.* 24:2362-2376.
- Gartner, B.L. 2005. Assessing wood characteristics and wood quality in intensively managed plantations. *J. For.* 103(2):75-77.
- Grace, J.C., W. Blundell, and D. Pont. 1998. Branch development in *pinus radiata* – model outline and data collection. *N. Z. J. For. Sci.* 28:182-194.
- Grace, J.C., D. Pont, and C.J. Goulding. 1999. Modelling branch development for forest management. *N. Z. J. For. Sci.* 29:391-408.
- Maguire, D.A., J.A. Kershaw, Jr., and D.W. Hann. 1991. Predicting the effects of silvicultural regime on branch size and crown wood core in Douglas fir. *For. Sci.* 37:1409-1428.
- Max, T.A., and H.E. Burkhart. 1976. Segmented polynomial regression applied to taper equations. *For. Sci.* 22:283-289.
- Sharma, M., H.E. Burkhart, and R.L. Amateis. 2002. Modeling the effect of density on the growth of loblolly pine trees. *South. J. Appl. For.* 26:124-133.
- Whiteside, I.D., M.D. Wilcox, and J.R. Tustin. 1977. New Zealand Douglas-fir timber quality in relation to silviculture. *N. Z. Journal of Forestry* 22: 24-45.

# Chapter 6

## Conclusions and Recommendations

### 6.1 Modeling knot shape in simulated trees

A simple model to represent a variety of knot shapes was developed. The knot model assumes that the live portion of a knot can be represented by a one-parameter equation and the dead portion by assuming the shape of a cylinder. The relative shape of the live portion of a knot was related with its maximum diameter. Branches with small diameter are assumed to be more cylindrical, whereas those with larger diameters assume conical. The developed model is simple and flexible for representing a great variety of knot shapes and allows for deriving explicit expressions for computing the volume of internal branches (live and dead portions). Another important characteristic is that the developed model can be linked to a taper equation to maintain spatial information of internal branches during the simulation. This approach facilitates computational implementation and reduces considerably the amount of data generated during the simulation of branch dynamics for a single tree. Both issues were important constraints when developing the proposed knot model in order to guarantee practical usefulness.

One important limitation is that the developed model assumes that knots do not exhibit curvature, which indeed may not be valid for other tree species. In this study the analysis of dissected branches indicated that for most of the knots curvature was not significant. However, this conclusion could have been influenced by the dissection techniques utilized to obtain the necessary branch data. Under the assumption that curvature was present but was not detected, it is unclear whether or not a more complex knot model is required for forest management purposes to make inference on the effect of internal branches on wood quality. Modeling of knot shape was a difficult task considering the effort required to obtain data from dissected branches as well as the observed variety in knot shapes.

The reconstruction technique utilized to recover information on knot shape required a minimum of five slices per knot; this technique is not recommended for small whorl sections. Sampling of whorl sections with the goal of obtaining information on knot shape should be concentrated in a small number of sample trees measured intensively along the stem and in management regimes oriented to produce sawtimber trees where branch diameter will have an influence on wood quality.

Additional research is required to determine if the assumed non-curvature of knots is completely valid for short-rotation loblolly pine plantations. Probably, the curvature of internal branches varies along the stem. Branches that stay for longer period of time within the live crown may show more pronounced curvature because of their size. It will require a more intensive sampling of whorl sections along the complete stem and utilization of other dissection techniques to investigate the effect that the dissection technique could have when investigating the curvature of knots.

## **6.2 Modeling branch dynamics and knot formation**

A stochastic modeling framework to represent the dynamics of first-order branches and knot formation was developed. Both external and internal information on branch dimensions and their location along and around the stem can be obtained. The branch model is intended to simulate the effect of silvicultural decisions on the quality of sawlogs produced. Because the branch model is distance-independent it can be linked to any individual-tree growth model that provides information on diameter at breast height, total tree height, and crown recession over time. The main assumptions are that branch diameter growth is driven by tree stem growth and crown recession. The modeling approaches selected were based on the type and amount of data available. At present, very limited research has been done to develop forest management oriented models to simulate the complete process of branch dynamics.

The use of a multcategory logistic regression was found to be a sound methodology to predict the number of whorls per growing season. However, data limitations did not permit evaluation of the inclusion of other predictor variables. Location of whorls within

each growing season was very difficult to model and therefore was predicted using observed average locations. Even though the reconstruction procedure used to recover information on whorl dynamics was useful, longitudinal data (e.g. direct measurements) on this process under a variety of growing conditions is required. This type of information can allow development of a predictive equation for the location of whorls within a growing season, and identification of important predictor variables in the multcategory logistic regression. Accurate predictions of clear-wood between successive whorls will require better understanding and modeling of whorl dynamics for a variety of growing conditions.

Most of the components that determine branch dynamics were included in the simulation systems. However, limited information was available for model construction and especially for model validation. Information was obtained using destructive sampling of trees and whorl sections. The main challenge was that no additional information on branch dynamics for loblolly pine trees is currently available. The modeling of some components (e.g. self-pruning process) was based on observational studies and modeled as a stochastic process. Similar approaches were required for other components (e.g. branch inclination, initial branch diameter and number of branches per whorl), mainly because of the difficulty for developing empirical equations with the available information. Mortality of branches located within the live crown was not modeled, because of insufficient information about this process.

The development of empirical equations requires longitudinal data. The measurement of branch characteristics (e.g. angle of inclination of branches, initial branch diameter and number of branches per whorl) in conjunction with other whorl, tree, stand and environmental variables is required. In this study, it was clear that additional information is necessary to explore possible relationships, but such information cannot be obtained from external stem measurements and dissection of whorl sections. Some of the required variables can be measured on standing trees at younger ages in established growth and yield trials, which until now has not been considered in the measurement protocols.

In this study, whorl sections were sampled below the base of live crown to recover information on branch development and knot formation. However, in similar studies where sample trees have been measured annually it is necessary to consider the measurement of the location of whorls and branch diameters (minimum and maximum) above the base of the live crown. This type of information could be highly valuable to validate the developed branch model. Simulations could be performed under the same initial spacing conditions and stand ages. After that, simulated trees with similar size could be compared to measured trees in terms of predicted and observed vertical trend in branch diameters within the live crown.

It was demonstrated that the developed framework can be linked with an existing individual-tree growth and yield simulation. Even though an adequate validation was not possible, the expected responses conformed to our general knowledge on branch dynamics. The model allows evolution of the effect of silvicultural regimes as initial spacing and thinning intensity on branch diameter growth and produces detailed 3D information on internal stem structure (e.g. knots). Simulated trees can permit the analysis of internal stem structure (e.g. distribution and volume of knots), which could otherwise be obtained only by applying destructive analysis techniques. Additionally, the framework is adequate to include predictive equations for other important wood properties (e.g. specific gravity).

The information on wood quality (internal and external) that can be obtained and its potential linkage with industrial processes (e.g. sawing simulation) to develop an integrated modeling system should motivate further studies on this topic. Currently, more information is required to better understand and model the process of branch dynamics.



### **6.3 Simulating the effects to initial spacing and thinning on sawlog quality**

The dynamic branch model was linked to PTAEDA3.1 to evaluate the effect of initial spacing and thinning intensity on sawlog quality. The quality of sawlogs produced was quantified using a measure of maximum branch diameter (e.g. Branch Index) and the number of whorls per log. The inclusion of the branch model allowed analysis of the quality of sawlogs produced by sawtimber trees between and within management regimes.

In all performed simulations, significant differences in terms of diameter of branches were detected between the first and second 16-ft sawlog. The second sawlog presented larger branch diameters than the first sawlog. The results indicated that initial spacing has an important effect on branch diameter in both the first and second sawlog. However, the most important impact occurred in the first sawlog, where sawtimber trees growing at a wider spacing have larger branch diameters. For the first sawlog trees with the same DBH but growing at wider spacing have larger branch diameters. Contrarily, for the second sawlog similar branch diameters are expected for trees with the same DBH but growing at different spacing. Thus, initial spacing is primarily affecting the bottom log, which is the most valuable portion of the bole. The outcome of the simulation permits a more accurate evaluation of the raw material produced, because measures of quality can be taken incorporated. Through simulation it is possible to determine the feasibility of producing sawtimber trees with a predetermined maximum branch diameter.

The simulation of thinning at stand age of 12 years old for an initial spacing of 8 ft x 8 ft (SI = 65 ft) demonstrated the effects on sawlog quality. The major impact in branch diameter was detected in the second sawlog when a heavy thinning was applied (60% of the basal area). Results showed that below this thinning intensity the quality of the bottom logs produced in sawtimber trees was not affected. However, thinning promotes the production of a second sawlog of larger dimensions. Comparatively, a simulated thinning intervention at 12 years old had a smaller impact on sawlog quality in comparison to initial spacing.

The predictive capability of the branch model in determining the number of whorls per log was influenced by differences in the height growth patterns between the juvenile and mature phases. Additionally, for the juvenile phase, trees growing at wider initial spacing had smaller growth rates in height and diameter. Consequently, trees planted at a wider spacings had a larger number of whorls for the first-sawlog, which is formed mainly during the juvenile phase. To allow a more consistent prediction of whorls per log rates of growth predicted by PTAEDA3.1 by the juvenile and mature phases need to be more consistent. Additionally, during the juvenile phase it can be assumed that trees growing at different spacing (same site) should have similar rate of growth, because of no inter-tree competition.

## Appendix. Simulator Input/Output and Fortran Code

### INPUT FILE: TreesSim.txt (from modified PTAEDA3.1)

| Variable | Format | Description  |
|----------|--------|--|
| AGE      | I3     | Tree age (years)                                       |
| XC       | F8.2   | X-Coordinate simulated tree (ft)                       |
| YC       | F8.2   | Y-Coordinate simulated tree (ft)                       |
| D        | F8.2   | Ground line diameter or Diameter at breast height (in) |
| H        | F8.2   | Total tree height (ft)                                 |
| CL       | F8.2   | Crown length (ft)                                      |
| LMORT    | I3     | Status according to PTAEDA3.1                          |
| ACRES    | F8.2   | Number of acres simulated                              |

**OUTPUT FILE: Tree2.sim**

| Variable                  | Format | Description   |
|---------------------------|--------|---|
| i                         | I3     | Tree age (years)  |
| XC                        | F8.2   | X-Coordinate simulated tree (ft)  |
| YC                        | F8.2   | Y-Coordinate simulated tree (ft)  |
| DBH(i)                    | F6.2   | Ground line diameter or DBH at age "i" (cm)   |
| TH(i)                     | F6.2   | Total tree height at age "i" (m)  |
| HINC(i)                   | F6.2   | Height increment at age "i" (m)   |
| HLC(i)                    | F6.2   | Height to base of live crown (m) at age "i"   |
| ACRES                     | F7.4   | Number of acres simulated   |
| NUMW(i)                   | I3     | Number of whorls formed at age "i"  |
| j                         | I3     | "j-th" whorl formed at age "i"  |
| WHEIGHT(i,j) <sup>a</sup> | F6.2   | Stem height of the "j-th" whorl formed at age "i"                                       |
| NUMB(i,j)                 | I3     | Number of branches of the "j-th" whorl formed at age "i"                                |
| k                         | I3     | "k-th" branch of the "j-th" whorl formed at age "i"                                     |
| BAGE(i,j,k)               | F5.1   | Age of the "k-th" branch at the end of the simulation period                            |
| BDEATH(I,j,k)             | F5.1   | Last year when the "k-th" branch was alive  |
| BANGLE(I,j,k)             | F7.2   | Angle of insertion (grade) to the stem pith of the "k-th" branch                        |
| BAZIM(i,j,k)              | F7.2   | Azimuth (degree) of the "k-th" branch   |
| BDIAM(i,j,k)              | F7.2   | Diameter of the "k-th" branch (mm) at the end of the simulation period                  |
| BHEIGHT(i,j,k)            | F7.2   | Height of the "k-th" branch (m) outside of the stem at the end of the simulation period |
| STATUS                    | I3     | Status of the "k-th" branch at the end of the simulation period (0: dead or 1:live)     |
| BTYPE                     | I3     | Type of branch (1: live, 2: non-occluded dead branch and 3: occluded dead branch)       |
| SPAGE                     | F5.1   | Age (years) when self-pruning is predicted to occur for the "k-th" branch               |
| XLIMB                     | F6.3   | Length (mm) of the limb left during the self-pruning process                            |
| XA                        | F8.3   | X-Coordinate (cm) for the end of the live portion of the "k-th" branch                  |
| YA                        | F8.3   | Y-Coordinate (cm) for the end of the live portion of the "k-th" branch                  |
| ZA                        | F8.3   | Z-Coordinate (cm) for the end of the live portion of the "k-th" branch                  |
| XD <sup>b</sup>           | F8.3   | X-Coordinate (cm) for the end of the dead portion of the "k-th" branch                  |
| YD                        | F8.3   | Y-Coordinate (cm) for the end of the dead portion of the "k-th" branch                  |
| ZD                        | F8.3   | Z-Coordinate (cm) for the end of the dead portion of the "k-th" branch                  |
| VLIVE                     | F8.3   | Volume of the live portion of the "k-th" branch   |
| VDEAD <sup>c</sup>        | F8.3   | Volume of the dead portion of the "k-th" branch   |
| VTOTAL                    | F8.3   | Total volume of the "k-th" branch   |

<sup>a</sup> it represents the point of origin for all branches formed in the same whorl, thus spatial location is (0,0,WHEIGHT).

<sup>b</sup> XD,YD,ZD coordinates can be outside of the stem bole for non-occluded branches (BTYPE=2).

<sup>c</sup> calculation considers only the portion attached internally to the stem.

## FORTRAN CODE

```
C -----
C SIMULATION OF BRANCH DEVELOPMENT AND KNOT FORMATION
C
C by GULLERMO TRINCADO
C RESEARCH GRADUATE STUDENT
C DEPARTMENT OF FORESTRY
C VIRGINIA POLYTECHNIC INSTITUTE AND STATE UNIVERSITY
C
C APRIL, 2006
C -----
C DESCRIPTION OF VARIABLES
C -----
C ----
C ACRES = Acres simulated
C AGE = Tree age
C BAGE = Number of years a branch was alive
C BAngle(i,j,k) = Angle of inclination of branch "k" located in whorl "j"
C formed at age "i" respect to stem pith (degrees)
C BAZIM(i,j,k) = Azimut of branch "k" located in whorl "j" formed at age "i" (degrees)
C BDEATH(i,j,k) = Tree age until branch(i,j,k) was still alive (years)
C BDIAM(i,j,k) = Diameter of branch "k" located in whorl "j" formed at age "i" (mm)
C BHEIGHT(i,j,k) = Height of branch "k" located in whorl "j" formed at age "i" (m)
C BTYPE(i,j,k) = Type of branch at the end of the simulation, used to estimate branch
C volume (1: live, 2: live/dead portions (non-occluded, with external
limb)
C and 3: live/dead portions (occluded)
C CL(i) = Crown Length (m) at age "i"
C DBH(i) = Diameter at breast height (m) at age "i"
C DUMMY, DUMMY1 = Dummy variables
C HINC(i) = Height increment (m) at age "i"
C HLC = Height live crown (m)
C NUMW(i) = number of whorls formed at age "i"
C NUMB(i,j) = number of branches of whorl "j" formed at age "i"
C SPAGE(i,j,k) = Self-pruning age of branch "k" located in whorl "j" formed at age "i"
C STATUS = Status of the branch at the end of the simulation (1:live, 0:dead)
C TH = Total tree height (m)
C WHEIGHT(i,j) = Height of the Whorl above the ground "j" (m)
C XLIMB(i,j,k) = Limb size of branch "k" located in whorl "j" formed at age "i"
C XC, YC = Coordinates of simulated trees
C XA, YA, ZA = Spatial coordinates of live part of the knot (end point)
C XD, YD, ZD = Spatial coordinates of dead part of the knot (end point)
C VLIVE = volume (cm3) of the live portion of a branch attached internally to
the stem
C VDEAD = volume (cm3) of the dead portion of a branch attached internally to
the stem
C VTOTAL = total volume of a branch attached internally to the stem
C -----
C ----
REAL XC, YC, HINC(50)
REAL CL(50), DELTAL, ALPHA, X, Y, Z
INTEGER Status
INTEGER i, j, k, l, m, Dummy, Dummy1

COMMON /Blok1/WHEIGHT(50,10), BAGE(50,10,10), BDEATH(50,10,10),
1 NUMB(50,10), BNUM(50,10,10), BANGLE(50,10,10), BAZIM(50,10,10),
2 BDIAM(50,10,10), BHEIGHT(50,10,10), BLENGTH(50,10,10),
3 BTYPE(50,10,10), SPAGE(50,10,10), XLIMB(50,10,10)
COMMON /Blok2/DBH(50), TH(50), HLC(50), LMORT(50), AGE(50), ACRES(50),
1 XCOORD(50), YCOORD(50)

C
C Growth series of each simulated trees
C
C CALL SERIES
CALL SEED(500)

C
C INPUT/OUTPUT files used during the simulation
```

```

C
OPEN(UNIT=3, FILE='Trees.txt',STATUS='old')
OPEN(UNIT=4, FILE='tree1.sim')
OPEN(UNIT=5, FILE='tree2.sim')

DUMMY = 1
DUMMY1 = 1
i = 0

DO WHILE (DUMMY.EQ.1)
  i = i + 1
  READ(3,30,END=99)AGE(i),XCOORD(i),YCOORD(i),DBH(i),TH(i),
*          CL(i),HLC(i),LMORT(i),ACRES(i)

C
C      identification of the age when TH > 1.37
C
C      IF ((TH(i).GT.1.37).AND.(Dummy1.EQ.1)) THEN
C          l = i
C          DUMMY1 = 0
C      ENDIF

C
C      required to check when the records for each tree are finished
C
C      IF (i.EQ.1) THEN
C          XC = XCOORD(i)
C          YC = YCOORD(i)
C      ENDIF

C
C      when the growth series of a tree is read, the simulation
C      of branch development starts
C
C      IF ((XCOORD(i).NE.XC).OR.(YCOORD(i).NE.YC)) THEN
C          m=i-1
C          CALL SIMULATION(m,l,XC,YC)
C          i = 0
C          DUMMY1 = 1

C
C          continue reading the growth series for the next tree
C
C          BACKSPACE 3
C          ENDIF

C          ENDDO

99  CONTINUE

m=i-1
CALL SIMULATION(m,l,XC,YC)

CLOSE(3)
CLOSE(4)
CLOSE(5)

30  FORMAT(I3,6(F8.2),I3,F8.2)
STOP
END

SUBROUTINE SERIES

C
C      Subroutine SERIES generate growth series of surviving trees.
C      (LINKAGE WITH PTAEDA)
C      -----
C      REAL XC(20000),YC(20000),D(20000),H(20000),CL(20000)
C      REAL HLC(20000),ACRES(20000)
C      INTEGER AGE(20000),LMORT(20000),DUMMY,i,j,n,ENDAGE

OPEN(UNIT=1, FILE='TreesSim.txt', STATUS='old')

```

```

OPEN(UNIT=2, FILE='Trees.txt')

  DUMMY = 1
  i = 0

  DO WHILE (DUMMY.EQ.1)
    i=i+1
    READ(1,10,END=99)AGE(i),XC(i),YC(i),D(i),H(i),
*          CL(i),LMORT(i),ACRES(i)
C
C   Changing units to metric
C
    D(i) = D(i)*2.54
    H(i) = H(i)*.3048
    CL(i) = CL(i)*.3048

C
C   Computing height to live crown
C
    IF (CL(i).NE.0) THEN
      HLC(i) = H(i)-CL(i)
    ELSE
      HLC(i)=0.0
    ENDIF

  ENDDO

99  CONTINUE

  n= i-1
  ENDAGE=AGE(n)

  DO i=1,n
    IF ((AGE(i).EQ.ENDAGE).AND.(LMORT(i).EQ.2)) THEN
      DO j=1,n
        IF ((XC(i).EQ.XC(j)).AND.(YC(i).EQ.YC(j))) THEN
          WRITE(2,20)AGE(j),XC(j),YC(j),D(j),H(j),CL(j),
*          HLC(j),LMORT(j),ACRES(j)
          ENDIF
        ENDDO
      ENDDO
    ENDIF
  ENDDO

  CLOSE(1)
  CLOSE(2)
10  FORMAT(I3,5F8.2,I3,F8.2)
20  FORMAT(I3,6F8.2,I3,F8.2)
RETURN
END

  SUBROUTINE SIMULATION(m,h,XC,YC)
C
C   Subroutine SIMULATION branch development and knot formation
C   -----
REAL Hinc(50),RATIO,XC,YC
REAL XA,YA,ZA,XD,YD,ZD,VLIVE,VDEAD,VTOTAL,DIF
INTEGER i,j,k,l,m,h,NUMW(50),STATUS
COMMON /Blok1/WHEIGHT(50,10),BAGE(50,10,10),BDEATH(50,10,10),
1 NUMB(50,10),BNUM(50,10,10),BANGLE(50,10,10),BAZIM(50,10,10),
2 BDIAM(50,10,10),BHEIGHT(50,10,10),BLENGTH(50,10,10),
3 BTYPE(50,10,10),SPAGE(50,10,10),XLIMB(50,10,10)
COMMON /Blok2/DBH(50),TH(50),HLC(50),LMORT(50),AGE(50),ACRES(50),
1 XCOORD(50),YCOORD(50)

  DO i=1, m

C
C   Linear interpolation of HLC for initial ages
C

```

```

        IF (i.LT.h) THEN
            HLC(i) = i*(HLC(h)/h)
        ENDIF

C
C      Assigning new values for groundline diameter when TH <= 1.37m
C
        RATIO = (2 * SRADIUS(DBH(h),TH(h),0.0))/TH(h)

        DO j=1, (h-1)
            DBH(j) = TH(j)*RATIO
        ENDDO

C
C      Computing annual height increment
C
        IF (i.EQ.1) THEN
            HINC(i) = TH(i)
        ELSE
            HINC(i) = TH(i)-TH(i-1)
        ENDIF

C
C      Assigning number of whorls for each growing season
C
        CALL WHORLS(HINC(i),NUMW(i))

C
C      Assigning the location of whorls within each growing season
C
        CALL WHORLHEIGHT(i,TH(i),HINC(i),NUMW(i))

C
C      Assigning initial branch characteristics (end of the first year)
C
        DO j=1,NUMW(i)
C
C          Assigning number of branches per whorl
C
            CALL BRANCHES(i,j,NUMB(i,j))

C
C          Assigning branch characteristics: inclination, azimuth and initial branch
C          diameter
C
            CALL BRANCHATTRIB(i,j)

C
C          Assigning initial branch height
C
            CALL BRANCHHEIGHT(DBH(i),TH(i),i,j,NUMW(i),NUMB(i,j))

        ENDDO

    ENDDO

C
C      OUTPUT of branch characteristics at branch age = 1 (File: Trees1.txt)
C
        DO i=1, m
            DO j=1,NumW(i)
                DO k=1,NumB(i,j)

C
C          Assigning BAge(i,j,k) equal to 1
C
                    BAGE(i,j,k) = 1
                    WRITE(4,40)i,XC,YC,DBH(i),TH(i),HINC(i),HLC(i),
*                        ACRES(i),NUMW(i),j, WHEIGHT(i,j),
*                        NUMB(i,j),k,BAGE(i,j,k),
*                        BANGLE(i,j,k),BAZIM(i,j,k),BDIAM(i,j,k),
*                        BHEIGHT(i,j,k), BLENGTH(i,j,k)

                ENDDO
            ENDDO
        ENDDO
    ENDDO
C

```



```

C      Recursive simulation of branch development
C
      DO l=2,m
        DO i=1,(l-1)
          DO j=1,NUMW(i)
            DO k=1, NUMB(i,j)
C
C              Determining wheather the Branch(i,j,k) is within the live crown at age "l-
1"
C
              IF (BHeight(i,j,k).GE.HLC(l-1)) THEN
                CALL BranchGrowth(i,j,k,l)
                BAGE(i,j,k) = BAGE(i,j,k) + 1
              ENDIF
            ENDDO
          ENDDO
        ENDDO
      ENDDO

C
C      OUTPUT of branch development for each tree until age "m" (projection period)
C
      DO i=1, m
        DO j=1,NUMW(i)
          DO k=1,NUMB(i,j)
            BDEATH(i,j,k) = i+BAGE(i,j,k)-1
C
C              Status of each branch at the end of the simulation
C              Status = 0 (dead branch, live/dead portions)
C              Status = 1 (live branch)
C
              IF ((m.EQ.BDeath(i,j,k)).AND.
*              (BHEIGHT(i,j,k).GE.HLC(m))) THEN
                STATUS = 1
              ELSE
                STATUS = 0
              ENDIF

C
C              Spatial location of the live part of the knots (XA,YA,ZA)
C
              IF (TH(BDEATH(i,j,k)).LE.TH(h)) THEN
C
C              For small trees simulation assumes conical shape
C
                CALL Cone(DBH(BDEATH(i,j,k)),TH(BDEATH(i,j,k)),
*              WHEIGHT(i,j),BANGLE(i,j,k),
*              BAZIM(i,j,k),XA,YA,ZA)
              ELSE

C
C              For trees with TH > 1.37 simulation uses taper equation
C
                CALL TaperEq(DBH(BDEATH(i,j,k)),
*              TH(BDEATH(i,j,k)),
*              WHEIGHT(i,j),BANGLE(i,j,k),
*              BAZIM(i,j,k),XA,YA,ZA)
              ENDIF

C
C              Spatial location of the death part of the knots (XD,YD,ZD)
C
              IF (STATUS.EQ.0) THEN

C
C              The coordinates (XD,YD,ZD) represent the end of the limb. Therefore,
C              this end part can be located inside or outside of the stem at the
C              end of the simulation
C
                CALL SELFPRUNING(i,j,k,m,XD,YD,ZD)
C
C

```

```

C          Location of the end point of the dead portion for those branches
C          were self-pruning didn't occur
C
C          IF (ZD.EQ.0) THEN
C              CALL TAPEREQ(DBH(m),TH(m),WHEIGHT(i,j),
*              BANGLE(i,j,k),BAZIM(i,j,k),XD,YD,ZD)
C          ENDIF
C
C          ELSE
C
C              Live branches do not have end point for the dead portion
C
C              XD=0.0
C              YD=0.0
C              ZD=0.0
C          ENDIF
C
C          Identification of branch type, used later to calculated volume
C          of branches attached internally to the stem using empirical equations
C          derived from the knot model
C
C          IF (Status.EQ.1) THEN
C
C              Live branch
C
C              BTYPE(i,j,k) = 1
C          ELSE
C
C              Stem radius of the dead branch according to XD coordinate
C              and angle of inclination
C
C              ALPHA = BAZIM(i,j,k)*0.017453293
C              r = XD/SIN(ALPHA)
C
C              Determination if a dead branch is located inside or outside
C              the stem at the end of the simulation period
C
C              IF (SRADIUS(DBH(m),TH(m),WHEIGHT(i,j)) .LE. r) THEN
C
C                  Death branch (non-occluded i.e. with an external limb)
C
C                  BTYPE(i,j,k) = 2
C              ELSE
C
C                  Dead branch (occluded)
C
C                  BTYPE(i,j,k) = 3
C
C              Always SRadius=r, but approximation in decimals make that
C              SRadius > r, even though the difference is minimal
C
C              DIF = (SRADIUS(DBH(m),TH(m),WHEIGHT(i,j))-r)
C              IF (DIF .LE. 0.0001) THEN
C                  BTYPE(i,j,k) = 2
C              ENDIF
C          ENDIF
C
C          ENDIF
C
C          Calculation of branch volume attached internally to the stem
C
C          CALL BVOLUME(i,j,k,m,XA,YA,ZA,XD,YD,ZD,
*          VLIVE,VDEAD,VTOTAL)
C
C          WRITE(5,50)i,XC,YC,DBH(i),TH(i),HINC(i),HLC(i),
*          ACRES(i),NUMW(i),j, WHEIGHT(i,j),NUMB(i,j),

```

```

*          k, BAGE(i,j,k),BDEATH(i,j,k),
*          BANGLE(i,j,k),BAZIM(i,j,k),BDIAM(i,j,k),
*          BHEIGHT(i,j,k),STATUS,INT(BTYPE(i,j,k)),
*          SPAGE(i,j,k),XLIME(i,j,k),XA,YA,ZA,
*          XD,YD,ZD,VLIVE,VDEAD,VTOTAL
      ENDDO
    ENDDO
  ENDDO
40  FORMAT(I3,2(F8.2),4(F6.2),F7.4,2(I3),F7.4,2(I3),F5.1,3(F7.2),
*        2(F7.4))
50  FORMAT(I3,2(F8.2),4(F6.2),F7.4,2(I3),F6.2,2(I3),2(F5.1),4(F7.2),
*        2(I3),F5.1,F6.3,9(F8.3))

  RETURN
END

      SUBROUTINE WHORLS(HINC,NUMW)
C
C      Subroutine WHORLS compute number of whorls for each growing
C      season
C      -----
      REAL P2,P3,P4,P5,T,RAND
      INTEGER NUMW,DUMMY

C
C      Polythomous logistic regression for a nominal variable
C
      P2 = EXP(8.1075-5.0902*HInc)
      P3 = EXP(5.2983-2.0670*HInc)
      P4 = EXP(2.0261-0.1546*HInc)

      T = 1+P2+P3+P4

C
C      Computing response probability
C
      P2 = P2/T
      P3 = P3/T
      P4 = P4/T
      P5 = 1-(P2+P3+P4)

C
C      Cumulative probabilities
C
      P3 = P2+P3
      P4 = P3+P4
      P5 = 1-P4

      CALL RANDOM(RAND)

C
C      Assigning Number of Whorls
C
      IF (HINC.LE.0) THEN
        NUMW = 0
      ELSE
        IF (Rand.LE.P2) THEN
          NUMW = 2
        ELSE
          IF (Rand.LE.P3) THEN
            NUMW = 3
          ELSE
            IF (Rand.LE.P4) THEN
              NUMW = 4
            ELSE
              NUMW = 5
            ENDIF
          ENDIF
        ENDIF
      ENDIF

```

```

        ENDIF

        RETURN
        END

        SUBROUTINE WHORLHEIGHT(i,TH,HINC,NUMW)
C
C   Subroutine WHORLHEIGHT computes the location of whorls within
C   each growing season
C   -----
        REAL TH,HINC
        INTEGER i,NUMW
        COMMON /Blok1/WHEIGHT(50,10),BAGE(50,10,10),BDEATH(50,10,10),
1 NUMB(50,10),BNUM(50,10,10),BANGLE(50,10,10),BAZIM(50,10,10),
2 BDIAM(50,10,10),BHEIGHT(50,10,10),BLENGTH(50,10,10),
3 BTYPE(50,10,10),SPAGE(50,10,10),XLIMB(50,10,10)

        SELECT CASE (NumW)
        CASE(2)
            WHEIGHT(i,1)=TH-(HInc*.46)
            WHEIGHT(i,2)=TH
        CASE(3)
            WHEIGHT(i,1)=TH-(HInc*.595)
            WHEIGHT(i,2)=TH-(HInc*.249)
            WHEIGHT(i,3)=TH
        CASE(4)
            WHEIGHT(i,1)=TH-(HInc*.689)
            WHEIGHT(i,2)=TH-(HInc*.425)
            WHEIGHT(i,3)=TH-(HInc*.187)
            WHEIGHT(i,4)=TH
        CASE(5)
            WHEIGHT(i,1)=TH-(HInc*.786)
            WHEIGHT(i,2)=TH-(HInc*.575)
            WHEIGHT(i,3)=TH-(HInc*.349)
            WHEIGHT(i,4)=TH-(HInc*.166)
            WHEIGHT(i,5)=TH
        END SELECT

        RETURN
        END

        SUBROUTINE BRANCHES(i,j,NUMB)
C
C   Subroutine BRANCHES computes the number of branches per whorl.
C   -----
        INTEGER i,j,k,NUMB,DUMMY
        REAL THETA,PROB(7),SUM

C
C   computing the parameter value for the double truncated Poisson
C   distribution
C
        THETA = 3.46799 - (0.65751/j)

        SUM = 0.0

        DO k = 1, 7
            SUM = SUM + (THETA**k)/FACT(k)
        ENDDO

        PROB(1) = THETA/SUM

        DO k = 2, 7
C
C   cumulative probability
C
            PROB(k) = PROB(k-1) + ((THETA**k)/FACT(k))/SUM
        ENDDO

```

```

CALL RANDOM(RAND)

  DUMMY = 1
  k = 0

  DO WHILE (DUMMY.EQ.1)
    k = k + 1
    IF (PROB(k).GE.RAND) THEN
      DUMMY = 0
      NUMB = k
    ENDIF
  ENDDO

RETURN
END

FUNCTION FACT(k)
C
C   Function FACT computes factorial
C   -----
  INTEGER j,k
  REAL FACT
  FACT = 1

  DO j=2, k
    FACT = FACT*j
  ENDDO

RETURN
END

SUBROUTINE BRANCHATTRIB(i,j)
C
C   Subroutine BRANCHATTRIB computes initial branch attributes:
C   azimuth, angle of inclination and initial branch diameter
C   -----
  INTEGER i, j, k
  REAL RAND, DIFFANGLE, STEP
  COMMON /Blok1/WHEIGHT(50,10),BAGE(50,10,10),BDEATH(50,10,10),
  1 NUMB(50,10),BNUM(50,10,10),BANGLE(50,10,10),BAZIM(50,10,10),
  2 BDIAM(50,10,10),BHEIGHT(50,10,10),BLENGTH(50,10,10),
  3 BTYPE(50,10,10),SPAGE(50,10,10),XLIMB(50,10,10)

C
C   Assigning branch azimuth for the first whorl
C
  IF (j.EQ.1) THEN
    DO k=1,NUMB(i,j)
      IF (NUMB(i,j).LE.2) THEN
        CALL RANDOM(RAND)
        BAZIM(i,j,k) = RAND*360
      ELSE
        IF (k.EQ.1) THEN
          CALL RANDOM(RAND)
          BAZIM(i,j,k) = RAND*360
        ELSE
          BAZIM(i,j,k) = (360/NUMB(i,j))*(k-1)+BAZIM(i,j,1)
          IF (BAZIM(i,j,k).GT.360) THEN
            BAZIM(i,j,k) = BAZIM(i,j,k) - 360 ;
          ENDIF
        ENDIF
      ENDIF
    ENDDO
  ENDIF

C
C   Assigning branch azimuth for the second, third, .. whorls

```

```

C
  IF (j.GT.1) THEN
    IF (NUMB(i,j).EQ.NUMB(i,j-1)) THEN

      SELECT CASE(NUMB(i,j))
      CASE(3)
        DIFFANGLE = 12
      CASE(4)
        DIFFANGLE = -5
      CASE(5)
        DIFFANGLE = -3
      CASE(6,7)
        DIFFANGLE = -53
      END SELECT

      DO k=1,NUMB(i,j)
      BAZIM(i,j,k) = BAZIM(i,j-1,k) + DIFFANGLE
      IF (BAZIM(i,j,k).GT.360) THEN
        BAZIM(i,j,k) = BAZIM(i,j,k) - 360
      ENDIF

      IF (BAZIM(i,j,k).LT.0) THEN
        BAZIM(i,j,k) = 360 + BAZIM(i,j,k)
      ENDIF
      ENDDO

    ELSE
      DO k=1,NUMB(i,j)
      IF (NUMB(i,j).LE.2) THEN
        CALL RANDOM(RAND)
        BAZIM(i,j,k) = RAND*360
      ELSE
        IF (k.EQ.1) THEN
          CALL RANDOM(RAND)
          BAZIM(i,j,k) = RAND*360
        ELSE
          BAZIM(i,j,k) = (360/NUMB(i,j))*(k-1)+BAZIM(i,j,1)
          IF (BAZIM(i,j,k).GT.360) THEN
            BAZIM(i,j,k) = BAZIM(i,j,k) - 360
          ENDIF
        ENDIF
      ENDIF
      ENDDO

    ENDIF
  ENDIF
C
C   Assigning branch inclination
C
  DO k=1,NUMB(i,j)
  CALL RANDOM(RAND)
  BANGLE(i,j,k) = 29.1483+18.9318*(-LOG(1-RAND*0.999))**(1/2.973)
  ENDDO
C
C   Assigning initial branch diameter
C
  DO k=1,NUMB(i,j)
  CALL RANDOM(RAND)
  BDIAM(i,j,k) = 1.6556+11.6227*(-LOG(1-RAND*0.999))**(1/2.826)
  ENDDO

  RETURN
  END

  SUBROUTINE BRANCHHEIGHT(DBH,TH,i,j,NUMW1,NUMB1)
C
C   Subroutine BRANCHHEIGHT computes the location of branches
C   above the ground
C   -----
C   INTEGER i, j, k, NUMW1,NumB1

```

```

REAL DBH, TH, ANGLE, X, Y
COMMON /Blok1/WHEIGHT(50,10), BAGE(50,10,10), BDEATH(50,10,10),
1 NUMB(50,10), BNUM(50,10,10), BANGLE(50,10,10), BAZIM(50,10,10),
2 BDIAM(50,10,10), BHEIGHT(50,10,10), BLENGTH(50,10,10),
3 BTYPE(50,10,10), SPAGE(50,10,10), XLIMB(50,10,10)

      IF (j.EQ.NUMW1) THEN
C
C      branches located in the last whorl of a growing season
C
      DO k=1, NUMB1
        BHEIGHT(i, j, k) = WHEIGHT(i, j)
        BLENGTH(i, j, k) = 0.0
      ENDDO
      ELSE
      DO k=1, NumB1
C
C      transforming to radians
C
        ALPHA = (90-BAngle(i, j, k))*0.017453293
        X = SRADIUS(DBH, TH, WHEIGHT(i, j))
        Y = X * TAN(ALPHA)
        BHEIGHT(i, j, k) = WHEIGHT(i, j) + (Y/100)
        BLENGTH(i, j, k) = (Y*10)/SIN(ALPHA)
      ENDDO
      ENDIF

      RETURN
      END

      SUBROUTINE BRANCHGROWTH(i, j, k, l)
C
C      Subroutine BRANCHGROWTH computes branch growth
C      -----
      INTEGER i, j, k, l
      REAL DELTAL, Z, X, Y
      COMMON /Blok1/WHEIGHT(50,10), BAGE(50,10,10), BDEATH(50,10,10),
1 NUMB(50,10), BNUM(50,10,10), BANGLE(50,10,10), BAZIM(50,10,10),
2 BDIAM(50,10,10), BHEIGHT(50,10,10), BLENGTH(50,10,10),
3 BTYPE(50,10,10), SPAGE(50,10,10), XLIMB(50,10,10)
      COMMON /Blok2/DBH(50), TH(50), HLC(50), LMORT(50), AGE(50), ACRES(50),
1 XCOORD(50), YCOORD(50)

      DELTAL = BLENGTH(i, j, k)
      Z = (TH(1-1)-BHEIGHT(i, j, k))/(TH(1-1)-HLC(1-1))
      ALPHA = (90-BANGLE(i, j, k))*0.017453293
      X = SRADIUS(DBH(1), TH(1), WHEIGHT(i, j))
      Y = X * TAN(ALPHA)
      BHeight(i, j, k) = WHEIGHT(i, j) + (Y/100)
      BLENGTH(i, j, k) = (Y*10)/SIN(ALPHA)
      DELTAL = BLENGTH(i, j, k) - DELTAL

      BDIAM(i, j, k) = BDIAM(i, j, k)+0.5533*(DELTAL**0.92)*
*      EXP(-1.0925*Z)

      RETURN
      END

      FUNCTION SRADIUS(DBH, TH, H)
C
C      Function SRADIUS computes stem radius at any given height
C      -----
      REAL DBH, TH, D, X, X1, X2, b1, b2, b3, b4, a1, a2

      b1 = -3.0257
      b2 = 1.4586
      b3 = -1.4464

```

```

b4 = 39.1081
a1 = 0.7431
a2 = 0.1125

X=H/TH
X1=X-1
X2=X*X-1

IF (TH.GE.1.37) THEN

  IF (X.GE.a1) THEN
    D =DBH*SQRT(b1*X1+b2*X2)
  ELSE
    IF ((a2.LE.X).AND.(X.LT.a1)) THEN
      D=DBH*SQRT(b1*X1 + b2*X2 + b3*(a1-X)**2)
    ELSE
      D=DBH*SQRT(b1*X1 + b2*X2 + b3*(a1-X)**2 + b4*(a2-X)**2)
    ENDIF
  ENDIF

  SRADIUS = D/2

ELSE
C
C   assuming the shape of a cone
C
  SRADIUS =(DBH-(H*100)*(DBH/(TH*100)))/2
ENDIF

END FUNCTION

SUBROUTINE SELFPRUNING(i,j,k,m,XD,YD,ZD)
C
C   Subroutine SELFPRUNING simulates the self-pruning process
C   -----
  INTEGER i,j,k,l,m,n,DEGIN,AGESP,DUMMY
  INTEGER DELTAT
  REAL XD,YD,ZD,F,RAND,RAND2,LIMBSIZE,H,ALPHA,THETA,R

  COMMON /Blok1/WHEIGHT(50,10),BAGE(50,10,10),BDEATH(50,10,10),
1 NUMB(50,10),BNUM(50,10,10),BANGLE(50,10,10),BAZIM(50,10,10),
2 BDIAM(50,10,10),BHEIGHT(50,10,10),BLENGTH(50,10,10),
3 BTYPE(50,10,10),SPAGE(50,10,10),XLIMB(50,10,10)
  COMMON /Blok2/DBH(50),TH(50),HLC(50),LMORT(50),AGE(50),ACRES(50),
1 XCOORD(50),YCOORD(50)

  n = BDEATH(i,j,k) + 1
  DELTAT = 0.0
  LIMBSIZE = 0.0
  AGESP = 0.0
  DUMMY = 0

  DO l=n,m
    DELTAT = DELTAT + 1

    IF (DELTAT.LE.4) THEN
      F = 0.0
    ELSE
      F = 0.142857143 * (DELTAT - 4)
    ENDIF

    CALL RANDOM(RAND)

    IF ((F.GT.RAND) .AND. (DUMMY.EQ.0)) THEN
      CALL RANDOM(RAND2)
C
C       Units in cm (3 inches = 7.62 cm)
C
      LIMBSIZE = 7.62 * RAND2

```



```

C
C           Age when the branch dropped off
C
      AGESP = 1
      DUMMY = 1
      ENDIF

      ENDDO

      IF (LIMBSIZE.GT.0) THEN

          CALL TAPEREQ(DBH(AGESP),TH(AGESP),WHEIGHT(i,j),BANGLE(i,j,k),
*              BAZIM(i,j,k),XD,YD,ZD)

C
C           Calculating length of the branch attached internally
C
      ALPHA = BAZIM(i,j,k)*0.017453293
      THETA = (90-BANGLE(i,j,k))*0.017453293

      H = (XD/SIN(ALPHA))/COS(theta)

C
C           Adding length of the limb, which can or can not be covered
C           completely in the following growing seasons.
C
      H = H + (BDIAM(i,j,k)/20)/TAN(BANGLE(i,j,k)*0.017453293)
*
      r = H*COS(theta)

      XD = r * SIN(ALPHA)
      YD = r*COS(ALPHA)
      ZD = WHeight(i,j)+(r*TAN(theta))/100

      ELSE

C
C           Spatial location of branches without self-pruning
C
      CALL TAPEREQ(DBH(m),TH(m),WHEIGHT(i,j),BANGLE(i,j,k),
*              BAZIM(i,j,k),XD,YD,ZD)

      ENDIF

      XLIMB(i,j,k) = LIMBSIZE
      SPAGE(i,j,k) = AGESP

      RETURN
      END

      SUBROUTINE TAPEREQ(DBH,TH,H,ANGLE,AZIM,X,Y,Z)

C
C           Subroutine TAPEREQ computes upper stem diameter to locate branches
C           on the stem surface (taper equation)
C           -----
      REAL DBH,TH,H,D,r,ALPHA,THETA

      D = SRADIUS(DBH,TH,H)*2

C
C           Transformation of angle of branch inclination to radians
C
      THETA = (90-ANGLE)*0.017453293

C
C           Transformation of azimuth to radians
C
      ALPHA = AZIM*0.017453293

      r = D/2
      X = r*SIN(ALPHA)
      Y = r*COS(ALPHA)

```

```

C
C   Divided by 100 to compute Z in meters (stem radius in cm)
C
Z = H + (r*TAN(THETA))/100

RETURN
END

SUBROUTINE CONE(DBH,TH,H,ANGLE,AZIM,X,Y,Z)
C
C   Subroutine CONE computes upper stem diameters to locate branches
C   on the stem surface for trees with TH < 1.37
C   -----
REAL DBH,TH,ANGLE,AZIM,X,Y,Z,r,THETA,ALPHA

C
C   Transformation of angle of branch inclination to radians (remember
C   that inclination is measured with respect to the stem pith).
C
THETA = (90-ANGLE)*0.017453293

C
C   Transformation of azimuth to radians
C
ALPHA = AZIM*0.017453293

r = (DBH - H*(DBH/TH))/2
X = r*SIN(ALPHA)

Y = r*COS(ALPHA)

C
C   Divided by 100 to compute in meters (stem radius in cm)
C
Z = H + (r*TAN(THETA))/100

RETURN
END

SUBROUTINE BVOLUME(i,j,k,m,XA,YA,ZA,XD,YD,ZD,VLIVE,VDEAD,VTOTAL)
C
C   Subroutine BVOLUME estimates internal branch volume (cm3)
C   -----
INTEGER i,j,k,TYPEB
REAL ALPHA,BETA,THETA,H,R,R1,R2,R3,D1,D2,DIF
REAL XA,XD,VLIVE,VDEAD,X1,X2,L1,L2,l,DUMMY1,DUMMY2
REAL H1,H2
COMMON /Blok1/WHEIGHT(50,10),BAGE(50,10,10),BDEATH(50,10,10),
1 NUMB(50,10),BNUM(50,10,10),BANGLE(50,10,10),BAZIM(50,10,10),
2 BDIAM(50,10,10),BHEIGHT(50,10,10),BLENGTH(50,10,10),
3 BTYPE(50,10,10),SPAGE(50,10,10),XLIME(50,10,10)
COMMON /Blok2/DBH(50),TH(50),HLC(50),LMORT(50),AGE(50),ACRES(50),
1 XCOORD(50),YCOORD(50)

ALPHA = BANGLE(i,j,k)*0.017453293
THETA = BAZIM(i,j,k)*0.017453293

C
C   Coefficients of the knot model
C
BETA = 0.0377 * ((BDIAM(i,j,k)**1.17380))

C
C   ALPHA = BAZIM(i,j,k)*0.017453293
C   THETA = (90-BANGLE(i,j,k))*0.017453293

C
C   Branch volume estimate considers only the part of the branch attached internally

```

```

C      to the stem. Therefore, for those non-occluded branches (BType=2) the external limb
C      is not considered in the calculations. But, they are displayed graphically using
C      the assigned (XD,YD,ZD) coordinates.
C
TYPEB = INT(BTYPE(i,j,k))

      IF (i.EQ.m) THEN
C
C      Assumed that branches formed in the last growing season
C      do not have volume. It avoids possible errors when running
C      the program
C
VLIVE = 0.0
VDEATH = 0.0
VTOTAL = VLIVE + VDEAD

      ELSE

      SELECT CASE(TypeB)

C      Live Branches
C
CASE(1)
      R = BDIAM(i,j,k)/20
      H = SQRT(XA**2 + YA**2 + (100*WHEIGHT(i,j)-100*ZA)**2)
      L1 = H + R/TAN(ALPHA)
      l = (2*R)/TAN(ALPHA)
      IF (L1.GT.l) THEN
          VLIVE = (1 + ((L1-l)/L1)**(BETA+1))/(2*(BETA+1))
          VLIVE = (3.141592*(R**2)*L1)*VLIVE
          VDEAD = 0.0
      ELSE
          VLIVE = 0.0
          VDEAD = 0.0
      ENDIF

C      Non-occluded branches
C
CASE(2)
      R = BDIAM(i,j,k)/20
      R1 = XA/SIN(THETA) + R*COS(ALPHA)
      R2 = SRADIUS(DBH(m),TH(m),WHEIGHT(i,j))

      IF (R2.GT.R1) THEN
C
C      Type of knot 2A
C
      H = SQRT(XA**2 + YA**2 + (100*WHEIGHT(i,j)-100*ZA)**2)
      L1 = H + R/TAN(ALPHA)

      VLIVE = (3.1415926*(R**2)*L1)/(BETA+1)

      H = SRADIUS(DBH(m),TH(m),WHEIGHT(i,j))
      H = H/COS(1.57079637-ALPHA)
      L2 = H + R/TAN(ALPHA) - L1
      l = (2*R)/TAN(ALPHA)

      VDEAD = 3.141592*(R**2)*(L2-(l/2))

      ELSE
      H = SQRT(XA**2 + YA**2 + (100*WHEIGHT(i,j)-100*ZA)**2)
      L1 = H + R/TAN(ALPHA)
      R3 = L1*COS(1.57079637-ALPHA)

      H = R2/COS(1.57079637-ALPHA)
      L1 = H + R/TAN(ALPHA)
      l = (2*R)/TAN(ALPHA)

      VLIVE = (1 + ((L1-l)/L1)**(BETA+1))/(2*(BETA+1))
      VLIVE = (3.141592*(R**2)*L1)*VLIVE

```

```

C          IF (R2.LT.R3) THEN
C
C          Type of knot 2B
C
D1 = R - ((R3-R2)/COS(1.57079637-ALPHA))
D2 = D1/COTAN(1.57079637-ALPHA)

VDEAD = (3.141592*(R**2)*D2)*(D1/(2*R))*0.5
VLIVE = VLIVE - VDEAD

ELSE
C
C          Type of knot 2C
C

D1 = R + ((R2-R3)/COS(ALPHA))
D2 = D1/COTAN(1.57079637-ALPHA)

VDEAD = (3.141592*(R**2)*D2)*(D1/(2*R))*0.5
VLIVE = VLIVE - VDEAD

ENDIF

ENDIF

C
C          Occluded branches
C
CASE(3)
R = BDIAM(i,j,k)/20
H = SQRT(XA**2 + YA**2 + (100*WHEIGHT(i,j)-100*ZA)**2)
L1 = H + R/TAN(ALPHA)

H = SQRT(XD**2 + YD**2 + (100*WHEIGHT(i,j)-100*ZD)**2)
L2 = H-L1

IF (L2.GT.0) THEN
VLIVE = (3.1415926*(R**2)*L1)/(BETA+1)
VDEAD = 3.1415926*(R**2)*L2
ELSE
C
C          Only live portion of a branch stays inside the stem
C

VLIVE = (3.1415926*(R**2)*H)/(BETA+1)
VDEAD = 0.0
ENDIF

END SELECT

VTOTAL = VLIVE + VDEAD

ENDIF

RETURN
END

```